การคืนสภาพทองแดงจากสารละลายผสมของทองแดงและตะกั่ว
โดยใช้การดูดซับและการคายซับ

นางสาวอภิปรียา คงสุวรรณ

RECOVERY OF COPPER(II) FROM COPPER-LEAD MIXTURE SOLUTION
USING ADSORPTION AND DESORPTION

Miss Apipreeya Kongsuwan

A Thesis Submitted in Partial Fulfillment of the Requirements

for the Degree of Master of Engineering Program in Chemical Engineering

Department of Chemical Engineering

Faculty of Engineering

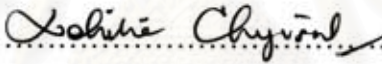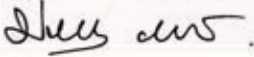Chulalongkorn University

Academic Year 2006

Thesis Title	RECOVERY OF COPPER(II) FROM COPPER-LEAD MIXTURE SOLUTION USING ADSORPTION AND DESORPTION
By	Miss Apipreeya Kongsuwan
Field of study	Chemical Engineering
Thesis Advisor	Associate Professor Prasert Pavasant, Ph.D.

Accepted by the Faculty of Engineering, Chulalongkorn University in Partial Fulfillment of the Requirements for the Master's Degree

....Dean of the Faculty of Engineering

(Professor Direk Lavansiri, Ph.D.)

THESIS COMMITTEE

....Chairman

(Assistant Professor Vichitra Chongvisal, Ph.D.)

....Thesis Advisor

(Associate Professor Prasert Pavasant, Ph.D.)

....Member

(Associate Professor Deacha Chatsiriwech, Ph.D.)

....Member

(Vorapot Kanokkantapong, Ph.D.)

อภิปรียา คงสุวรรณ : การคืนสภาพทองแดงจากสารละลายผสมของทองแดงและตะกั่วโดย
ใช้การดูดซับและการคายซับ. (RECOVERY OF COPPER(II) FROM COPPER-LEAD
MIXTURE SOLUTION USING ADSORPTION AND DESORPTION) อาจารย์ที่ปรึกษา :
รศ.ดร.ประเสริฐ ภวสันต์, 101 หน้า.

การผลิตถ่านกัมมันต์จากเปลือกไม้ยูคาลิปตัสด้วยกรดฟอสฟอริกนำมาศึกษาเพื่อดูดซับน้ำ
เสียปนเปื้อนโลหะหนัก ซึ่งโลหะหนักที่นำมาศึกษาคือทองแดงและตะกั่วทั้งในระบบหนึ่ง
องค์ประกอบและสององค์ประกอบ ค่าความเป็นกรดด่างที่เหมาะสมในการดูดซับทองแดงและ
ตะกั่วคือพีเอช 5 และอัตราเร็วในการดูดซับสามารถทำนายด้วยสมการอัตราการเกิดปฏิกิริยาอันดับ
สอง และความสามารถในการดูดซับสูงสุดในการดูดซับทองแดงและตะกั่วมีค่าเท่ากับ 0.45 และ
0.53 มิลลิโมลต่อกรัม ซึ่งหมู่ฟังก์ชันที่เกี่ยวข้องในการดูดซับคือ หมู่คาร์บอกซิลิก หมู่เอมีน และหมู่
เอไมด์ กลไกในการเกิดปฏิกิริยาการกำจัดโลหะหนักจะเป็นการดูดซับทางกายภาพ ในการดูดซับ
สององค์ประกอบของทองแดงและตะกั่วพบว่าถ่านกัมมันต์มีความสามารถในการดูดซับตะกั่วได้
มากกว่าทองแดงและความสามารถในการดูดซับของโลหะแต่ละชนิดลดลงเมื่อเปรียบเทียบกับการ
ดูดซับโลหะหนักหนึ่งองค์ประกอบ

ในการคายซับโลหะหนักด้วยกรดซิตริกจากการทดลองพบว่า เมื่อเพิ่มความเข้มข้นของกรด
ซิตริกและอุณหภูมิในการคายซับจะทำให้ประสิทธิภาพการคายซับสูงขึ้น กรดซิตริกที่มีความเข้มข้น
1 โมลต่อลิตร และอัตราส่วนของแข็งต่อของเหลวเท่ากับ 4 หรือ 8 สามารถสกัดโลหะหนักหนึ่ง
องค์ประกอบได้เกือบ 100 เปอร์เซนต์ แต่ในการแยกโลหะหนักสององค์ประกอบให้ได้มากที่สุด
ควรใช้กรดซิตริกที่ความเข้มข้น 0.01 โมลต่อลิตร และอัตราส่วนของแข็งต่อของเหลวเท่ากับ 16
และอัตราเร็วในการคายซับการสกัดสามารถทำนายได้ด้วยสมการอัตราการเกิดปฏิกิริยาอันดับสอง
เช่นเดียวกัน

ภาควิชา.........วิศวกรรมเคมี.................... ลายมือชื่อนิสิต...

สาขาวิชา.......วิศวกรรมเคมี.................... ลายมือชื่ออาจารย์ที่ปรึกษา........................

ปีการศึกษา 2549

4870554721 : MAJOR   CHEMICAL ENGINEERING
KEY WORD: ADSORPTION / HEAVY METALS / DESORPTION / CITRIC ACID / ACTIVATED CARBON

APIPREEYA KONGSUWAN: RECOVERY OF COPPER(II) FROM COPPER-LEAD MIXTURE SOLUTION USING ADSORPTION AND DESORPTION. THESIS ADVISOR: ASSOC. PROF. PRASERT PAVASANT, Ph.D., 101 pp.

Eucalyptus bark was used to produce activated carbon through the phosphoric acid activation process. This activated carbon was then used for the adsorption of copper and lead ions. The results indicated that the optimal pH for adsorption was 5 and the rate of adsorption could be predicted with the pseudo second order model. The maximum adsorption capacities for Cu(II) and Pb(II) were 0.45 and 0.53 mmol g^{-1}. Carboxylic, amine and amide groups were found to involve in the adsorptions of Cu(II) and Pb(II). Ion exchange should not be a major mechanism for the uptakes of both heavy metals and the actual mechanism should simply be physical adsorption. For binary components adsorptions, activated carbon could adsorb more Pb(II) than Cu(II) where the presence of the secondary metal ions suppressed the adsorption of the primary metal ions. However, Pb(II) was found to have stronger negative effect on the adsorption of Cu(II) than vice versa.

Citric acid was used to desorb Cu(II) and Pb(II) from the loaded activated carbon. The results showed that increasing desorbing agent concentration and desorption temperature increased desorption efficiency. For single component systems, the desorption best took place at the citric acid concentration of 1 mol L^{-1} whereas the solid/liquid (S/L) ratio of either 4 or 8 was found to give satisfactorily desorption results. For the binary systems, citric acid concentration of 0.01 mol L^{-1} and the solid/liquid (S/L) ratio of 16 were found to be suitable conditions for the separation of both metal ions. The rate of desorption could be predicted with the pseudo second order model.

Department…..Chemical Engineering…Student's signature……………………………

Field of study...Chemical Engineering…Advisor's signature ……………………

Academic year 2006.

ACKNOWLEDGEMENTS

CONTENTS

LIST OF TABLES

LIST OF FIGURES

CHAPTER I

INTRODUCTION

1.1 Motivations

With a rapid increase in global industrial activities, pollution derived from the uncontrolled escape of heavy metals such as copper, nickel, chromium, and zinc has become serious. Heavy metals are detected in waste streams from mining operations, tanneries, electronics, electro plating and petrochemical industries in large quantities. These heavy metals have harmful effects on human physiology and other biological systems when they exceed tolerance levels. The most widely used methods for removing heavy metals from wastewaters include chemical precipitation, solvent extraction, oxidation, reduction, dialysis/electrodialysis, electrolytic extraction, reverse osmosis, ion exchange, evaporation, cementation, dilution, filtration, flotation, air stripping, flocculation, sedimentation, soil flushing/washing chelation, membrane filtration and adsorption (Bartosh et al., 2000; Mohan and Singh, 2002). Among various treatment technologies, activated carbon adsorption is commonly used because the design is simple and can use with the low concentration of heavy metal. Nevertheless, adsorption of binary or multiple component mixture processes generates solid waste in large quantity and does not provide any recovery or recycling options for the metal components that have potential economic value as non-renewable natural resources.

For many years, desorption techniques for the purposes of recovery heavy metals are studied. Unfortunately, the various effective desorbing agents such as benzene and chlorine could cause cancer and environmental pollution. Recently, the development of low molecular weight organic acid desorption of heavy metals was proposed as an environmental friendly desorbing agent which provided reasonable level of recovery of heavy metals (Wu et al., 2003).

Recent work at the Department of Chemical Engineering, Faculty of Engineering, Chulalongkorn University, Thailand, has demonstrated a successful conversion of eucalyptus bark to activated carbon. This work therefore intended to employ this activated carbon product in the recovery of heavy metal from the binary mixture solution. Fundamentally, each type of heavy metal was selectively adsorbed

to the activated carbon surface at certain pH. Hence, with a proper adjustment of pH, a recovery of each specific metal was made possible. A recovery with a more environmental friendly desorbing agent such as citric acid was thereafter investigated. In this work, a synthetic mixture solution of copper and lead was arbitrarily selected as a modeled adsorption system.

1.2 Objectives of this work

1. To investigate the adsorption characteristics of heavy metals in the synthetic wastewater using activated carbon from *Eucalyptus camaldulensis Dehn* bark

Sub-objectives:

- To determine adsorption isotherms and adsorption kinetics of the adsorption of heavy metals
- To determine appropriate pH for the adsorption of heavy metals

2. To recover heavy metal from heavy metal mixture solution that adsorbed on activated carbon surface by desorption.

Sub-objectives:

- To determine desorption kinetics.
- To determine appropriate conditions, i.e. concentration of desorbing agent, solid/liquid *(S/L)* ratio, temperature for desorption.

1.3 Scopes of this work

1. Adsorption experiments were performed in a batch system with both single and binary mixture synthetic solutions.

- The heavy metals investigated in this work included copper (Cu), lead (Pb).
- The range of heavy metals concentration was 0.1-10 mmol L^{-1}
- The range of pH of solution was 1-6.

2. Desorption experiments were performed in a batch system.

- The desorbing agent investigated in this work was citric acid.
- The range of citric solution concentration was 0.005-1 mol L^{-1}.
- The range of solid/liquid *(S/L)* ratio was 1-16 (amount of activated carbon loaded metals 0.05-0.4 g).
- The temperature was in the range from 25-75°C.

CHAPTER II

BACKGROUNDS & LITERATURE REVIEW

2.1 Heavy metals

Heavy metals are a group of elements that are generally presented in the Periodic Tables Group I B to VIII B and have an atomic number of between 26 and 84. The most commonly occurring heavy metals in the environment include chromium, iron, nickel, copper, zinc, silver, cadmium, platinum, gold, mercury, lead and arsenic. Within the environment there are a number of different chemical forms in which heavy metals can exist. Whether the heavy metals are present in water or organisms, their biological properties and availability are intensely affected by their chemical status (Krenkel, 1975). Heavy metals can exist in water as free metal ions, inorganic complexes and compounds, or associated with colloidal and particulate matter.

2.1.1 Sources of heavy metals

Heavy metals or metallic compounds are used during the manufacturing of variety of products. As a result of a loop hole in conventional thermodynamics, industries that involve the use of heavy metals always generate wastes containing them. This section characterizes wastes generated by major metal-waste-producing industries and address current waste management practices. The industries discussed include coating, smelting and refining of non-ferrous metals, paint, ink and associated products, iron and steel manufacturing, photographic industry, leather tanning and finishing, wood preserving and battery manufacturing. Waste streams from each of these industries have their own unique characteristics. However, they also contain a number of common metals, such as aluminium, arsenic, cadmium, chromium, copper, lead, nickel, silver and zinc.

Table 2.1 summarizes a comprehensive list of industries that use heavy metals and the effluents from those which contain high concentrations of heavy metals. A number of other industries such as automotive manufacturers, computer manufacturers, mining and food processing industries may also employ heavy metals in their processes and therefore potentially produce heavy metal-containing effluents.

Table 2.1 List of industries involved the use of heavy metals (Kaewsarn, 2000)

Name of Industry	Heavy metals								
	Ag	Al	As	Cd	Cr	Cu	Ni	Pb	Zn
Metal coating	•			•	•	•		•	•
Smelting and refining	•	•		•		•		•	•
Paint, ink and associated products		•			•	•		•	
Petroleum refining					•			•	
Iron and steel manufacturer				•	•	•	•	•	•
Photographic industry	•								
Leather, tanning and fishing					•				
Wood preserving			•		•	•			
Battery manufacturer	•						•	•	

2.1.2 Environmental problems associated with heavy metals

The problems that heavy metals pose to the environment differ greatly from most other form of pollution. This is primarily because metals do not undergo biodegradation. While all forms of pollution have potential to affect living organisms, most heavy metals only require relatively low dosages to cause toxicity. Evaluation of the impact of heavy metals in wastewater systems which applies to our environment necessitates consideration of their potential toxicity to plants, animals and humans.

A toxic material is a substance that has an adverse effect on health. Many chemicals could be classified as toxic, but some more so than others. The level of toxicity of a substance relates to the amount that causes an adverse effect and to some extent the type of effect. Many chemicals elements are also essential or at least beneficial to human health, but they also can become toxic when taken in excess. The toxic effects of an element are measured by its dose-response relationship, where the response is the sign of an adverse effect. At times the symptoms of acute and chronic exposure are different and thus, the effects may also differ. Another feather that affects the response to a toxic metal is that some people are more sensitive, and therefore more at risk than others.

A comprehensive review of the toxicological details of all of these heavy metals is beyond the scope of this study. Thus, some examples of the effects of each heavy metal on the health of human being are listed in Table 2.2. It can be seen that threshold-limiting values for all of the metals are typically very low.

Table 2.2 Heavy metals, threshold limiting values (TLV-TWA) and effect of poisoning. (Patnaik, 1999)

Heavy metals	TLV-TWA (mg/m^3)	Effect of poisoning
Lead	0.15	<u>Acute toxic</u> Ataxia, headache, stupor, hallucinations, tremors, convulsions and coma <u>Chronic exposure</u> Weight loss, central nervous system effects, anemia, and damage to the kidney
Copper	1.0	Irritation of eyes and mucous membranes, nasal perforation, cough, dry throat, muscle ache, chills, and metal fever.

2.2 Legal controls for heavy metal contamination

Legislation around the world is rapidly catching up with the fears of the environmentalists in regards to heavy metals pollution. For example the last few years have seen directives issued by various organizations such as European Commission and the United State Environmental Protection Agency that set stricter limits for heavy metal discharges from industries. The limits are usually associated with a total discharge from the industry. Furthermore, with the growing realization of the toxicity of heavy metals, fueled by some infamous accounts of poisoning such as Minamata and Itai Itai incidents, worldwide legislation is becoming stricter. Clearly, industries which use or produce metals will be obligated to examine their processes for all possible sources of emission more closely and meet the stringent effluent discharge standards.

2.3 Metal removal technologies from wastewater

Because of the strict limits, effluent or water contaminated with heavy metals must be treated. The degree of treatment may range from a main process stream for a seriously polluted industrial waste to a polishing process to remove the trace concentration which can remain after the main treatment. Thus, the type of process or combination of processes will depend on the heavy metals involved and ultimate concentration allowed. Many technologies are used for removal heavy metals such as chemical precipitation, electrolytic recovery, membrane separation, ion exchange, evaporation, biological treatment systems, use of activated carbon for adsorption and other physic-chemical treatment methods. Comparison of properties of treatment technologies for heavy metal removal is concluded in Table 2.3.

Table 2.3 Comparison of treatment technologies for heavy metal removal (Kaewsarn, 2000)

Properties	Technology					
	Adsorption	Biosorption	Precipitation	Ion Exchange	Membrane	Evaporation
Low concentration	OK	OK	No	OK	No	No
Effluent quality (mg/L)	<1	<1	2-5	<1	1-5	1-5
pH variation	OK	OK	No	OK	OK	OK
Selectivity	No	OK	No	OK	No	No
Versatility	OK	OK	No	OK	OK	No
Organic tolerance	OK	OK	OK	No	No	OK
Regeneration	OK	OK	No	OK	No	No
Cost	OK	OK	OK	No	No	No

2.4 Activated Carbon (AC)

Activated carbon, a microcrystalline, nongraphitic form of carbon, possesses a large capacity for adsorbing chemicals from gases or liquids. Activated carbons are characterized by a large specific surface area of 300-2,500 m^2/g, and large distribution of pore sizes. It has a very complex structure, with pore sizes ranging from microspores (<20 A˚ slit width) to macrospores (>500 A˚ slit width), and has a variety

of surface groups as listed in Table 2.4. Activated carbon is distinguished from elemental carbon by the removal of all non-carbon impurities and the oxidation of the carbon surface.

Table 2.4 Surface groups on activated carbon and their effect on adsorbability (Eckenfelder, 2000)

Groups	Adsorbability
Hydroxyl	Generally reduces adsorbability. Extent of decrease depends on structure of host molecule.
Amino	Effect similar to that of hydroxyl but somewhat greater. Many amino acids are not adsorbed to any appreciable extent.
Carbonyl	Effect varies according to host molecule. Glyoxylic acid more adsorbable than acetic but similar increase does not occur when introduced into higher fatty acids
Double bonds	Variable effects as with carbonyl.
Halogens	Variable effects.
Sulfonic	Usually decreases adsorbability.
Nitro	Often increases adsorbability.

AC is available in either powder (PAC) or granular forms (GAC). GAC is more convenient for use in conventional unit processes and regeneration equipment, whereas the powder form offers higher surface area and maximum rate for sorption of contaminants. AC has a fixed adsorption capacity for each type of metallic compound. Once this capacity is saturated, contaminants will no longer be adsorbed and the AC must be regenerated or replaced. Using a strong acid or base to remove metal particles and bring them back into the solution can reactivate the carbon.

Production of Activated carbon

Activated carbon is normally produced using two different processes where the raw materials could come from a variety of carbonaceous source materials, e.g. nutshells, wood, coal. The two processes include:

1. *Physical activation*: The carbon precursor is developed into activated carbons using gases. This is generally done by using one or combining the following processes:

- Carbonization: Material with carbon content is pyrolyzed at temperature in the range 600-900°C, in absence or air (usually in inert atmosphere with gases like argon)

- Activation: Raw material or carbonized material is exposed to oxidized atmospheres (carbon dioxide, oxygen, or steam) at temperature above 250°C, usually in the temperature range of 600-1200°C.

2. *Chemical activation*: Impregnation with chemical such as acids like phosphoric acid or bases like potassium hydroxide or salts like zinc chloride, followed by carbonization at temperature in the range of 450-900°C, It is believed that carbonization and activation step proceeds simultaneously in chemical activation. This technique can be problematic in some cases because, for example, zinc trace residues may remain in the end product. However, chemical activation is preferred over physical activation owing to the lower temperature and shorter time needed for activating material.

2.5 Adsorption theory

Adsorption onto solid adsorbent has great environmental significance, since it can effectively remove pollutants from both aqueous streams. Due to the high degree of purification that can be achieved, this process is often used at the end of a treatment sequence.

2.5.1 Fundamental

Adsorption is mass transfer process that can generally be defined as the accumulation of materials at the interface between two phases. These phases can be any of the following combination: liquid-liquid, liquid-solid, gas-liquid and gas-solid. In the adsorption process, molecules, as shown in Figure 2.1, or atom or ions in a gas or liquid diffuse to the surface of a solid, where they bond with the solid surface or are held there by weak intermolecular forces. The adsorbed solutes are referred to as *adsorbate,* whereas the solid material is the *adsorbent.* Adsorption processes in microporosity are the most difficult to describe accurately. The adsorption processes

occurring within mesopores are more easily understood. Macroporosity accounts for < 1% of the adsorption processes within microporous carbon.

For the adsorption of a solute onto the porous surface of an adsorbent, there are essentially four stages in the adsorption process as shown in Figure 2.1 and they are described below:

(1) Transport of molecules from the bulk of solution to the exterior surface of the adsorbent;

(2) Movement of molecules across the interface and adsorption onto external surface sites;

(3) Migration of molecules within the pores of the adsorbent, and

(4) Interaction of molecules with the available sites on the interior surfaces, bounding the pore and capillary spaces of the adsorbent.
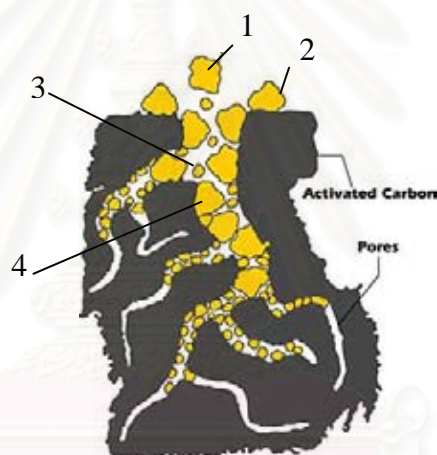
Figure 2.1 Adsorption with solid-particle adsorbent

Thermodynamic system of the adsorption is simply that various compounds strive for equilibrium. The process of adsorption occurs in both steady-state and unsteady-state conditions. The primary force driving the interaction between the adsorbate and the adsorbent is the electrostatic attraction and repulsion between molecules of the adsorbate and the adsorbent. These driving forces can be either physical or chemical. In discussing the fundamentals of adsorption, it is useful to distinguish between physical and chemical adsorption. Table 2.5 shows some differences between physical and chemical adsorptions.

Table 2.5 Distinctions between physical and chemical adsorptions

Physical adsorption	Chemical adsorption
- Dipole-dipole interactions dispersing interactions, and hydrogen bonding	- Formation of chemical bonds
- Rapid and Reversible interaction	- Slow and irreversible interaction
- Monolayer or multilayer	- Monolayer only
- Low heat of adsorption, 40 Btu per lbmole of the adsorbate (<2 or 3 times latent heat of evaporation)	- High heat of adsorption, 80 to 400 Btu per lbmole of the adsorbate (>2 or 3 times latent heat of evaporation)
- Non specific site	- Highly specific site
- No electron transfer although polarization of adsorbate may occur	- Electron transfer leading to bond formation between adsorbate and surface
- No dissociation of adsorbed species	- May involve dissociation
- Only significant at relatively low temperatures	- Possible over a wide range of temperatures

2.5.2 Adsorption kinetics

Quantifying the changes in sorption with time requires that an appropriate kinetic model is used. Lagergren's kinetics equation (Lagergren, 1898) has been most widely used to describe the solute adsorption on various adsorbents. The first-order Lagergren expression based on the solid capacity is

$$\frac{dq}{dt} = k_1(q_e - q) \tag{2.1}$$

where q_e and q are the amount of adsorbed adsorbate on the adsorbent at the equilibrium and at time t, respectively (mmolg^{-1}), and k_1 is the rate constant of first-order adsorption (min^{-1}). After integrating and applying boundary condition, $t=0$-$t=t$ and $q=0$-$q=q$; the integrated form of Eq. (2.1) becomes

$$\log(q_e - q) = \log q_e - \frac{k_1}{2.303}t \tag{2.2}$$

A pseudo second-order rate expression based on sorption equilibrium capacity was derived by Ho and McKay (1999). The sorption capacity is assumed to be proportional to the number of active sites occupied on the adsorbent, or

$$\frac{dq}{dt} = k_1(q_e - q)^2 \tag{2.3}$$

where k_2 are the second-order rate constant with a unit of g mmol^{-1}min^{-1}. After integrating and applying boundary condition, $t=0$-$t=t$ and $q=0$-$q=q$; Eq. (2.3) becomes

$$\frac{1}{q_e - q} = \frac{1}{q_e} + k_2 t \tag{2.4}$$

Eq. (2.4) can be rearranged to the linear form as follows:

$$\frac{t}{q} = \frac{1}{k_2 q_e^2} + \frac{1}{q_e} t \tag{2.5}$$

2.5.3 Adsorption isotherms

Adsorption in a solid-liquid system result in the removal of solute from solution and their concentration at the surface of the solid, to such time as the concentration of the solute remaining in solution is in a dynamic equilibrium with that at the surface. At this position of equilibrium, there is a defined distribution of solute between the liquid and solid phases. This distribution express the quantity q_e as a function of C at fixed temperature, the quantity q_e being the amount of solute adsorbed per unit weight of solid adsorbent, and C the concentration of solute remaining in solution at equilibrium. An expression of this type is termed an *adsorption isotherm*. Commonly, the amount of adsorbed material per unit weight of adsorbent increases with increasing concentration, but not in direct proportion.

Several types of isothermal adsorption relations may occur. The most common relationship between q_e and C obtains for systems in which adsorption from solution leads to the deposition of an apparent single layer of solute molecule on the surface of solid. Occasionally, multimolecular layers of solute may take place, and therefore an appropriate isotherm relation must be selected to explain such phenomena. Two of the most commonly used isotherm models are described below.

Single component adsorption

Langmuir isotherm

The Langmuir adsorption model is based on the assumptions that maximum adsorption corresponds to a saturated monolayer of solute molecules on the adsorbent surface, that the energy of adsorption is constant, and that there is no transmigration of adsorbate in the plane of the surface. The Langmuir isotherm is

$$q_e = \frac{q_m bC}{1+bC} \tag{2.6}$$

where q_m is the maximum adsorption capacity (mg/g), b a constant related to bonding energy of adsorption

Graphically the Langmuir isotherm has the form in Figure 2.2
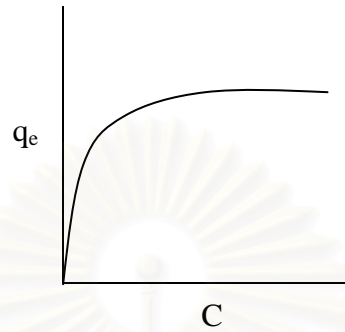
Figure 2.2 Langmuir adsorption pattern

Two convenient linear forms of the Langmuir isotherm are

$$\frac{C}{q_e} = \frac{1}{bq_m} + \frac{C}{q_m} \tag{2.7}$$

or

$$\frac{1}{q_e} = \frac{1}{q_m} + \left(\frac{1}{bq_m}\right)\left(\frac{1}{C}\right) \tag{2.8}$$

Freundlich isotherm

The Freundlich isotherm is a special case for heterogeneous surface adsorption where a multilayer adsorption could occur. The Freundlich isotherm is

$$q_e = K_F C^{1/n} \tag{2.9}$$

where K_F and n are constants, and $n > 1$. The Freundlich isotherm is usually fitted to the logarithmic form

$$\log q_e = \log K_F + \frac{1}{n}\log C \tag{2.10}$$

Eq. (2.10) gives a straight line with a slope of 1/n and intercept equal to the value of $\log K_F$. The intercept is roughly an indicator of adsorption capacity and the slope, 1/n, of adsorption intensity.

Binary components adsorption (Pavasant et al, 2003)

The binary components isotherm models based on Langmuir assumption can be derived using the same principle. In case of binary components adsorption, the adsorption reaction can be expressed by two chemical reaction equations

$$B + M_1 \xleftrightarrow{K_1} BM_1 \; ; \; K_1 = \frac{[BM_1]}{[B][M_1]} \tag{2.11}$$

$$B + M_2 \xleftrightarrow{K_2} BM_2 \; ; \; K_2 = \frac{[BM_2]}{[B][M_2]} \tag{2.12}$$
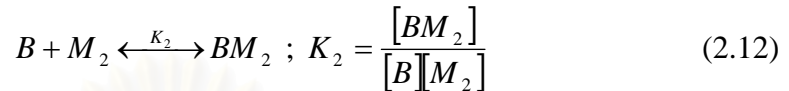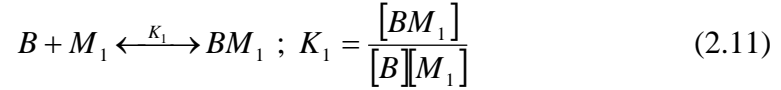
where B are the free binding sites, M_1 and M_2 the first and second adsorbate in the solution, BM_1 and BM_2 the adsorbent uptake for the first and second metals and K_1 and K_2 the equilibrium constants of reactions

The mass balance equation of binding site can be written as

$$[B_t] = [B] + [BM_1] + [BM_2] \tag{2.13}$$

Therefore, Eqs. (2.11) and (2.12) are

$$[BM_1] = \frac{K_1[B_t][M_1]}{1 + K_1[M_1] + K_2[M_2]} \tag{2.14}$$

$$[BM_2] = \frac{K_2[B_t][M_2]}{1 + K_1[M_1] + K_2[M_2]} \tag{2.15}$$

The expressions of Eqs. (2.14) and (2.15) in form of adsorption capacity are

$$q_1 = \frac{b_1 q_{m,1} C_{e,1}}{1 + b_1 C_{e,1} + b_2 C_{e,2}} \tag{2.16}$$

$$q_2 = \frac{b_2 q_{m,2} C_{e,2}}{1 + b_1 C_{e,1} + b_2 C_{e,2}} \tag{2.17}$$

where $q_{m,1}$ and $q_{m,2}$ are the maximum adsorption capacities for components 1 and 2, b_1 and b_2 the affinity constants of Langmuir model for components 1 and 2, $C_{e,1}$ and $C_{e,2}$ the equilibrium concentrations for components 1 and 2, and q_1 and q_2 are the adsorption capacities for components 1 and 2.

2.6 Desorption

Desorption is necessary as a means to recover the spent adsorbents, particularly those expensive, high efficiency types. The desorption side of the process should:

- yield the metals in a concentrated form;
- restore the adsorbent to close to the original condition for effective reuse with:
  - undiminished metals uptake;
  - no physical change or damage.

The desorption or regeneration can be accomplished by washing the adsorbent with an appropriate solution. The type, strength and quantity of the desorbing solution must be determined and optimized. Screening for the most effective regenerating solution is imperative, and most often, cationic species are generally released by a simple mild acidic wash.

Due to different affinities of metal ions for the predominant sorption site there will be a certain degree of metal selectivity by the adsorbent on the uptake. Similarly, selectivity may be achieved upon the elution-desorption operation. It should be born in mind that this selectivity on the desorption side of the operation may serve as another means of separating metals from one another if desirable.

One of the primary factors often used to indicate the operation of the system is the solid to liquid or S/L ratio, where S represents the amount of adsorbent (loaded with metal), and L is the volume of desorbing agent.

2.6.1 Desorption kinetics

The pseudo first order expression:

$$-\frac{dq}{dt} = k_{d,1}(q - q_e) \tag{2.18}$$

where q_e and q are the amount of adsorbate on the adsorbent at the equilibrium and at time t, respectively (mmolg^{-1}), and $k_{d,1}$ is the rate constant of first-order desorption (min^{-1}). After integrating and applying boundary condition, $t=0$ - $t=t$ and $q=q_0$ - $q=q$; Eq. (2.18) becomes

$$\log(q - q_e) = \log(q_0 - q_e) - k_{d,1}t \tag{2.19}$$

The pseudo second order expression:

$$-\frac{dq}{dt} = k_{d,2}(q - q_e)^2 \tag{2.20}$$

where $k_{d,2}$ are the second-order rate constant with a unit of g mmol^{-1} min^{-1}. After integrating and applying boundary condition, $t=0$ - $t=t$ and $q=q_0$ - $q=q$; Eq. (2.20) becomes

$$\frac{1}{(q - q_e)} - \frac{1}{(q_0 - q_e)} = k_{d,2}t \qquad\qquad (2.21)$$

2.7 Literature review

2.7.1 Adsorption of heavy metals

- Adsorption kinetics

From literature reviews on the kinetic models (Table 2.6), both first and second order models were found to be able to explain the sorption systems for the heavy metals. Generally, the first order kinetic model is suited for the system with high initial concentration whereas the second order is for the low initial concentration cases. It is apparent from this literature search that most adsorption systems of heavy metals followed the second order rather than the first order. This could be due to the fact that the investigation on the adsorption of heavy metals was only carried out in the low initial concentration range which corresponds to the actual range in the common wastewater treatment outlet. Therefore the sorption can take place quite rapidly leading to an appropriate use of the second order kinetic expression. In both cases, there was an increasing trend in rate constant value with an increase in initial concentration and temperature of the metal solution.

- Adsorption isotherm

Table 2.7 summarizes the literature review on the adsorption isotherms which shows that most heavy metal adsorption systems with activated carbon fitted well to Langmuir isotherm. Note that this literature was only selected from those which employed activated carbon for the adsorption of heavy metals. This indicates that the adsorption of heavy metals onto the activated carbon surface was mostly monolayer. There were certain cases where Freundlich isotherm could apply but among these cases, there was only one case where the parameter *1/n* was greater than one. This demonstrates that there were only few cases where a multilayer adsorption could take place for the heavy metal sorption onto activated carbon. From this table, it can be seen that activated carbon generally can uptake heavy metals in the range of a few milligram to a few hundred milligram per gram (of AC). Pb was often found to be taken at the highest content whereas the

capacity for Cu was usually quite low when compared with other heavy metals.

- Effect of pH for adsorption

The adsorption of metals was found to be strongly dependent on the pH of the solution. The appropriate pH for Cu and Pb are summarized in Table 2.8. Most literature demonstrated that adsorption of heavy metals were conducted at acidic condition. In fact, at low pH (< 3), there is excessive protonation of the active sites at carbon surface and this often refuses the formation of links between metal ion and the active site. At moderate pH values (3-6), linked H^+ is released from the active sites and adsorbed amount of metal ions is generally found to increase. At higher pH values (>6), the precipitation is dominant or both ion exchange and aqueous metal hydroxide formation (not necessarily precipitation) may become significant mechanisms in the metal removal process. This condition is often not desirable as the metal precipitation could lead to a misunderstanding for the adsorption capacity. And in practice, metal precipitation is generally not a stabilized form of heavy metal removal as the precipitation can some time be very small in size, and upon the neutralization of the effluent from the wastewater treatment plant, the solubility of the metals increases resulting in a re-contamination of the waste outlet stream.

Table 2.6 Literature reviews on the kinetic model of various adsorption systems

Adsorbent	Heavy metals	Initial concentration	Condition	Kinetic model	Rate Constant	Ref.
Sago waste	Cu(II), Pb(II)	50,100 mgL^{-1}	150±5 rpm, 25±5 ℃	Second order	-	Quek et al., 1998
Commercial AC	Mn(II), Fe(II), Ni(II), Cu(II)	200 ppm	140 rpm, 30 ℃	First order	k_1 = 0.017, 0.0209, 0.0308, 0.0395 h^{-1}	UZUN and GÜZEL, 2000
AC from waste walnut shell	Cu(II)	50, 100, 200, 300 mgL^{-1}	-	First order	k_1 = 0.016, 0.036, 0.060, 0.080 min^{-1}	Kim et al., 2001
Steam activated sulphurised carbon	Cd(II)	50, 100, 150, 250, 400 mgL^{-1}	200 rpm, 30℃	Second order	k_2 = 7.88×10^{-3}, 4.74×10^{-3}, 3.40×10^{-3}, 2.33×10^{-3}, 1.64×10^{-3} g mg^{-1}min^{-1}	Krishnan and Anirudhan, 2003
Steam activated sulphurised carbon	Cd(II)	250 mgL^{-1}	200 rpm, 30, 40, 50, 60℃	Second order	k_2 = 2.33×10^{-3}, 2.8×10^{-3}, 3.58×10^{-3}, 4.46×10^{-3}, g mg^{-1}min^{-1}	Krishnan and Anirudhan, 2003
Sago waste activated with H$_2$SO$_4$ and (NH$_4$)$_2$S$_2$O$_8$	Hg(II)	20, 30, 40, 50 mgL^{-1}	170 rpm, 30±2 ℃	First order	k_1 = 2.37×10^{-2}, 1.83×10^{-2}, 2.38×10^{-2}, 2.23×10^{-2} min^{-1}	Kadirvalu et al., 2004
Unmodified carbon, HCl, H$_2$SO$_4$, H$_3$PO$_4$, CTAB modified carbon	Pb(II)	300 mgL^{-1}	160 rpm, 30℃	Second order	k_2 = 0.0085, 0.0052, 0.0060, 0.0062, 0.0087 g mg^{-1}min^{-1}	Nadeem et al., 2006

Table 2.7 Literature reviews on the adsorption isotherm of various adsorption systems

Adsorbent	Heavy metals	Variation	Condition	Isotherm	Ref.
Sago waste	Cu(II), Pb(II)	pH 2-6	150±5 rpm, 25±5°C, 24 h	Langmuir q_m = 12.42, 46.64 mg/g b = 0.069, 0.246 $(mg/L)^{-1}$	Quek et al., 1998
AC	Cu(II)	Initial conc. 100-300 mg/L	140 rpm, 30 °C	Freundlich K_F = 2.394 mg/g $1/n$ = 0.38	UZUN and GÜZEL, 2000
AC from waste walnut shell	Cu(II)	Initial conc. 50-300 mg/L	-	Freundlich K_F = 1.66 mg/g $1/n$ = 2.79	Kim et al., 2001
AC pretreated with 1 M citric acid	Cu(II)	pH 3-11	25°C, 48 h	Langmuir q_m = 14.92 mg/g b = 0.08 $(mg/L)^{-1}$	Chen et al., 2003
AC pretreated with CO_2	Ni(II)	Initial conc. 25-250 mg/L	20°C, 100 rpm	Langmuir q_m = 30.769 mg/g b = 0.025 $(mg/L)^{-1}$	Hasar,2003
AC pretreated with H_2SO_4	Ni(II)	Initial conc. 25-250 mg/L	20°C, 100 rpm	Langmuir q_m = 37.175 mg/g b = 0.091 $(mg/L)^{-1}$	Hasar,2003
Steam activated sulphurised carbon	Cd(II)	Initial conc. 50-1000 mg/L	30, 40, 50, 60°C, 200 rpm	Langmuir q_m = 149.93±5.44, 163.32±7.16, 172.81±4.17, 190.48±12.07 mg/g b = 0.161±0.015, 0.213±0.077, 0.317±0.028, 0.421±0.046, $(mg/L)^{-1}$	Krishnan and Anirudhan, 2003

Table 2.7 Literature reviews on the adsorption isotherm of various adsorption systems (cont.)

Adsorbent	Heavy metals	Variation	Condition	Isotherm	Ref.
AC pretreated with HNO$_3$	Cu(II)	Dosage 0.01-2.5 g	25ºC, 48 h	Langmuir q_m = 15.34 mg/g b = 0.23 (mg/L)$^{-1}$	Chen and Wang, 2004a
GAC	EDTA disodium salt + Cu(II), Pb(II)	Dosage	25ºC, 2 day	Langmuir q_m = 0.02, 0.07 mol/kg b = 2.39×10^4 (mol/m^3)$^{-1}$	Chen and Wu, 2004b
Rice husk ash	Pb(II), Hg(II)	Initial conc.	15ºC, 30 min	Langmuir q_m = 12.346, 9.32 mg/g b = 0.3250, 0.0115 (mg/L)$^{-1}$	Feng et al., 2004
Rice husk ash	Pb(II), Hg(II)	Initial conc.	30ºC, 30 min	Langmuir q_m = 12.61, 6.72 mg/g b = 0.163, 0.018 (mg/L)$^{-1}$	Feng et al., 2004
GAC pretreated with tannic acid	Cu(II), Fe(II), Cd(II), Zn(II), Mn(II)	Dosage 0.02-2.0 g	-	Langmuir q_m = 2.73, 2.8, 2.46, 1.8, 1.73 mg/g b = 4.76, 0.88, 1.67, 1.29, 0.72 (mg/L)$^{-1}$	Ücer et al., 2006

Table 2.8 Literature reviews on effect of pH on various adsorption systems

Adsorbent	Heavy metals	Studies range	Condition	Optimum pH	Ref.
Sago waste	Cu(II), Pb(II)	pH 2-6	150±5 rpm, 25±5°C, 24 h	5, 4.5	Quek et al., 1998
ACs pretreated with NaCl	Cu(II), Pb(II), Ni(II)	pH 2-10	20±1°C, 12 h	5	Faur-Brasquet et al., 2002
ACs pretreated with citric acid	Cu(II)	pH 3-11	25°C, 48 h	3-4	Chen et al., 2003
ACs pretreated with CO_2 and H_2SO_4	Ni(II)	pH 2-7	25°C, 48 h	5	Hasar, 2003
Hazelnut shell ACs	Cr(II)	pH1-8	30°C, 200 rpm	1	Kobya, 2004
ACs from apricot stone	Cu(II), Pb(II)	pH 1-6	200 rpm 25°C, 48 h,	3-4	Kobya et al., 2005
ACs pretreated with tannic acid	Cu(II)	pH 2-7	-	5.4	Ücer et al., 2006
CTAB modified carbon	Pb(II)	pH 1-10	30°C, 160 rpm	5.5	Nadeem et al., 2006

2.7.2 The desorption of heavy metals

The recovery of heavy metals is generally carried out using desorption unit where heavy metals are forced to dissolve into an external, immiscible liquid stream and therefore separated from the waste (which could be in solid or liquid forms).

Kakitani et al., 2006:

This work seemed to be the extension of the previous work mentioned above as it focused on the extraction of Cr-Cu-As from contaminated wood (chromium as CrO_3, 45-51%; copper as CuO, 17-21%; arsenic as As_2O_5, 30-38%). A two steps extraction by solvents was employed with different conditions as follows;

1. 1st Oxalic acid (1N, 75ºC, 1h) for extraction chromium and arsenic,
    2nd Sulfuric acid (1N, 75ºC, 1-3h) for extraction copper and remaining arsenic

2. 1st Oxalic acid (1N, 75ºC, 1h) for extraction chromium and arsenic ,
    2nd Phosphoric acid (1N, 75ºC, 1-3h) for extraction copper and remaining arsenic

3. 1st Citric acid (1N, 75ºC, 1h) for extraction copper and arsenic ,
    2nd Sulfuric acid (1N, 75ºC, 1-3h) for extraction chromium and remaining arsenic

4. 1st Citric acid (1N, 75ºC, 1h) for extraction copper and arsenic ,
    2nd Phosphoric acid (1N, 75ºC, 1-3h) for extraction chromium and remaining arsenic

5. 1st Citric acid (1N, 75ºC, 1h) for extraction copper and arsenic ,
    2nd H_2O_2/NaOH (3%/1%, 75ºC, 1-3h) for extraction chromium and remaining arsenic

6. 1st Oxalic acid (1N, 75ºC, 1h) for extraction chromium and arsenic ,
    2nd Ammonia water(10%, 75ºC, 1-3h) for extraction copper and remaining arsenic

7. 1st Citric acid (1N, 75ºC, 1h) for extraction chromium and arsenic ,
    2nd Sodium-oxalate solution (pH 11.2 and 3.2, 75ºC, 1-3h) for extraction copper and remaining arsenic

Conclusion

% removal of heavy metals from each method could be summarized as shown below:

1. 100% As, 91.6% Cu, 88.0% Cr

2. 98.0% As, 74.9% Cu, 77.1% Cr

3. 100% As, 87.7% Cu, 90.0% Cr

4. 100% As, 99.1% Cu, 95.7% Cr

5. 97.3% As, 85.7% Cu, 95.6% Cr

6. 100% As, 74.4% Cu, 93.3% Cr

7. 100% As, 61.4% Cu, 81.2% Cr

With regard to those two literatures mentioned above, researchers did not concentrate on the recovery a single of each metal. The obtained extracted solution could be reused within the process for the preservation of wood.

Park et al., 2006:

This work focused on the leaching of Cu-Ni-Co from artificial matte composed of 24.95%Cu, 35.05%Ni, 4.05%Co, 11.45%Fe, 24.5%S. Matte was a mixture of molten metallic sulfides and produced from Pacific Ocean nodules. The leaching process employed $FeCl_3$ and HCl as leaching reagents where the extraction was done at 300 rpm of shaking rate. Ranges of concentration and temperature examined in this work were:

$FeCl_3$ conc. 0.5- 2.0 M

HCl conc. 0.1- 0.5 M

temp. 30-90°C

Conclusion

- The extraction of all metals increased with an increase in $FeCl_3$ conc. where 0.1 M $FeCl_3$ was sufficient for extraction.

- The extraction of all metals increased with an increase in temperature.

- Optimum condition for removal of 99.5% Cu, 93.2% Ni, 85.2% Co was 1.5M $FeCl_3$, 0.3 MHCl, 90°C and 7 h

Again, researchers did not concentrate on the separation of each metal because ferric chloride unselectively leached metals. Iron in resulting solution could be rejected as precipitate and other metals in the resulting solution without iron could be recovered using ion exchange resin.

.

Table 2.9 Literature reviews on type of desorbing agent and desorbing agent concentration for desorption

desorbing agent	Heavy metal	q_e	desorbing agent concentration	Desorption Efficiency (%)	Authors
EDTA, Citric acid, Oxalic acid, Malic acid	Cu(II)	-	2.59, 0.09, 0.05, 0.05 mgL^{-1}	8.4, 52.7, 46.4, 42.9	Wu et al., 2003
	Pb(II)	-	3.82, 0.98, 0.38, 1.19 mgL^{-1}	5.8, 95.9, 82.0, 43.0	
	Zn(II)	-	14.0, 3.0, 2.8, 12.8 mgL^{-1}	5.8, 95.9, 82.0, 43.0	
	Cd(II)	-	0.67, 0.25, 0.08, 0.91 mgL^{-1}	12.0, 36.9, 43.4, 46.5	
NTA	Pb(II)	2.14 mmolg^{-1}	0.001, 0.005, 0.01, 0.05, 0.01 M	43, 68, 77, 75, 76	Jeon et al., 2005
EDTA	Cu(II)	-	1 mM	100	Hammaini et al., 2006

From the literature reviews on desorption of heavy metals, citric, acids can be used to desorbed copper. There was an increasing trend in %removal of metal when increasing in desorbing agent concentration and temperature in shaking process

CHAPTER III

MATERIALS & METHODS

3.1 Materials

3.1.1 Equipments

- Analytical balance 2 digit (Sartorius, BP 3100S)
- Muffle furnace (Cabolite, England,AAF 11/18/20)
- Oven, WTB Binder, FD 115(E2)
- X-ray diffraction spectroscopy (SIEMENS XRD D5000)
- Scanning electro microscope (SEM)
- Fourier transform infrared spectrometer (FT-IR), Perkin Elmer, Model 1760X
- Flame & graphite furnace atomic adsorption spectrophotometer (AAS) (ZEEnit 700)
- Inductively couple plasma (ICP), Vista
- Rotary shaker
- pH-meter, Hanna, HI 98240
- Spectrophotometer, Spectronic® UV/VIS Helios Alpha spectrophotometer with Vision32 software –v1.25
- Micropipette 1, 5 mL
- Fraction collector, Amersham Biosciences FRAC-100,325
- Filter paper GF/C, Toyo
- Vacuum pump, KNF Neuberger, NO35AN. 18-IP20
- Filter Paper (Whatman No. 42 and 93)
- Conical tube
- Magnetic stirrer, Clifton UK, MSU-3
- Magnetic bar
- Desiccators
- Water purification system (For making DI water), ELGA, Ultaanalytic
- Refrigerator

3.1.2 Glassware

- Erlenmeyer flasks
- Volumetric flasks
- Filtering flasks
- Bushner Flasks
- Beakers
- Pipettes
- Cylinders
- Dropper
- Funnels
- Burette

3.1.3 Chemicals

- Deionized water (DI water)
- Phosphoric acid (85% by weight)
- Hydrochloric acid
- Citric acid
- Sodum thiosulfate
- Iodine solution
- Potassium iodate solution
- Starch solution
- potassium dihydrogen phosphate (KH_2PO_4)
- disodium hydrogen phosphate (Na_2HPO_4)
- Methylene blue
- Analytical grade $Cu(NO_3)_2 * 2.5\ H_2O$
- Analytical grade $Pb(NO_3)_2$
- Ammonium acetate
- Acetic acid
- Nitric acid (HNO_3)
- Sodium hydroxide (NaOH)
- pH buffer solution 4.00 ± 0.02, Scharlau chemie
- pH buffer solution 7.00 ± 0.02, HACH

- Mix metal standard solution for ICP, MERCK

3.2 Methods

3.2.1 Eucalyptus bark collection

Eucalyptus camaldulensis Dehn was collected from the pulping process in commercial plantation area in Prachinburi province, Thailand.

3.2.2 Activated carbon preparation

1. Wash eucalyptus bark with tab water
2. Dry in an oven at 105°C for 4 h
3. Crush and sieve through the mesh number 10 (approx. 2 mm).
4. Impregnate into phosphoric acid (85% by weight) by using the weight ratio of raw material and phosphoric acid at 1:1
5. Stir thoroughly until well mixed at room temperature
6. Carbonize in a muffle furnace at 500 $^\circ$C for 1 h
7. Wash the product with hot distilled water until the pH of the leachate is 6
8. Dry in an oven at 105°C for 4 h
9. Crush and sieve in the size ranged between mesh number 325 (0.045 mm) and 100 (0.150 mm)
10. Store in a desiccators

3.2.3 Activated carbon characteristics

- The surface morphology of activated carbon was visualized via scanning electron microscopy (SEM), the corresponding SEM micrographs being obtained using a scanning electron microscope (XL 30 ESEM FEG).

- Surface areas were calculated from adsorption isotherms using the method of Brunauer, Emmet and Teller (BET method). The BET surface area was determined by nitrogen adsorption (- 196°C) on surface area analyzer (Thermo Finnigan, Sorptomatic 1990).

- The ash content of the carbon was determined using a standard method according to ASTM D 2866-94. This method involved pre-drying the sample at 150°C, followed by burning in a muffle furnace at 650°C for 4 h in the presence of air.

The ash content was calculated from the combustion residue. This test was repeated until constant ash content was obtained.

- Apparent (bulk) density of all samples was calculated as the ratio between weight and volume of packed dry material.

- The yield of activated carbon was defined as the ratio of the weight of the activated carbon to product that of the original eucalyptus bark, both weights on a dry basis, i.e.

$$\text{Yield} \quad = \quad \frac{W_1}{W_0} \times 100 \quad\quad\quad (3.1)$$

where W_0 is the original mass of the precursor on a dry basis and W_1 is the mass of the carbon after activation, washing, and drying.

- The ultimate analysis of eucalyptus bark was performed in CHNS/O analyzer (Perkin Elmer PE2400 Series II), using gaseous products freed by pyrolysis in high-purity oxygen, and chromatographic was detected with a thermal conductivity detector and the proximate analysis was developed following ASTM standards for chemical analysis of wood charcoal (ASTM D 1762-84).

- Iodine number was determined according to the standard method, ASTM Designation: 4607-94. Details follow in Section 3.3.1.

- Methylene blue number was determined according to the standard method, JIS K 1470-1991. Details follow Section 3.3.2.

3.2.4 Preparation of synthetic wastewater by using buffer solution

1. Pipet the desired volume of acitic acid and weigh the desired weight of ammonium acetate and metal nitrate
2. Transfer into volumetric flask 2 L
3. Add deionized water until level of solution reach to the mark
4. Stock in polyethylene bottles

3.2.5 Adsorption studies

- **Effect of pH for adsorption**
    1. Weigh 0.1 g of activated carbon
    2. Place into a conical tube
    3. Add 25 mL solution with copper nitrate solution (pH 1)

4. Mix the solution with a rotary shaker with stirring rate 200 rpm at room temperature

5. Separate activated carbon from solution (at 30 min)

6. Triplicate the experiments

7. Analyze for the metal ions by Flame & Graphite Furnace Atomic Adsorption Spectrophotometer (AAS)

8. Repeat Steps 1-7 with lead nitrate solution and change pH of solution to 2, 3, 4, 5 and 6

- **Determination of adsorption kinetics and adsorption isotherm of single component**

   1. Weigh 0.1 g of activated carbon

   2. Place the carbon into a conical tube

   3. Add 25 mL solution of copper nitrate 0.1 mM

   4. Mix the solution with a rotary shaker at 200 rpm, room temperature

   5. Separate activated carbon from solution of specified tube (at pre-determined intervals of time)

   6. Triplicate the experiments

   7. Analyze for the metal ions by Flame & Graphite Furnace Atomic Adsorption Spectrophotometer (AAS)

   8. Repeat Steps 1-7 with 0.2, 0.3, 0.4, 0.5, 1, 2.5, 5, 10 mM of copper nitrate solution and 0.1, 0.2, 0.3, 0.4, 0.5, 1, 2.5, 5, 10 mM of lead nitrate solution

- **Determination of adsorption kinetics and adsorption isotherms of binary component**

   1. Weigh 0.1 g of activated carbon

   2. Place the carbon into a conical tube

   3. Add 25 mL solution of copper – lead nitrate 0.2 mM (equimolar concentration)

   4. Mix the solution with a rotary shaker at 200 rpm, room temperature

   5. Separate activated carbon from solution of specified tube (at pre-determined intervals of time)

   6. Triplicate the experiments

7. Analyze for the metal ions by Flame & Graphite Furnace Atomic Adsorption Spectrophotometer (AAS)

8. Repeat Steps 1-7 with 0.4, 0.6, 2.5, 5, 10 mM

3.2.6 Desorption studies

- **Effect of *(S/L ratio)* and desorbing agent concentration for desorption**

1. Add 25 mL of citric acid solution (0.005 M) into a conical tube

2. Add 0.025 g of heavy metal loaded activated carbon

3. Mix the solution in a rotary shaker at 200 rpm at room temperature for 24 h

4. Separate activated carbon from solution

5. Triplicate the experiments

6. Analyze for the metal ions by Flame & Graphite Furnace Atomic Adsorption Spectrophotometer (AAS)

7. Repeat Steps 1-7 with 0.1, 0.2, 0.3, 0.4 g of heavy metal loaded activated carbon and 0.005, 0.01, 0.05, 0.1, 1 M of Citric solution

- **Determination of desorption kinetics**

1. Add 25 mL of citric acid solution (0.01 M) into a conical tube

2. Add 0.4 g of heavy metal loaded activated carbon

3. Mix the solution in a shaker water bath with a stirring rate of 200 rpm at room temperature for 24 h

4. Separate activated carbon from solution of specified tube (at pre-determined intervals of time)

5. Triplicate the experiments

6. Analyze for the metal ions by Flame & Graphite Furnace Atomic Adsorption Spectrophotometer (AAS)

7. Repeat Steps 1-7 with operating temperature of 50 and 75 °C

3.3 Analytical methods and calculations

3.3.1 Determination of iodine number (ASTM D4607)

Procedure

1. Crush and sieve the activated carbon in the size ranged between mesh number 325 (0.045 mm) and 100 (0.150 mm)

2. Dry in an oven at 105°C for 4 h and cool to room temperature

3. Determine of iodine number requires an estimation of three carbon dosages

4. Weigh three appropriate amounts of activated carbon

5. Transfer to 250 ml Erlenmeyer flask equipped with a ground glass stopper

6. Pipet 10.0 mL of 5 wt % hydrochloric acid solution into each flask containing carbon

7. Stopper each flask and swirl gently until the carbon is completely wetted

8. Loose the stoppers to vent the flasks

9. Place on a hot plate in a fume hood

10. Boil gently for 30 ± 2 s

11. Remove the flasks from the hot plate and cool to room temperature

12. Pipet 100.0 mL of 0.100 N iodine solutions into each flask

13. Stopper the flasks, and shake vigorously for 30 ± 1 s

14. Filter each mixture through filter paper (Whatman No. 42) into a beaker

15. Pipet 50 mL of each filtrate into a clean 250 mL Erlenmeyer flask

16. Titrate each with standardized 0.100 N sodium thiosulfate solutions until the solution is a pale yellow

17. Add 2 mL of the starch indicator solution

18. Continue the filtration with sodium thiosulfate until one drop produces a colorless solution

19. Record the volume of sodium thiosulfate used

Calculation of iodine number (X/M) (mg g^{-1})

$$X/M = \frac{[A-(DF)(B)(S)]}{M} \qquad (3.2)$$

where S is sodium thiosulfate volume (mL), M the weight of carbon (g).

To calculate the value of X/M, first device the following value:

$$A = (N_2)(12693.0) \qquad (3.3)$$

where N_2 is iodine concentration (N).

$$B = (N_1)(126.93) \tag{3.4}$$

where N_1 is sodium thiosulfate concentration (N).

$$DF = \frac{[I+H]}{F} \tag{3.5}$$

where DF is dilution factor, I iodine volume (mL), H hydrochloric acid volume (mL) and F filtrate volume (mL).

- *Calculation of carbon dosage (M) (g)* for calculation iodine number, Eq. 3.2

$$M = \frac{[A-(DF)(C)(126.93)(50)]}{E} \tag{3.6}$$

where C is residual filtrate (N) and E estimated iodine number of the carbon.

for approximation carbon dosage (M) may be use Table 3.1.

Table 3.1 Approximation carbon dosage (M)

	M				M		
E	C=0.01	C=0.02	C=0.03	E	C=0.01	C=0.02	C=0.03
300	3.766	3.300	2,835	1550	0.729	0.639	0.549
350	3.228	2.829	2.430	1600	0.706	0.619	0.531
400	2.824	2.475	2.126	1650	0.684	0.600	0.515
450	2.510	2.200	1.890	1700	0.664	0.582	0.500
500	2.259	1.980	1.701	1750	0.645	0.566	0.486
550	2.054	1.800	1.546	1800	0.628	0.550	0.472
600	1.883	1.650	1.417	1850	0.610	0.535	0.460
650	1.738	1.523	1.308	1900	0.594	0.521	0.447
700	1.614	1.414	1.215	1950	0.579	0.508	0.436
750	1.506	1.320	1.134	2000	0.565	0.495	0.425
800	1.412	1.237	1.063	2050	0.551	0.483	0.415
850	1.329	1.164	1.000	2100	0.538	0.471	00405
900	1.255	1.100	0.945	2150	0.525	0.460	0.396
950	1.189	1.042	0.895	2200	0.513	0.450	0.388
1000	1.130	0.990	0.850	2250	0.502	0.440	0.378
1050	1.076	0.943	0.810	2300	0.491	0.430	0.370
1100	1.027	0.900	0.773	2350	0.481	0.421	0.362

Table 3.1 Approximation carbon dosage (M) (cont.)

	M				M		
E	C=0.01	C=0.02	C=0.03	E	C=0.01	C=0.02	C=0.03
1150	0.982	0.861	0.739	2400	0.471	0.412	0.354
1200	0.941	0.792	0.680	2450	0.461	0.404	0.347
1250	0.904	0.792	0.680	2500	0.452	0.396	0.340
1300	0.869	0.761	0.654	2550	0.443	0.388	0.333
1350	0.837	0.733	0.630	2600	0.434	0.381	0.327
1400	0.807	0.707	0.607	2650	0.426	0.374	0.321
1450	0.799	0.683	0.586	2700	0.418	0.367	0.315
1500	0.753	0.666	0.567	2750	0.411	0.360	0.309

- *Calculation of residual filtrate (C) (N)* for calculation iodine number, Eq. 3.2

$$C = \frac{(N_1 \cdot S)}{F} \qquad (3.7)$$

Using logarithmic paper, plot *X/M* versus *C* for each of the three carbon dosages. Calculate the least squares fit for the three points and plot. The iodine number is the *X/M* value at a residual iodine concentration (*C*) of 0.02 N. The regression coefficient for the least squares fit should be greater than 0.995.

3.3.2 Determination of methylene blue number

Preparation of solutions2

- *Potassium dihydrogen phosphate solution*
    1. Dry of potassium dihydrogen phosphate (KH_2PO_4) in the oven at 110-120 °C for 2 h
    2. Cool to room temperature in a desiccator
    3. Dissolve 9.07 g of KH_2PO_4 with distilled water
    4. Transfer to a 1 L volumetric flask and fill to the mark with distilled water

- *Disodium hydrogen phosphate solution*
    1. Dry of disodium hydrogen phosphate (Na_2HPO_4) in the oven at 110-120 °C for 2 h
    2. Cool to room temperature in a desiccator

3. Dissolve 23.88 g of dry Na_2HPO_4 with distilled water

4. Transfer to a 1 L volumetric flask and fill to the mark with distilled water.

- *Buffer solution*

Mix 400 mL of Potassium dihydrogen phosphate solution and 600 mL of Disodium hydrogen phosphate solution

- *Standard methylene blue solution*

1. Dry of methylene blue in the oven at 105 ± 5 °C For 4 h

2. Cool to room temperature in a desicator

3. Dissolve 1.2 g of dry methylene blue with buffer solution

4. Transfer to a 1L volumetric flask and fill to the mark with buffer solution.

Procedure

1. Add 0.05 g of activated carbon to 25 mL of a solution of methylene blue (1,200 mg/L).

2. Stir for 30 min at room temperature

3. Remove activated carbon by centrifuge at 10,000 rpm for 30 min.

4. Determine the dye concentration using light absorbance at 665 nm (UV-vis spectrophotometer, JIS K 1470-1991).

Calculation of methylene blue

- *Preparation of calibration curve*

1. Take methylene blue solution 10 mL into 50 mL one mark volumetric flask, and add buffer solution up to the marked line. From this solution, take 5, 10, 25 and 50 mL into 500 mL one mark volumetric flasks, and add buffer solution up to the marked line.

2. For these solutions, prepare the relation curve between the concentration of methylene blue solution (0.24 to 2.4 mg L^{-1}) and the absorbance at 665 nm in wavelength and obtain from this the remaining concentration of methylene blue.

Plot the remaining concentration of methylene blue solution on the abscissa and the adsorption amount of methylene blue obtained using the calculation method (Eq. 3.9) on the ordinate of both logarithm graph and prepare the adsorption isotherm. Adsorption isotherm obtain the methylene

blue amount (mg/g) of sample when the remaining concentration of methylene blue as the methylene blue adsorption performance is 0.24 mg/L.

Using the remaining concentration of methylene blue, the methylene blue amount (mg/g) shall be calculated using the following formula.

$$Q = \frac{(1200 - C)(25/1000)}{S} \qquad (3.8)$$

where Q is the amount of methylene blue being adsorbed per gram of adsorbent (mgg^{-1}), C the remaining concentration of methylene blue (mg L^{-1}), S the mass of activated carbon (g) and 1200 is the initial concentration of methylene blue solution (mgL^{-1}).

3.3.3 Determination of the adsorption capacity (Volesky, 1990)

The sorption capacity was calculated from Eq. (3.9)

$$q = \frac{V(C_i - C_e)}{1000W} \qquad (3.9)$$

where q is adsorption capacity (mmol g^{-1}), C_i the initial metal concentration (mmol L^{-1}), C_e the concentration of metal at equilibrium (mmol L^{-1}), W the adsorbent dosage (g) and V the solution volume (L).

3.3.4 Determination of the (S/L) ratio (Volesky, 1990)

$$(S/L) \; ratio = \frac{Amount \; of \; adsorbent \; (loaded \; with \; metals) \; (g)}{Volume \; of \; desorbing \; agent(L)} \qquad (3.10)$$

3.3.5 Determination of desorption efficiency (Volesky, 1990)

$$Desorption \; efficiency = \frac{Amount \; of \; released \; metal \; ion}{Amount \; of \; metal \; ion \; on \; AC} \times 100\% \qquad (3.11)$$

3.3.6 Determination of desorption ratio

$$Desorption \; ratio = \frac{Concentration \; of \; interested \; metals}{Overall \; concentration} \qquad (3.12)$$

CHAPTER IV

RESULTS AND DISCUSSION

4.1 Characteristics of eucalyptus bark raw material and activated carbon product

Table 4.1 shows the proximate and ultimate analysis of eucalyptus bark. It was shown that the bark contained relatively high carbon and low ash. Therefore this raw material was suitable for the synthesis of activated carbon. After the activated process, the morphology of the carbon changed and the external surface of activated carbon obtained from scanning electron micrographs (SEMs) was shown in Fig.4.1. This SEM image illustrates irregular structure with cracks and crevices on the surface of the activated carbon at 1000x magnification which confirmed amorphous and heterogeneous structures. Moreover, Table 4.1 shows the proximate and ultimate analysis of activated carbon obtained from this activation process. This demonstrated that the product contained a relatively higher fixed carbon and lower volatile matter than those in the raw material. This was because the volatile matters were removed during the activation process. However, the overall yield of the process which was calculated from the ratio between the weight of the product and the raw material was only 30% (see Table 4.2), and the weight loss was due to the gasification of such volatile and some of the carbon in the raw materials. This level of yield was considered moderate when compared with those prepared with other raw materials such as mangrove wood (38.07%) (Ninlanon, 1997), Eucalyptus camaldulensis Dehnh (33.14%) (Jindaphunphairoth, 2000), used tired (47.20%) (Isarasaenee, 1996), palm oil shell (19.66%) (Suravattanasakul, 1998).

Table 4.2 also summarizes other properties of the activated carbon obtained from the technique employed in this work. The BET result illustrated that the activated carbon product had a relatively high specific surface areas ($\sim$1,240 m^2g^{-1}) when compared with those prepared from other agricultural by-products such as peanut hull (208 m^2g^{-1}), coir pith (595 m^2g^{-1}), eichhornia (266 m^2g^{-1}), cassava peel (200 m^2g^{-1}), coconut tree sawdust carbon (325 m^2g^{-1}) and sago waste (625 m^2g^{-1}) (Kadirvalu et al., 2004). The difference could be due to the removal of different organic components and minerals presented in the different raw materials which could

react with phosphoric acid during the activation process (Chen et al., 2003). This led to a different formation of pore structure in the final activated carbon product. This reason could also explain the weight loss during activation process, as phosphoric acid reacted with char and volatile matters resulting in the gas products which diffused quickly out of the surface of particles and created pores (Patnukao and Pavasant, 2006).

The iodine and methylene blue numbers indicated the adsorption capacities of the activated carbon. The iodine number indicated the adsorption capacity of activated carbon in micropore (d < 20°A) (Jankowska et al., 1991) and the methylene blue number represent the adsorption capacity in mesopore (20°A < d < 500°A). Table 4.2 illustrates that the activated carbon product from this work had an iodine number of about 918 ± 7 mg g^{-1}. This was relative moderate when compared with those prepared from other activation processes. On the other hand, the activated carbon product had a relatively high methylene blue number which meant that the product had more micropore structure when compared with other activated carbon products of similar origin. Table 4.3 provides examples for the comparison between the iodine and methylene numbers obtained from the various activated products.

The inorganic composition of activated carbon determined by microwave digester was shown in Fig. 4.2. The results showed that the main compositions comprised alkaline and alkaline earth. These metals may be important for the adsorption of heavy metals in the case that ion exchange process prevailed.

4.2 Single component adsorption

4.2.1 Effect of pH for adsorption

The adsorption of metals was found to be strongly dependent on the pH of the solution. Fig. 4.3 demonstrates that the optimal pH for the adsorption of Cu(II) and Pb(II) (at 0.3 mmol L^{-1}) was about 5 which was rather acidic. At low pH (< 3), there was competitive of proton and metal ions for ion-exchange with releasing ions i.e. Na$^+$, Ca^{2+}, etc. by carbon into the solution. Hence, the formation of links between metal ion and the active site decreased. At moderate pH (3-6), increasing pH in metal solution saw a drop in proton density and this resulted in a decrease in the competition with the metal ions. Therefore an increase in the adsorption capacities was observed. At high pH (>6), however, the removal process could take place by metal-hydroxide precipitation, i.e. hydroxide ion from the solution could form complexes with Cu(II)

and Pb(II). Apiratikul (2003) studied the solubility of metal ion. It was shown that solubility dropped at high pH as shown in Table 4.4. This condition was often not desirable as the metal precipitation could lead to a misunderstanding for the adsorption capacity. In practice, metal precipitation was generally not a stabilized form of heavy metal as the precipitation could some time be very small in size, and upon the neutralization of the effluent from the wastewater treatment plant, the solubility of the metals increased resulting in a re-contamination of the waste outlet stream.

4.2.2 Single component adsorption

Adsorption kinetics

Batch experiments were carried out using Cu(II) and Pb(II) solutions at different initial metal concentrations (0.1-10 mmol L^{-1}). Fig. 4.4 shows the results on the adsorption kinetics of both metal ions. Kinetic curves were generally single, smooth and continuous, and the saturation was expected to occur which indicated a monolayer adsorption. All of metal ions were in contact with the surface layer of activated carbon and all adsorption processes were completed within 45 min. Cu(II) and Pb(II) adsorptions increased sharply during the initial stage and slowed down gradually when approaching equilibrium. This was due to the decrease in flux (concentration gradient) with time due to the transfer of solute onto solid phase (Dogan et al., 2006). The time required to reach equilibrium varied with the initial concentration. The metal solution with higher initial concentration required a slightly shorter time than the metal solution with a lower initial concentration. However, the slowest still did not take longer than 45 min.

The pseudo first-order and the pseudo second-order kinetic models were used to predict kinetic parameters for the adsorptions of Cu(II) and Pb(II). Table 4.5 demonstrates that adsorption kinetics fitted more favorably with the pseudo second-order than the pseudo first-order models (from R^2 results). Thus, the rate constant (k_2) and equilibrium adsorption capacities (q_e) were thereafter predicted by the pseudo second-order model. The results indicated that an increase in initial metal concentration increased the rate constant (k_2). This was because an increase in initial concentration enhanced the concentration gradient of metal ion concentration between aqueous and solid phases. As the external mass transfer rate depended significantly on

the concentration difference driving force, the transfer of adsorbate into adsorbent became more rapid and the rate of adsorption consequently increased.

Adsorption isotherm

Adsorption equilibrium is established when the concentration of metal ion in the bulk solution (C_e) was in dynamic with that of the interface (q_e). This level of equilibrium concentration depends significantly on the initial concentration of the metals and the isotherm results at 25°C are displayed in Fig. 4.5. As a general observation, Pb(II) exhibited a higher maximum adsorption capacity than Cu(II).

Langmuir and Freundlich isotherms as expressed in Eqs. 2.8 and 2.10 were selected to discuss experimental data. Table 4.6 reveals that experimental data fitted more favorably with Langmuir than Freundlich isotherms. This suggested that the adsorptions of Cu(II) and Pb(II) were potentially monolayer (Feng et al., 2004). A comparison between maximum adsorption capacities (q_m) between the two metal ions illustrated that Cu(II) and Pb(II) had maximum adsorption capacities of 0.45 and 0.53 mmol g^{-1}, respectively. In the next section (Section 4.2.3), the functional groups related to the adsorption is discussed and it was demonstrated that the activated carbon might have more functional group binding sites for Pb(II) than for Cu(II). Moreover, Pb(II) adsorption was found to have a higher *b* value indicating a stronger chemical and physical affinity than Cu(II).

4.2.3 Relationship between functional groups and heavy metals adsorption

The changes in functional groups after the adsorption were important in describing the mechanism of metal ions bound on the surface of activated carbon. FT-IR was used to analyze the functional groups of activated carbon. Fig. 4.6 (a) shows the FT-IR transmission spectrum for the original activated carbon whereas Figs. 4.6 (b) and (c) display the FT-IR transmission spectra for the spent activated carbon with Cu(II), Pb(II) and a mixture of both ions (Cu(II)-Pb(II)), respectively.

Initially, the original activated carbon constituted several functional groups such as carboxylic acid, amine and amide groups. After the adsorption, there seemed to be shifts (more than 10 cm^{-1}) in wave number of dominant peaks. These shifts indicated that there were binding processes taking places at specific functional groups on the surface of activated carbon (Pavasant et al., 2003). The carboxylic acid group

contained the following minor groups: O−H stretching, C=O stretching, C−O stretching and O−H bending. The O−H bending was observed to shift clearly at wave number 1417.04 cm^{-1} for both metals. Moreover, the O−H stretching and C−O stretching groups were observed to shift for both metal ions. There was a remarkable increase in the intensity of spectra for O−H stretching. This could be due to the use of acetic acid and ammonium acetate as buffer for adsorption. For C=O stretching group, there was a shift in the wave number from 1774.88 cm^{-1} of pure activated carbon to 1793.78 cm^{-1} of Cu(II) loaded activated carbon. Hence, the binding between C=O stretching group and Cu(II) was expected in the Cu(II) adsorption. Interestingly, this C=O stretching disappeared after the Pb(II) adsorption which could indicate a reaction between such functional group with Pb(II) during the adsorption.

For amine group, there were changes in wave number for N−H stretching in Cu(II) and Pb(II) adsorptions. The C−N stretching was found to be a clear peak at 1088.49 cm^{-1} for the sorption of Pb(II) adsorption while the Cu(II) adsorption did not seem to change the wave number of this group. The N−H bending group did not seem to change for both metal ion adsorptions. Therefore, N−H stretching and C−N stretching were involved in the Cu(II) and Pb(II) adsorptions, respectively, whereas N−H bending group should not have involved in adsorption of both metal ions.

The amide group contained two minor groups such as N−H stretching and C−O stretching. Only N-H stretching was found to have shift in wave number after the adsorption of both metals.

Summary of the changes in the wave numbers due to the adsorption of the heavy metals are given in Table 4.7 whereas the conclusion of possible function groups involved with the adsorption of the two metals are given in Table 4.8. In short, N−H stretching and C−N stretching of amine and amide groups seemed to be responsible for the adsorption of both metals. As a general observation, all functional groups responsible for Cu(II) adsorption was also available for Pb(II), but not vice versa. This could be the reason why the maximum adsorption capacity of Pb(II) was higher than that of Cu(II) as discussed in previous sections.

4.2.4 Mechanism for removal of heavy metals

Removal of heavy metals from wastewater could involve either adsorption or ion exchange, or both. To evaluate for the ion exchange mechanism of removal process,

the measurement of the released light metal ions that was the compositions of activated carbon (Fig. 4.2) was carried out. This was performed in a batch system with initial concentrations of Cu(II) and Pb(II) of 10 mmol L^{-1}. All metal ions in the solution before and after adsorption were analyzed by Inductively Couple Plasma (ICP). The plots of the various metal ion concentrations were shown in Fig. 4.7. In this figure, the difference between the two adjacent bars is the amount of metals adsorbed to or desorbed from the activated carbon. It can be seen that there were only marginal amounts of light metals being desorbed when compared with the amount adsorbed. The percentage of ion exchange in the removal process is then calculated from

$$\% \ ion \ exchange = \frac{\sum (C_{2,light} - C_{1,light})}{C_{1,heavy} - C_{2,heavy}} \times 100 \qquad (4.1)$$

where $C_{1,light}$ and $C_{2,light}$ is concentration of light metal ions before and after adsorption, respectively and $C_{1,heavy}$ and $C_{2,heavy}$ is the concentration of heavy metal ions before and after adsorption, respectively. The calculation revealed that the percentages of ion exchange for Cu(II) and Pb(II) were 1.05% and 10.4%, respectively. Therefore ion exchange should not be a major mechanism for the uptakes of both heavy metals and the actual mechanism should be adsorption. It should be noted that the uptake of Pb(II) was more contributed by ion exchange than Cu(II). It should be noted that ICP analysis was subject to some error of 2 %, therefore the difference in the % ion exchange could be due to the analytical error and not from the experiment itself. Therefore the results on %ion exchange for Cu(II) must be interpreted with extreme care.

4.3 Binary component adsorption

The binary components adsorption experiment was carried out in the same manner as a single component experiment. Binary components of Cu(II) and Pb(II) were studied in this work by using the mixture of equimolar concentration, e.g. binary components at 10 mmol L^{-1} was prepared from the mixture of Cu(II) at 5 mmol L^{-1} and Pb(II) at 5 mmol L^{-1}.

Adsorption kinetics

The concentrations of heavy metals used to study adsorption kinetics of binary components were 0.2, 0.4, 0.6, 5, 10 mmol L^{-1}. The binary component adsorption kinetic curves exhibited the same trend and characteristics as those for single component systems (Fig. 4.8). For instance, the adsorption processes were completed within 45 min where the rate constants of binary components adsorptions both Cu(II) and Pb(II) obtained from this work are summarized in Table 4.9. An increase in initial concentration of heavy metals resulted in increasing rate constants. Comparisons of the rate constants from the single and binary component adsorptions are shown in Table 4.10. The rate constants, k_2, for both metals varied with initial metal concentration for both single and binary component systems. The magnitude of the rate constant for the binary system was in the same order as the single component, but the values were slightly different. It was difficult to conclude on the effect of the presence of the secondary metal on the primary metal with this set of experimental data.

Adsorption isotherm

The range of concentration of heavy metals used to investigate adsorption kinetics of the binary component systems were from 0.625 to 10 mmol L^{-1}. Fig. 4.9 shows the adsorption isotherm of single and binary component adsorptions. In this figure, the labels: Cu/Cu-Pb and Pb/Cu-Pb: refer to the adsorption isotherms of Cu(II) and Pb(II) from binary components systems, whereas the labels: Cu and Pb, are for the adsorption isotherms of Cu(II) and Pb(II) from single component systems. Table 4.10 displays the equilibrium adsorption capacities of single and binary component adsorptions. It was shown that adsorption of Cu(II) in binary component adsorption had increasing trend of equilibrium adsorption capacities when increased initial concentration. As the initial concentration of Cu(II) reached 5 mmol L^{-1}, the adsorption capacity remained constant. For Pb(II) on the other hand, although there was increasing trend of equilibrium adsorption capacities in a similar manner with the adsorption of Cu(II), the adsorption capacity did not seem to reach the constant level with the range of concentration employed in this work.

It was also noticed that the adsorption capacities of both metals for the single and binary components were quite close at low initial concentration. For instance, q_e in Table 4.10 for the adsorption of Cu(II) at an initial concentration of 0.625 mmol L^{-1} was almost the same as that for the binary adsorption at an initial concentration of

1.25 mmol L^{-1} (Cu(II) = Pb(II) = 0.625 mmol L^{-1}). However, the adsorption capacity for the binary system seemed to be lowered than that of the single component at high initial concentration level. For Cu(II) in particular, the equilibrium sorption capacity in the binary system seemed to level off at 2.16×10^{-1} mmol g^{-1}. This could be because, at low concentration, there existed a large number of adsorption site compared with the amount of metal ion in the solution and therefore the level of competition between the two metals was not high. Therefore the adsorption capacities for both metals remained the same as those from single component systems. However, as the concentration became high, the competition for the adsorption site was more intense and this resulted in a decrease in the sorption capacity for both metals.

Langmuir isotherms as expressed in Eqs. 2.16 and 2.17 were selected to discuss experimental data to predict maximum adsorption capacities. The experimental data fitted more favorable with Langmuir than Freundlich isotherms for adsorption of heavy metals in binary system. The highest achievable adsorption capacities of Cu(II) and Pb(II) in binary components adsorption were 0.181 and 0.357 mmol g^{-1} in case of equimolar concentration, respectively. Section 4.2.3 indicated that Pb(II) could adsorb to a more variety of functional groups than Cu(II) and therefore the adsorption capacity for Pb(II) was slightly higher than that of Cu(II). The maximum adsorption capacities of Cu(II) and Pb(II) obtained from binary component adsorption were less than those obtained from the single component system where $q_{m,Cu}$=0.45 mmolg^{-1} and $q_{m,Pb}$=0.53 mmolg^{-1}. This could be due to the reason given above

The effect of ionic interaction on the binary component adsorption can be represented by the ratio of the adsorption capacity for one metal ion in the presence of the other metal ion (binary component system), q^{mix}, to the adsorption capacity for the same metal when it was presented alone in the solution (single component system), q^0, (Mohan et al., 2002). Three case scenarios could be formulated:

(i) $\dfrac{q^{mix}}{q^0} > 1$ the adsorption was promoted by the presence of other metal ions,

(ii) $\dfrac{q^{mix}}{q^0} = 1$ there was no observable net interaction, and

(iii) $\dfrac{q^{mix}}{q^0} < 1$ adsorption was suppressed by the presence of other metal ions.

Table 4.9 shows q^{mix}/q^0 from the binary components adsorption of Cu(II), all of which were less than unity. This indicated that Cu(II) adsorption was suppressed by Pb(II) adsorption. In the same manner, q^{mix}/q^0 of Pb(II) from binary component adsorption were less than unity. They could be indicated that Pb(II) adsorption was suppressed by Cu(II) adsorption.

4.4 Desorption

4.4.1 Effect of desorbing agent concentration and *(S/L) ratio* for desorption of single component system

The desorption of Cu(II) and Pb(II) from activated carbon was studied in this work. The metal loaded activated carbon from the adsorption experiment with 10 mmol L^{-1} of metal solution which gave the adsorption capacities of 0.45 and 0.53 mmol g^{-1} of Cu(II) and Pb(II), respectively. Desorbing agent concentration was an important factor for extraction. The desorbing agent used for the desorption was citric acid solution because it could form metal-citrate complex where proton replaced metal ions loaded on the activated carbon surface (Lee et al., 2005). This desorption mechanism can be explained as follows:

$$Cu^{2+} + 2HL \leftrightarrow CuL_2 + 2H^+ \tag{4.2}$$

$$Pb^{2+} + 2HL \leftrightarrow PbL_2 + 2H^+ \tag{4.3}$$

where HL represents the desorbing agent.

Fig. 4.10 illustrates the desorption efficiency calculated from Eq. 3.11 at various conditions. The parameter "C" referred to the desorbing agent concentration and the *S/L ratio* was defined as the ratio of the amount of adsorbent (loaded with metal) (mg) and volume of desorbing agent (mL). The results indicated that the desorption efficiency increased with desorbing agent concentration because an increase in desorbing agent concentration increased the density of ligands and proton for complexing with metal ions and replacing the adsorbed metals, respectively (Qin et al., 2004). At the desorbing agent concentration equal to 1 mol L^{-1}, the desorption efficiency approached 100%.

Fig. 4.10 also demonstrates that the optimal *S/L ratio* based on the highest desorption efficiency for each of the level of desorbing agent concentration (C) used in this experiment was 4. However, for the desorption operation, the optimal condition should be considered simultaneously from the desorbing agent

concentration and the *S/L ratio*. For this case, the optimal condition for desorption was at desorbing agent concentration equal to 1 mol L^{-1} and the *S/L ratio* of either 4 or 8 which provides almost 100% recovery of both metals. It is noted here that the desorbing agent concentration of 1 mol L^{-1} provided the best desorption efficiency. The experiment was not designed to look into detail of this parameter and it was possible that the desorbing agent concentration that gave appropriate level of desorption efficiency lied between 0.1 and 1 mol L^{-1}.

4.4.2 Effect of desorbing agent concentration and *S/L ratio* for desorption of binary component.

From the binary adsorption of Cu(II) and Pb(II) at equimolar concentration of 10 mmol L^{-1} (Cu(II) 5 mmol L^{-1} and Pb(II) 5 mmol L^{-1}), the amounts of Cu(II) and Pb(II) adsorbed onto one gram of activated carbon were 0.22 and 0.37 mmol, respectively. The purpose of this desorption work was to examine the possibility in using desorbing agent desorption in the recovery and separation of the two heavy metals from the activated carbon. In the previous section, the results on the desorption efficiency of the single component metal system were revealed. The separation of the two metals might be possible with the desorption conditions that provided rather different desorption efficiency for the two metals. An desorption ratio is then proposed as an indicator for this and is defined as the ratio between the amount of one species of metal released and the total amount of both species released from the activated carbon (Eq. 3.12). The last columns of Tables 4.11 and 4.12 illustrate the level of desorption ratio for Cu. Information from the single component desorption was used in the selection of conditions for the desorption and separation of Cu(II) and Pb(II) on the activated carbon. In this case, the desorbing agent at 0.01 mol L^{-1} and the *S/L ratio* at 8, 12 and 16 were preliminarily selected as these led to the highest Cu desorption ratio (high quantity of Cu(II) and low quantity of Pb(II) in desorbing agent) (Table 4.11). Fig. 4.11 shows the results on the binary desorption of Cu(II) and Pb(II) from the desorption at various *S/L ratio* whereas Table 4.12 illustrates that the best condition which gave the highest desorption ratio for Cu was the condition at desorbing agent concentration equal to 0.01 mol L^{-1} and *S/L ratio* equal to 16.

In the comparison of the desorption efficiency of Cu(II) with Pb(II), it was observed that the effectiveness of citric acid on the extract of Cu(II) was better than that of Pb(II). The reason for this could be described using the concept of the stability

of the metal-liqand system. This stability for a metal-ligand system is used to analyze complexation data at specific pH and ionic strength where a more stable solution exhibits a higher stability constant. Palma and Mecozzi, (2007) reported that the stability constant of citric acid with Cu(II) was higher than Pb(II) ($\log K_{Cu-CA}$ = 6.1, $\log K_{Pb-CA}$ = 4.1) and therefore Cu(II) had a higher potential in being extracted by citric acid than Pb(II). It could also be that the adsorption of Pb(II) was stronger than the adsorption of Cu(II) on the activated carbon and therefore the desorption could see a higher release of Cu(II) than that of Pb(II).

4.4.3 Desorption kinetics

In the desorption processes, heavy metals loaded on activated carbon are pushed back into the fresh desorbing agent. The concentration of heavy metals in the desorbing agent therefore increases with time, whereas the amount of heavy metals on the activated carbon decreases. This is exactly the reverse of the adsorption process where Figs. 4.12 - 4.13 display the desorption kinetics of Cu(II) and Pb(II) in the single and binary component systems, respectively. It was quite clear that the amount of loaded metal ions decreased with increasing reaction time for both Cu(II) and Pb(II) extractions. The equilibrium state was achieved in 150 min under the desorption conditions used in this work. This indicated that the desorption processes reached equilibrium much slower than the counterpart adsorption process. The kinetic parameters of the desorption were predicted by pseudo-second order because of high R-square value (Table 4.13).

Single component system

Desorption kinetics of Cu(II) and Pb(II) from loaded activated carbon was studied by using experiment condition at desorbing agent concentration equal to 1 mol L^{-1} and *(S/L) ratio* equal to 8 at 25 °C as this gave almost 100% recoveries (Fig.4.11). The rate constant of Cu(II) and Pb(II) desorptions were 18.63 and 63.18 g mmol^{-1} min^{-1}. The amount of metal ions at equilibrium state was 0.02×10^{-1} and 0.01×10^{-1} mmol g^{-1}.

The effect of desorption temperature was investigated by performing experiments with citric acid at different desorption temperatures: 25, 50, and 75 °C, and the results are presented in Table 4.13. An increase in the desorption temperature enhanced the desorption efficiency resulting in a lesser quantity of metal ion

remaining on the activated carbon. This increase in desorption efficiency could be due to thermodynamic equilibria where solubilities increased with temperature. In the case of the desorption of Pb(II), the amount of Pb(II) released from the activated carbon was not significantly affected by temperature. This meant that the adsorption of Cu(II) and Pb(II) on the activated carbon might be of different nature. Note that when deionized water was used as desorbing agent for extraction. Increasing desorption temperature from 25 to 75 °C caused the the desorption efficiency of Cu(II) and Pb(II) to increase from 3.52 and 0.28 to 7.66 and 2.88%, respectively. This suggested that the adsorption of metal ions on the activated carbon was of physical type.

Binary component system

Desorption kinetics of binary components of Cu(II) and Pb(II) loaded onto the activated carbon was studied using experiment conditions at desorbing agent concentration of 0.01 M and *S/L ratio* of 16 as this seemed to give the highest desorption ratio. Fig.4.12 displays the binary components desorption kinetics of Cu(II) and Pb(II) whilst Table 4.13 shows the rate constants of binary component desorption for both Cu(II) and Pb(II). The extractions of Cu(II) and Pb(II) with citric acid from the activated carbon exhibited a rather different character in the kinetic point of view. It was shown that the desorption of Cu(II) from the binary component system had higher rate constants than that of the single component desorption at the same desorption condition. The situation was opposite for Pb(II). Complex interaction between the presence of the secondary metal ion such as Pb(II) on the desorption of Cu(II) might be responsible for this finding, but the exact mechanism on this aspect could still not be concluded upon. One thing that could be summarized with confidence was that the desorption of Cu(II) had higher rate constants than desorption of Pb(II).

4.4.4 Iterative desorption

As one desorption process could not provide good desorption efficiency and ratio for both metal ions, the iterative desorption was carried out. Table 4.14 demonstrates the desorption efficiency obtained from each iterative desorption. For the single component and binary component iterative desorptions (Figs. 4.14-4.15), the second and third iterations gave lower desorption efficiency than the first as the remaining

metal ions in activated carbon decreased. In the third iteration of binary component desorption, it appeared that citric acid could no longer effectively separate the two metal ions. It was concluded at this point that the iterative desorption could enhance the desorption efficiency but not the desorption ratio.

Table 4.1 Proximate and ultimate analysis of eucalyptus bark and activated carbon

Parameter	Value (% by weight)	
	Eucalyptus bark	Activated carbon
Proximate		
Moisture content	10.50	7
Volatile matter	75.05	22.78
Fixed carbon	13.10	65.34
Ash content	1.35	4.88
Ultimate		
C	41.36	62
H	4.67	4
Others – N, O, S	53.97	34

Table 4.2 Characteristics of activated carbon

Parameter		Value
Yield	(%)	30
Apparent (bulk) density	(g cm^{-3})	0.251
BET specific surface area	(m^2 g^{-1})	1239.38
Pore specific volume	(cm^3 g^{-1})	1.572
Average pore diameter	(A°)	8.49
Pore size distribution		
- Micropore	(%)	88.5
- Mesopore	(%)	11.48
Iodine number	(mg g^{-1})	918$\pm$7
Methylene blue	(mg g^{-1})	427$\pm$2

Table 4.3 Comparison between properties of activated carbon from different origins

Authors	Raw material	Activation processes	Iodine number $(mg\ g^{-1})$	Methylene blue number $(mg\ g^{-1})$
This work	*camaldulensis Dehnh* wood	phosphoric acid	918 ± 7	427 ± 2
Arriagada et al., 1994	*Eucalyptus globulus* wood	steam	968	311
Castro et al., 2000	sugar cane bagasse	phosphoric acid	746	283
Jindaphunphairoth ,2000	*camaldulensis Dehnh* wood	steam	1,233	242
Girgis et al., 2002	Peanut hull	phosphoric acid	-	384.2

Table 4.4 The pH where a drop of solubility of Cu(II) and Pb(II) (Apiratikul, 2003)

Heavy metal	pH		
	K_{sp}*	MINEQL**	Experiment
Cu(II)	6	5.3	5.94
Pb(II)	7.5	5.8	7.02

* Ksp = estimates from solubility product values

** MINEQL = estimates from MINEQL program

Table 4.5 Kinetic parameters of pseudo first and second-order models for single component adsorptions of Cu(II) and Pb(II)

Heavy metals	Initial concentration (mmol L^{-1})	$q_{e,exp}$ (mmol g^{-1})	Pseudo-first order			Pseudo-second order		
			k_1 (min^{-1})	$q_{e,cal}$ (mmol g^{-1})	R^2	k_2 (g mmol^{-1} min^{-1})	$q_{e,cal}$ (mmol g^{-1})	R^2
Cu(II)	0.1	1.97×10^{-2}	4.05	1.92×10^{-2}	0.9976	3.22×10^{-4}	1.94×10^{-2}	0.9997
	0.2	3.91×10^{-2}	3.22	3.86×10^{-2}	0.9995	5.87×10^{-4}	3.90×10^{-2}	1.0000
	0.3	5.63×10^{-2}	3.13	5.51×10^{-2}	0.9971	8.00×10^{-4}	5.64×10^{-2}	1.0000
	0.4	7.99×10^{-2}	2.66	7.84×10^{-2}	0.9962	4.62×10^{-3}	7.95×10^{-2}	0.9998
	0.5	9.11×10^{-2}	2.05	9.16×10^{-2}	0.9882	5.01×10^{-3}	9.36×10^{-2}	0.9999
	1.0	1.73×10^{-1}	2.09	1.61×10^{-1}	0.9695	6.23×10^{-3}	1.74×10^{-1}	0.9997
	2.5	3.00×10^{-1}	1.16	2.72×10^{-1}	0.9368	1.38×10^{-2}	3.10×10^{-1}	0.9998
	5.0	3.66×10^{-1}	0.44	3.10×10^{-1}	0.8604	1.52×10^{-2}	3.77×10^{-1}	0.9930
	10.0	4.59×10^{-1}	0.49	3.86×10^{-1}	0.8468	2.92×10^{-2}	4.79×10^{-1}	0.9900
Pb(II)	0.1	1.74×10^{-2}	2.13	1.72×10^{-2}	0.9966	1.39×10^{-5}	1.77×10^{-2}	0.9995
	0.2	5.30×10^{-2}	2.38	4.94×10^{-2}	0.9892	2.00×10^{-4}	5.23×10^{-2}	0.9988
	0.3	6.45×10^{-2}	2.67	6.18×10^{-2}	0.9937	6.57×10^{-4}	6.42×10^{-2}	0.9993
	0.4	7.10×10^{-2}	3.56	6.92×10^{-2}	0.9978	1.11×10^{-3}	7.10×10^{-2}	0.9996
	0.5	9.40×10^{-2}	3.39	9.19×10^{-2}	0.9386	3.26×10^{-2}	9.56×10^{-2}	0.9997
	1.0	2.00×10^{-1}	3.07	2.02×10^{-1}	0.9967	3.61×10^{-2}	2.07×10^{-1}	0.9997
	2.5	3.89×10^{-1}	0.75	3.55×10^{-1}	0.9330	3.78×10^{-1}	3.97×10^{-1}	0.9997
	5.0	4.25×10^{-1}	0.87	3.96×10^{-1}	0.8562	4.00×10^{-1}	4.80×10^{-1}	0.9998
	10.0	5.30×10^{-1}	1.51	4.24×10^{-1}	0.8079	4.39×10^{-1}	5.51×10^{-1}	0.9996

Table 4.6 Parameters of Langmuir and Freundlich isotherms

Heavy metal ion	Langmuir isotherm			Freundlich isotherm		
	q_m (mmol g^{-1})	b (L mmol^{-1})	R^2	K_F	$1/n$	R^2
Cu(II)	0.455	6.125	0.9897	0.538	0.494	0.9041
Pb(II)	0.534	6.555	0.9964	0.372	0.392	0.7456

Table 4.7 Wave number (cm^{-1}) of dominant peaks obtained from transmission spectra

	Pure AC	AC with Cu(II)	AC with Pb(II)
Carboxylic acid			
O−H stretching	2943.07	2918.11	2920.20
C=O stretching	1774.88	1793.78	-*
C−O stretching	1200.85	1230.37	1225.86
O−H bending	1417.04	-*	-*
Amine			
N−H stretching	3390.59	3429.33	3404.93
N−H bending	1590.93	1590.24	1584.62
C−N stretching	1088.49	1093.76	-*
Amide			
N−H stretching	3390.59	3429.33	3404.93
C−O stretching	1693.14	1698.60	1695.61

* - refer that shift clearly of wave number

Table 4.8 Possible functional groups involved with the adsorption of Cu(II) and Pb(II)

	Cu(II)	Pb(II)
Carboxylic acid		
O−H stretching	*	*
C=O stretching	*	*
C−O stretching	*	*
O−H bending	*	*
Amine		
N−H stretching	*	*
N−H bending		
C−N stretching		*
Amide		
N−H stretching	*	*
C−O stretching		

Table 4.9 Kinetic parameters of pseudo first and second-order models for binary components adsorptions of Cu(II) and Pb(II)

Heavy metals	Initial concentration (mmol L^{-1})	$q_{e,exp}$ (mmol g^{-1})	q^{mix}/q^0	Pseudo-first order			Pseudo-second order		
				k_1 (min^{-1})	$q_{e,cal}$ (mmol g^{-1})	R^2	k_2 (g mmol^{-1} min^{-1})	$q_{e,cal}$ (mmol g^{-1})	R^2
Cu(II)	0.2	1.60×10^{-2}	7.72×10^{-1}	3.356	1.49×10^{-2}	0.9997	8.85×10^{-5}	1.50×10^{-2}	1.0000
	0.4	3.40×10^{-2}	8.64×10^{-1}	3.001	3.26×10^{-2}	0.9964	1.03×10^{-4}	3.37×10^{-2}	0.9995
	0.6	5.30×10^{-2}	9.03×10^{-1}	2.472	4.97×10^{-2}	0.9948	6.40×10^{-4}	5.09×10^{-2}	0.9997
	5.0	2.20×10^{-1}	7.09×10^{-1}	0.835	1.92×10^{-1}	0.9561	5.71×10^{-3}	2.20×10^{-1}	0.9987
	10.0	2.20×10^{-1}	5.79×10^{-1}	1.117	1.90×10^{-1}	0.9639	5.77×10^{-3}	2.18×10^{-1}	0.9981
Pb(II)	0.2	2.10×10^{-2}	1.12	2.897	1.97×10^{-2}	0.9982	7.02×10^{-4}	1.98×10^{-2}	0.9998
	0.4	3.51×10^{-2}	6.64×10^{-1}	2.16	3.40×10^{-2}	0.9970	2.80×10^{-4}	3.47×10^{-2}	0.9997
	0.6	5.70×10^{-2}	8.74×10^{-1}	2.393	5.49×10^{-2}	0.9968	1.15×10^{-3}	5.61×10^{-2}	0.9998
	5.0	3.10×10^{-1}	7.85×10^{-1}	1.839	2.85×10^{-1}	0.9778	3.18×10^{-2}	3.11×10^{-1}	0.9997
	10.0	3.74×10^{-1}	7.88×10^{-1}	1.303	3.34×10^{-1}	0.9385	3.50×10^{-2}	3.78×10^{-1}	0.9988

Table 4.10 Comparison of rate constants, k_2 (g mmol^{-1} min^{-1}), and equilibrium adsorption capacity, q_e (mmol g^{-1}), between single and binary adsorptions

Parameters	Initial Concentration (mmol L^{-1})	Cu(II)	Cu(II) from Binary components*	Pb(II)	Pb(II) from Binary components*
k_2	10	2.92×10^{-2}	5.77×10^{-3}	4.39×10^{-2}	3.50×10^{-2}
	5	1.52×10^{-2}	5.71×10^{-3}	4.00×10^{-2}	3.18×10^{-2}
	0.4	4.62×10^{-4}	8.85×10^{-4}	1.11×10^{-4}	2.80×10^{-4}
	0.2	5.87×10^{-4}	1.03×10^{-5}	2.00×10^{-5}	7.02×10^{-4}
q_e	10	4.59×10^{-1}	2.16×10^{-1}	5.31×10^{-1}	3.79×10^{-1}
	5	3.64×10^{-1}	2.16×10^{-1}	4.57×10^{-1}	3.10×10^{-1}
	2.5	3.00×10^{-1}	2.11×10^{-1}	3.89×10^{-1}	3.02×10^{-1}
	1.25	2.04×10^{-1}	1.24×10^{-1}	2.95×10^{-1}	1.29×10^{-1}
	0.625	1.27×10^{-1}		1.30×10^{-1}	

* Binary component is equimolar concentration, e.g. binary components 10 mmol L^{-1} was from Cu(II) 5 mmol L^{-1} and Pb(II) 5 mmol L^{-1}.

Table 4.11 Solvent extraction of Cu(II) and Pb(II) from single heavy metal component systems

Citric acid concentration (M)	(S/L) ratio	$q_{e,Ext}$ (mmol g^{-1})		Extraction Efficiency (%)		Cu(II) Extraction ratio
		Cu(II)	Pb(II)	Cu(II)	Pb(II)	
0.005	1	3.27×10^{-1}	3.88×10^{-1}	28.01	27.56	0.4636
0.005	4	2.39×10^{-1}	2.60×10^{-1}	47.49	51.43	0.4399
0.005	8	2.81×10^{-1}	3.77×10^{-1}	38.18	29.50	0.5239
0.005	12	3.10×10^{-1}	4.28×10^{-1}	31.91	19.94	0.5763
0.005	16	3.35×10^{-1}	4.52×10^{-1}	26.40	15.57	0.5905
0.01	1	2.99×10^{-1}	4.26×10^{-1}	34.31	20.29	0.5898
0.01	4	1.85×10^{-1}	3.57×10^{-1}	59.28	33.35	0.6018
0.01	8	2.33×10^{-1}	4.33×10^{-1}	48.87	19.12	0.6849
0.01	12	2.76×10^{-1}	4.62×10^{-1}	39.36	13.60	0.7110
0.01	16	2.98×10^{-1}	4.89×10^{-1}	34.52	8.58	0.7737
0.05	1	2.77×10^{-1}	4.09×10^{-1}	39.13	23.48	0.5862
0.05	4	1.38×10^{-1}	2.66×10^{-1}	69.66	50.20	0.5413
0.05	8	1.87×10^{-1}	3.13×10^{-1}	58.82	41.56	0.5461
0.05	12	2.06×10^{-1}	3.72×10^{-1}	54.64	30.40	0.6044
0.05	16	2.18×10^{-1}	3.88×10^{-1}	52.09	27.50	0.6169
0.1	1	2.56×10^{-1}	3.05×10^{-1}	43.73	42.98	0.4638
0.1	4	6.60×10^{-2}	1.01×10^{-1}	85.50	81.09	0.4727
0.1	8	6.95×10^{-2}	2.02×10^{-1}	84.73	62.31	0.5362
1	1	2.49×10^{-1}	2.91×10^{-1}	45.24	45.54	0.4579
1	4	2.26×10^{-2}	4.38×10^{-3}	95.02	99.18	0.4489
1	8	1.61×10^{-2}	7.05×10^{-3}	96.45	98.68	0.4539
1	12	1.68×10^{-2}	2.21×10^{-4}	96.30	99.96	0.4503
1	16	1.03×10^{-2}	5.29×10^{-3}	97.72	99.01	0.4563

Table 4.12 Solvent extraction of Cu(II) and Pb(II) from binary heavy metal
components systems

Citric acid concentration (M)	(S/L) ratio	$q_{e,Ext}$ (mmol g^{-1})		Extraction Efficiency (%)		Extraction ratio	
		Cu(II)	Pb(II)	Cu(II)	Pb(II)	Cu(II)	Pb(II)
0.01	1	1.97×10^{-1}	3.06×10^{-1}	12.99	19.23	0.2874	0.7126
0.01	4	1.45×10^{-1}	2.95×10^{-1}	35.75	22.28	0.4893	0.5107
0.01	8	1.47×10^{-1}	3.31×10^{-1}	35.03	12.80	0.6203	0.3797
0.01	12	1.61×10^{-1}	3.46×10^{-1}	28.88	8.84	0.6610	0.3390
0.01	16	1.72×10^{-1}	3.54×10^{-1}	24.08	6.64	0.6838	0.3162
0.05	1	2.02×10^{-1}	2.96×10^{-1}	21.80	22.00	0.2283	0.7717
0.05	4	1.28×10^{-1}	2.23×10^{-1}	43.25	41.15	0.3856	0.6144
0.05	8	1.28×10^{-1}	2.65×10^{-1}	43.28	30.03	0.4624	0.5376
0.05	12	1.34×10^{-1}	3.04×10^{-1}	40.85	19.92	0.5504	0.4496
0.05	16	1.36×10^{-1}	3.18×10^{-1}	39.77	16.09	0.5960	0.4040

Table 4.13 Kinetic parameters of single and binary component extraction systems (S/L=16)

Heavy metals	Condition	$q_{e,Ext,exp}$	Extraction efficiency (%)	Pseudo-first order			Pseudo-second order		
				k_1 (min^{-1})	$q_{e,Ext,cal}$	R^2	k_2 (g mmol^{-1} min^{-1})	$q_{e,Ext,cal}$	R^2
Cu(II)	25 °C	2.89×10^{-1}	35.63	0.09	3.04×10^{-1}	0.9867	0.69	2.78×10^{-1}	0.9918
	50 °C	2.78×10^{-1}	38.45	1.22	3.07×10^{-1}	0.9607	13.23	2.55×10^{-1}	0.9942
	75 °C	2.35×10^{-1}	48.05	1.67	2.51×10^{-1}	0.9658	15.36	2.44×10^{-1}	0.9925
	C=1 M, 25 °C	0.50×10^{-2}	97.35	2.50	0.30×10^{-1}	0.9916	18.63	0.02×10^{-1}	0.9981
Pb(II)	25 °C	4.90×10^{-1}	8.44	1.36	4.97×10^{-1}	0.8924	25.78	4.95×10^{-1}	0.9719
	50 °C	4.73×10^{-1}	11.62	1.03	4.81×10^{-1}	0.9398	31.91	4.79×10^{-1}	0.9908
	75 °C	4.65×10^{-1}	12.92	0.96	4.71×10^{-1}	0.9598	56.31	4.69×10^{-1}	0.9965
	C=1 M, 25 °C	0.30×10^{-2}	99.24	3.79	0.11×10^{-1}	0.9994	63.18	0.01×10^{-1}	0.9999
Cu(II) from (Cu-Pb)	25 °C	1.72×10^{-1}	23.48	0.08	1.86×10^{-1}	0.9568	4.71	1.84×10^{-1}	0.9605
	50 °C	1.57×10^{-1}	30.68	0.90	1.66×10^{-1}	0.9501	23.77	1.63×10^{-1}	0.9812
	75 °C	1.52×10^{-1}	32.81	1.88	1.56×10^{-1}	0.9829	61.20	1.54×10^{-1}	0.9935
Pb(II) from (Cu-Pb)	25 °C	3.54×10^{-1}	6.54	0.04	3.59×10^{-1}	0.9908	0.59	3.46×10^{-1}	0.9871
	50 °C	3.46×10^{-1}	8.48	0.18	3.52×10^{-1}	0.9353	7.04	3.48×10^{-1}	0.9451
	75 °C	3.36×10^{-1}	11.31	1.14	3.41×10^{-1}	0.9751	43.25	3.39×10^{-1}	0.9929

Table 4.14 Total desorption efficiency of iterative desorption

Heavy metals	Condition	Desorption efficiency			
		Iterative No. 1	Iterative No. 2	Iterative No. 3	Total
Cu(II)	S/L =8	49.11	30.27	10.29	89.67
	S/L =12	38.99	23.74	8.37	71.10
	S/L =16	33.97	18.31	6.33	58.61
Pb(II)	S/L =8	19.66	15.74	8.62	44.02
	S/L =12	13.34	10.13	7.13	30.60
	S/L =16	8.21	4.35	4.11	16.67
Cu(II) from	S/L =8	35.30	27.61	9.30	72.21
(Cu-Pb)	S/L =12	27.86	20.97	11.49	60.33
	S/L =16	23.83	14.30	5.92	44.05
Pb(II) from	S/L =8	13.10	11.74	9.29	34.13
(Cu-Pb)	S/L =12	9.81	9.50	8.27	27.58
	S/L =16	7.29	6.84	6.46	20.59
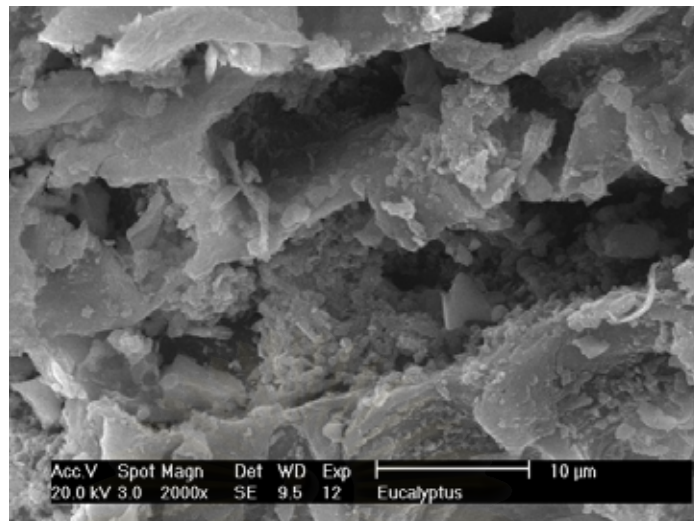
(a)
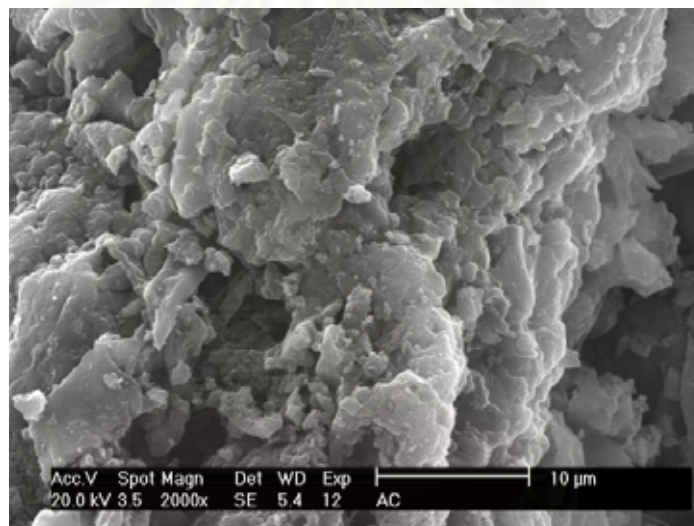
(b)

Figure 4.1 SEM photograph of eucalyptus bark (a) and activated carbon (b)
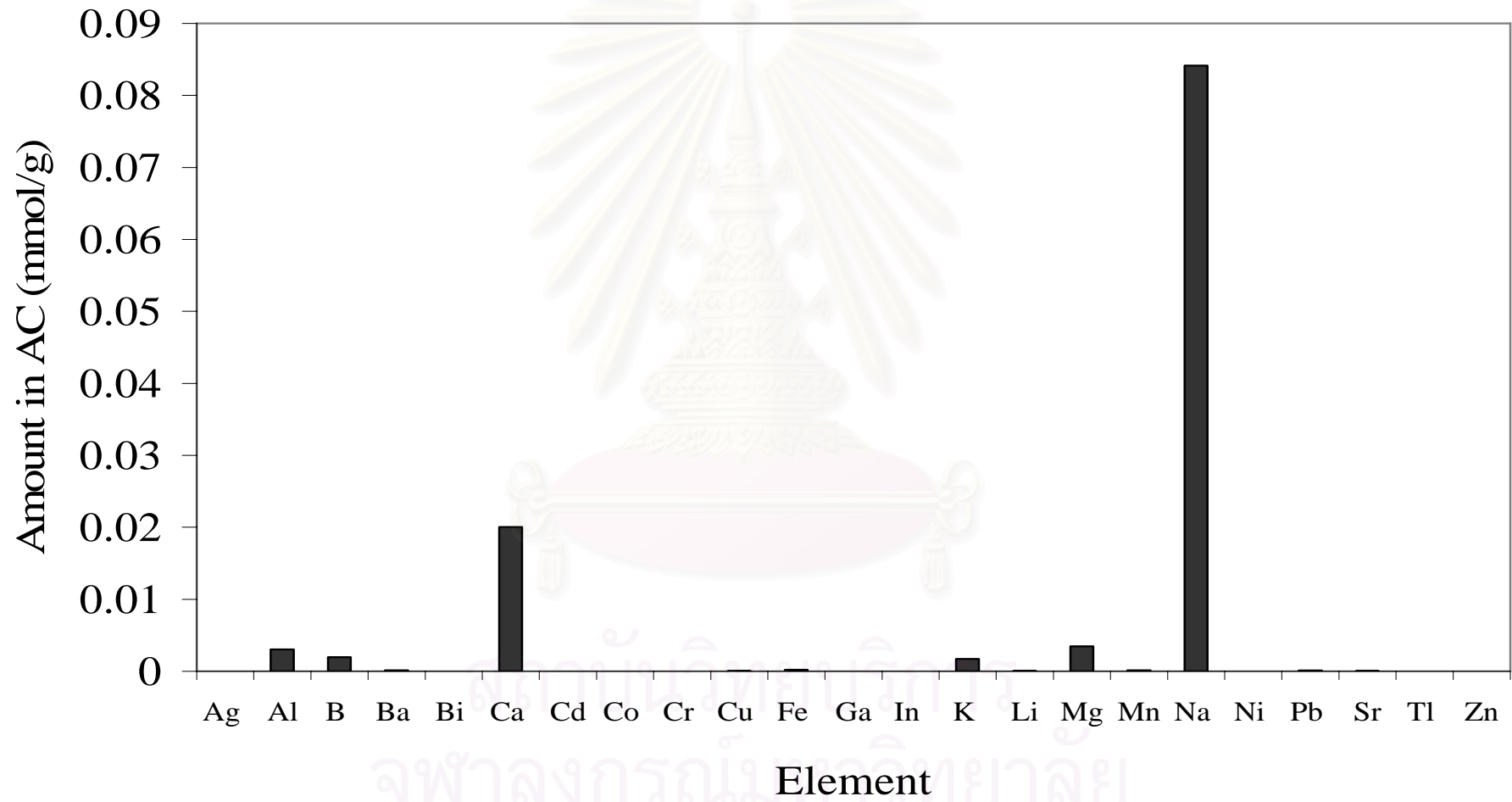
Figure 4.2 Metal compositions in activated carbon
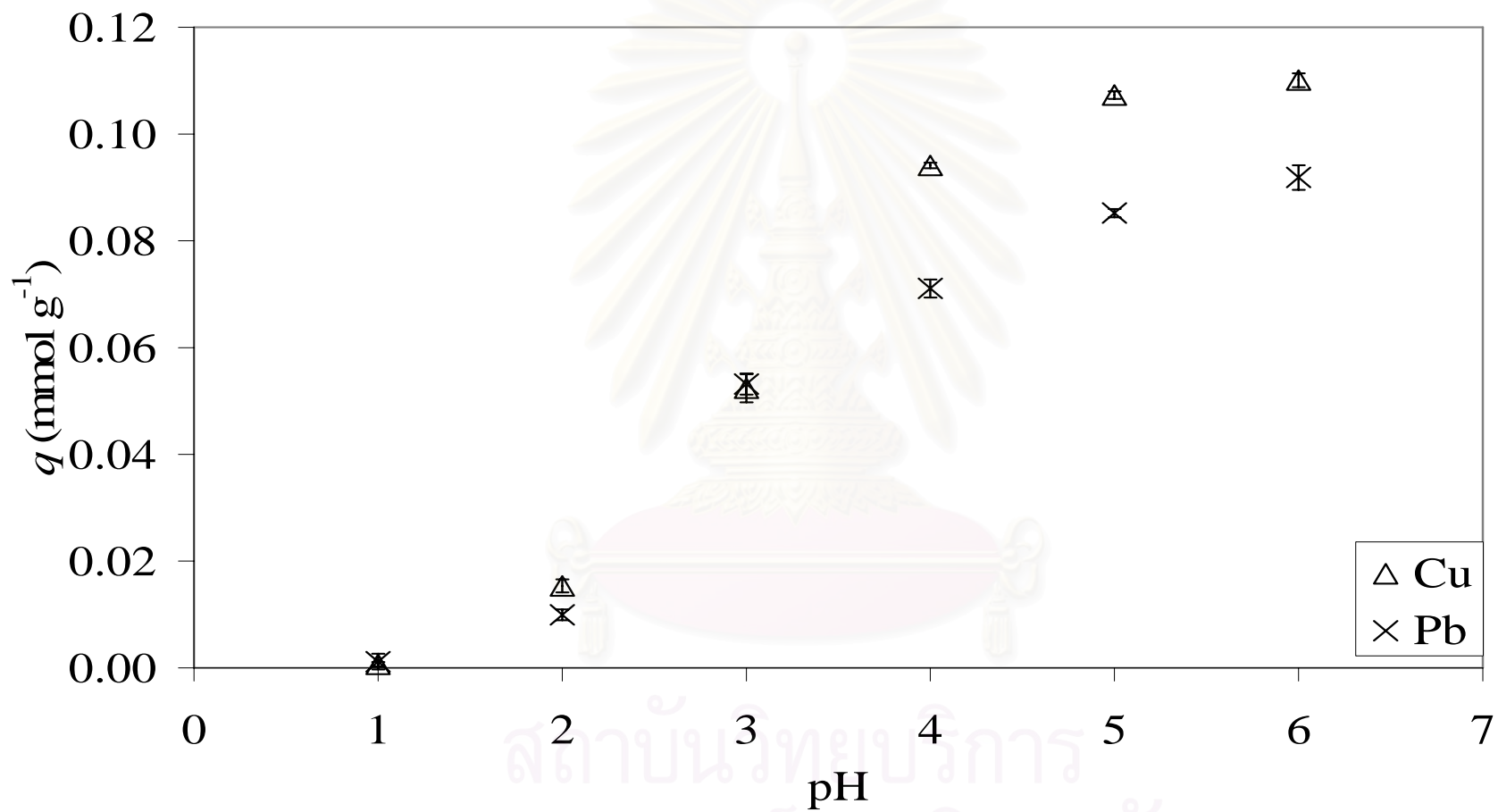
Figure 4.3 Effect of pH for adsorption (Initial concentration = 0.3 mmol L^{-1}, shaking rate = 200 rpm, 25°C)
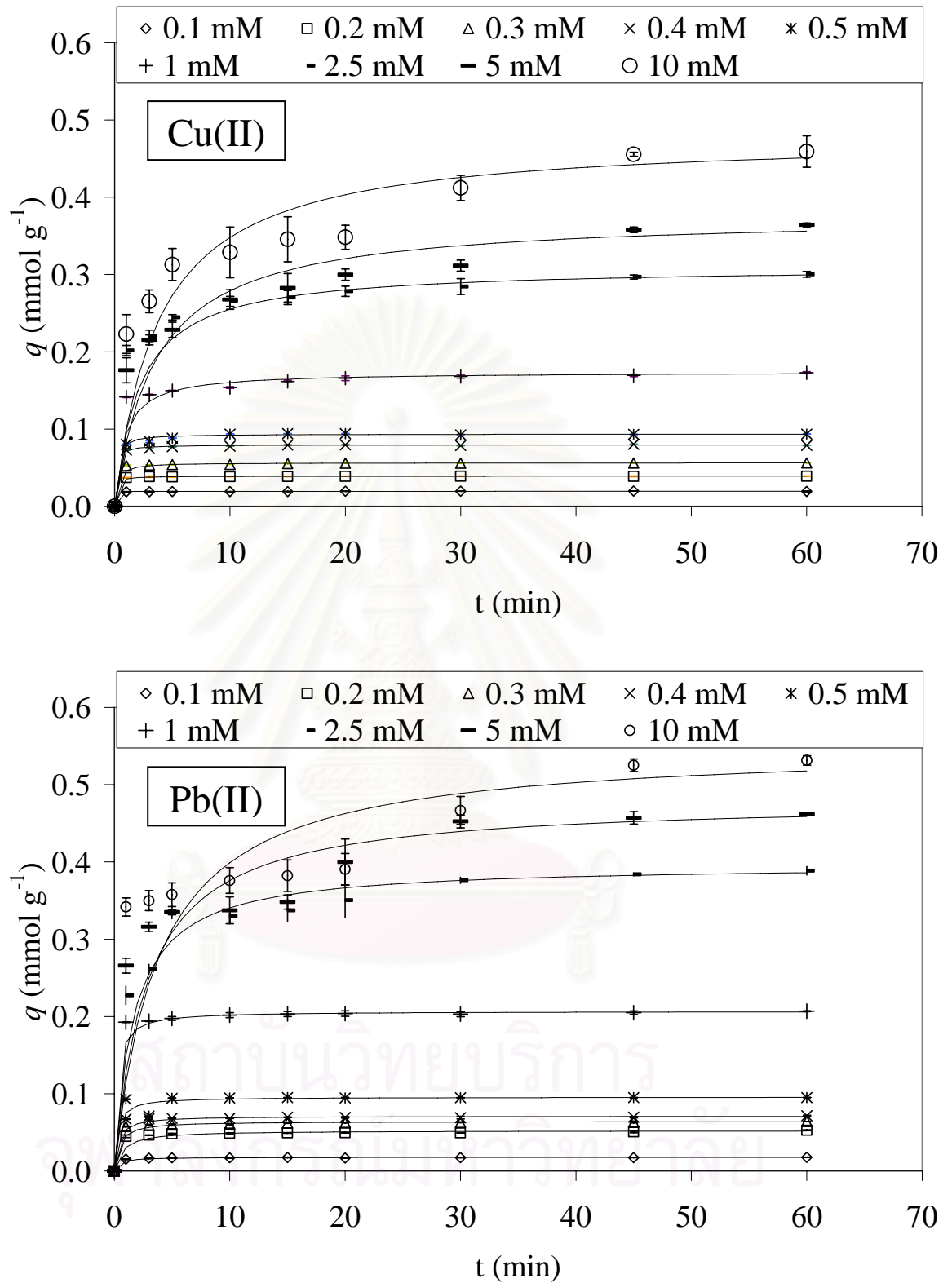
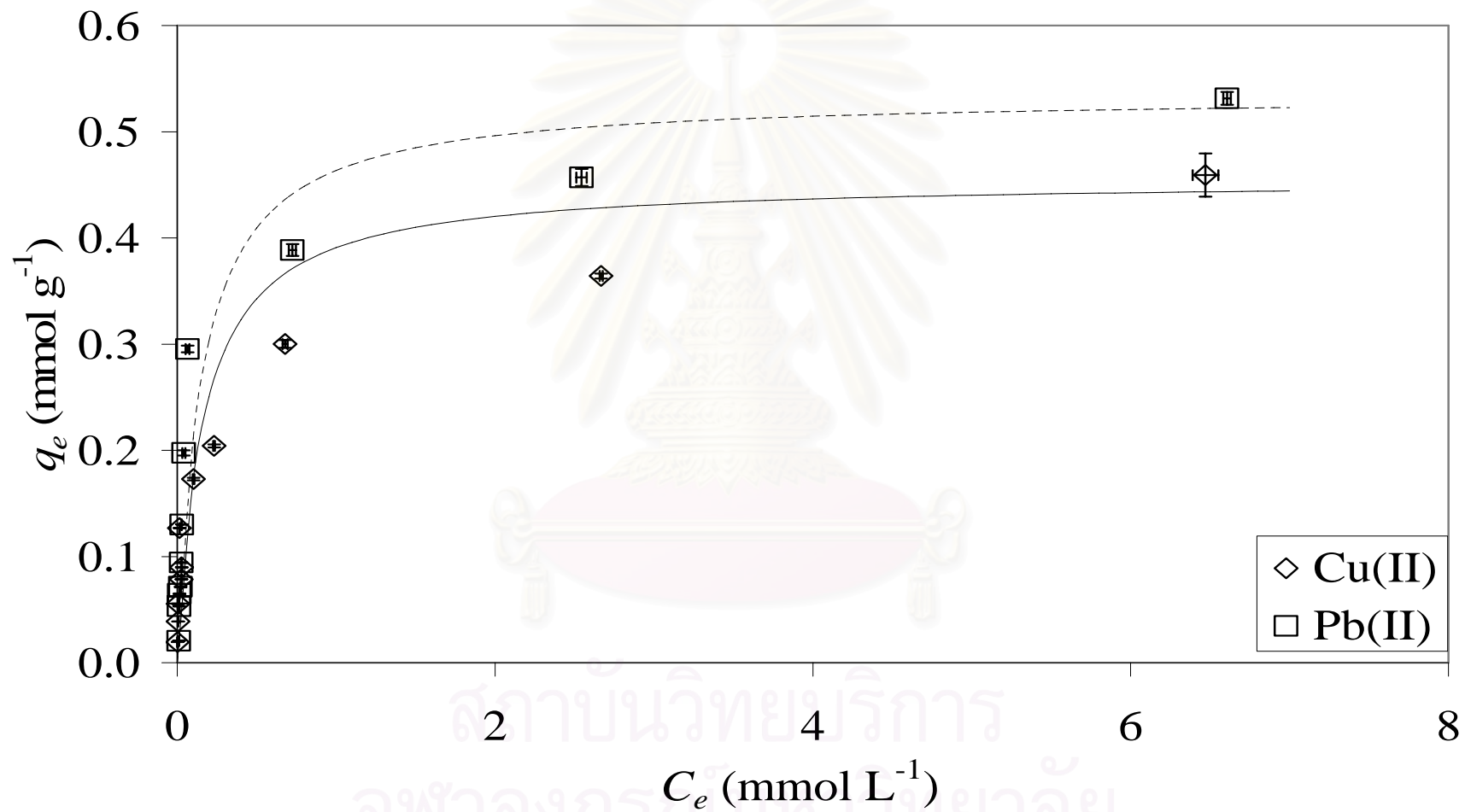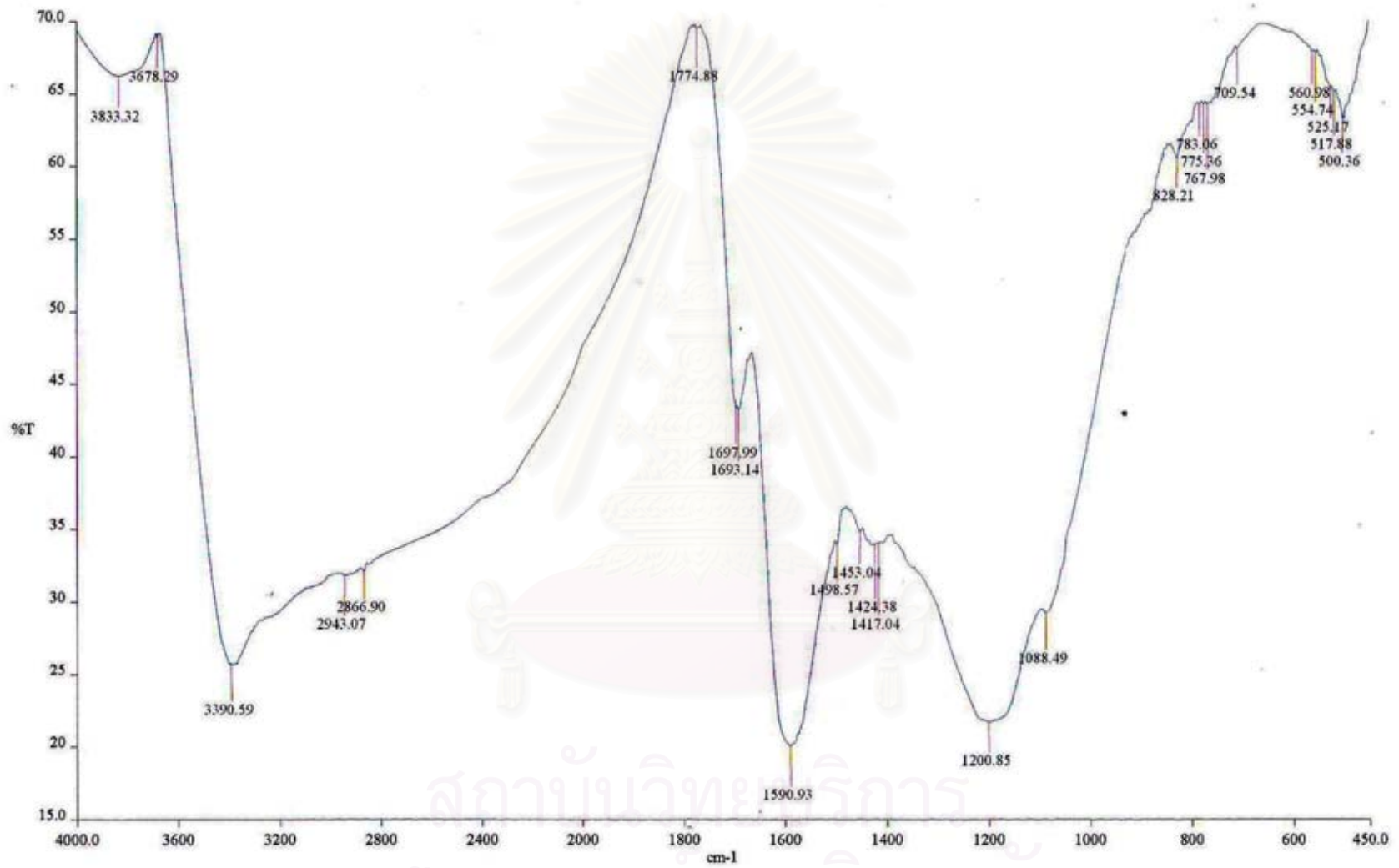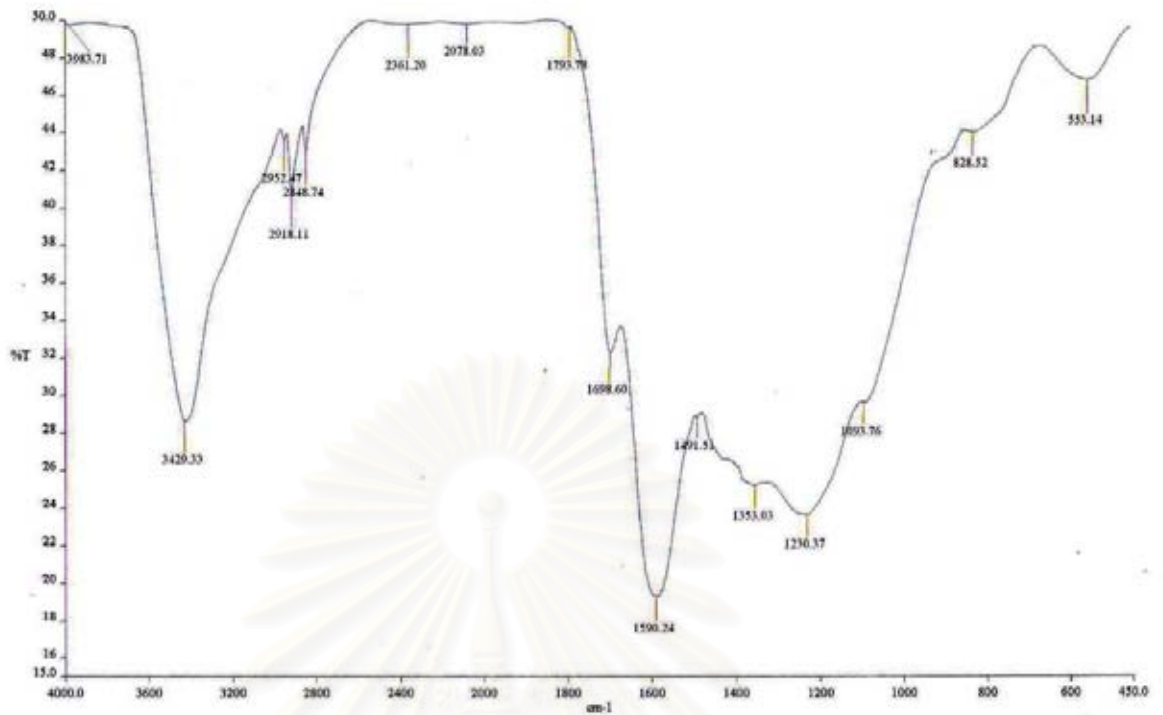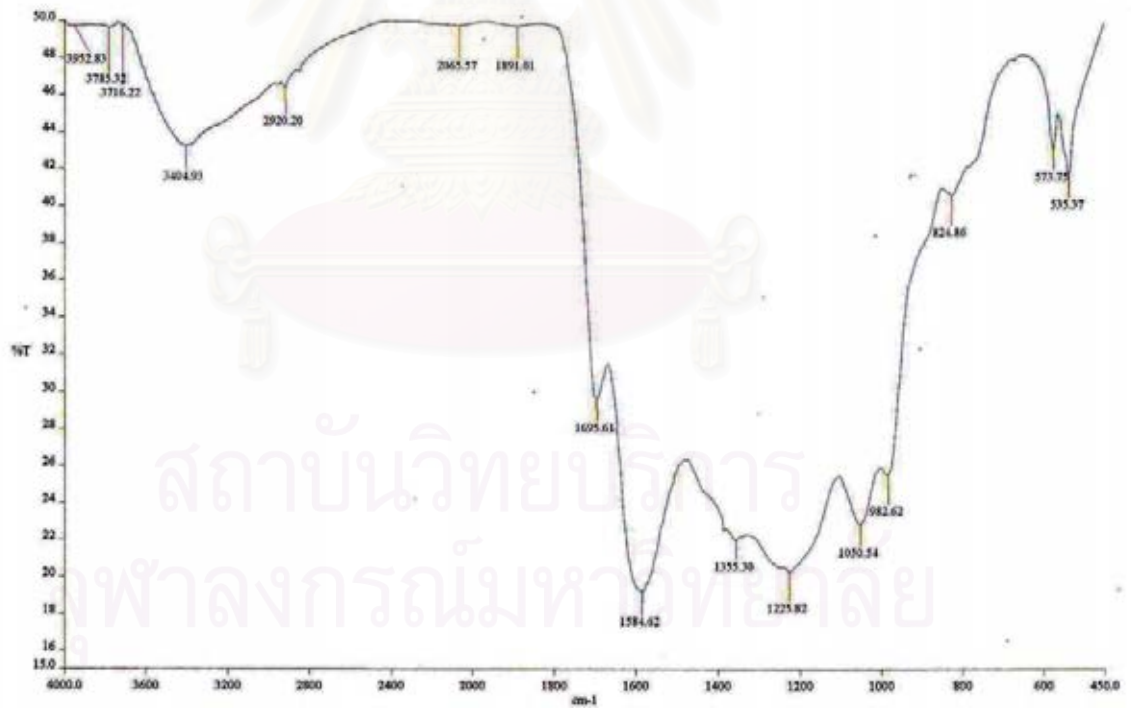Figure 4.4 Adsorption kinetics (shaking rate = 200 rpm, 25°C)

Figure 4.5 Adsorption isotherms of Cu(II) and Pb(II) (shaking rate = 200 rpm, 25°C)

(a) original activated carbon

(b) Cu(II) laden AC

(c) Pb(II) laden AC

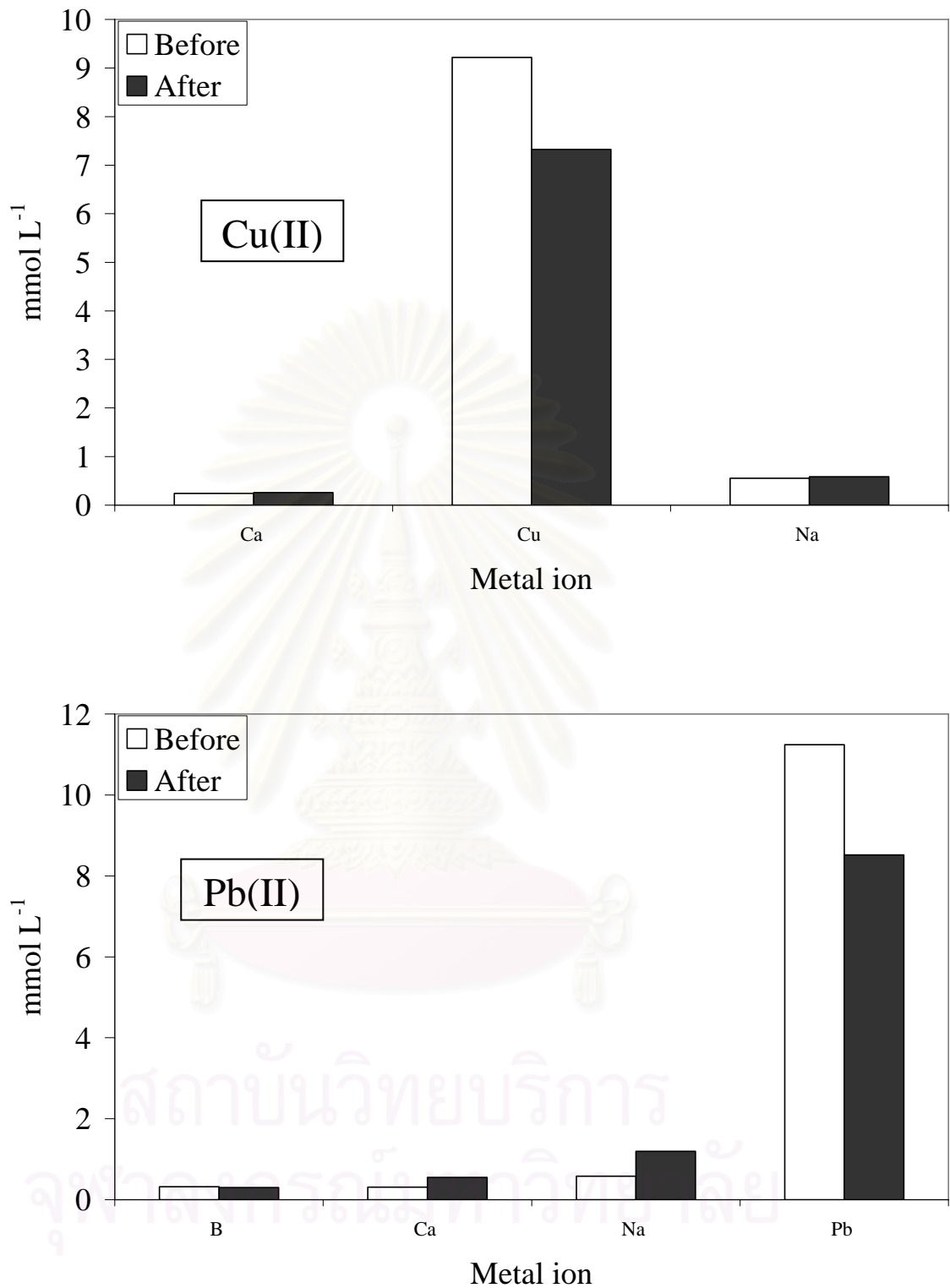Figure 4.6 FT-IR transmission spectra

Figure 4.7 Metal ions concentration before and after adsorption
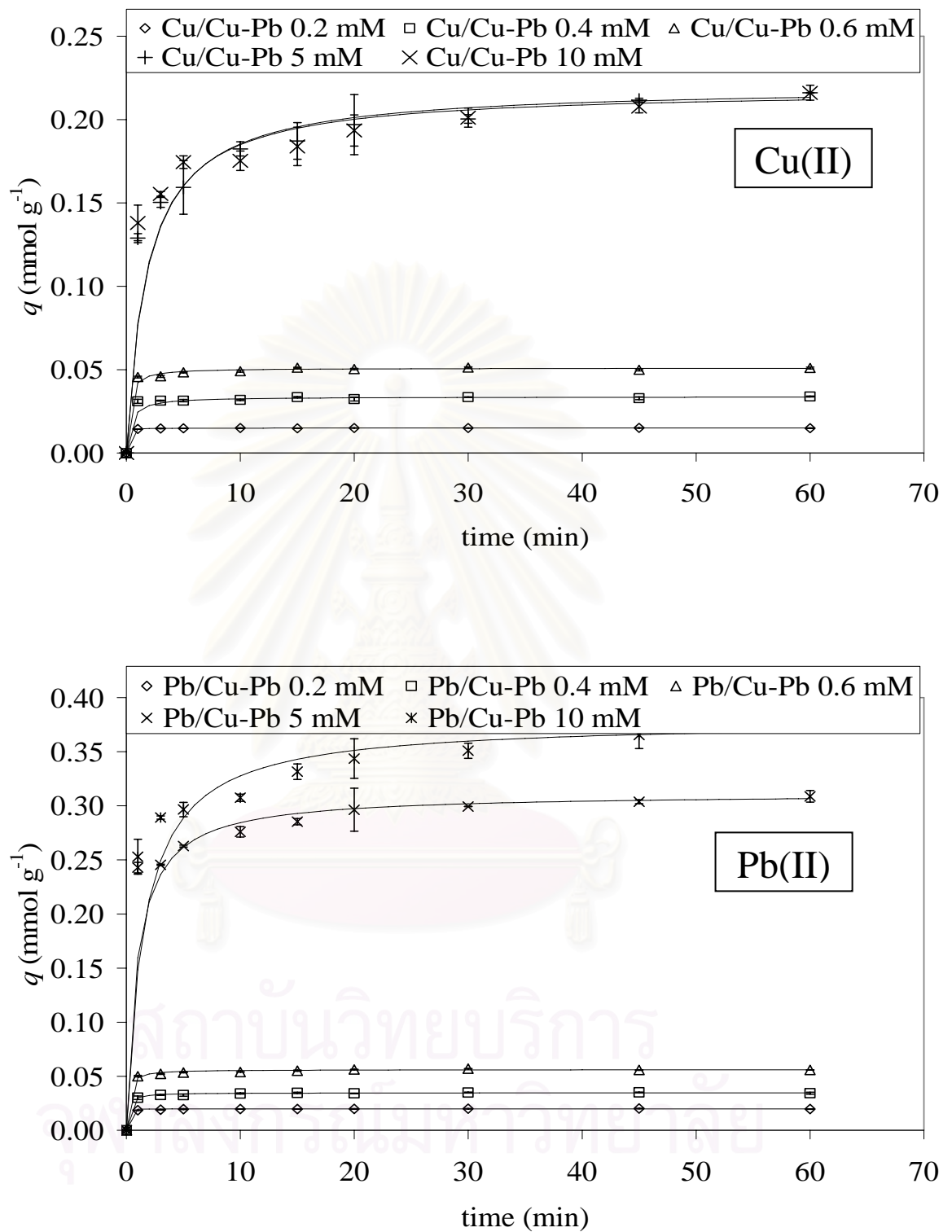
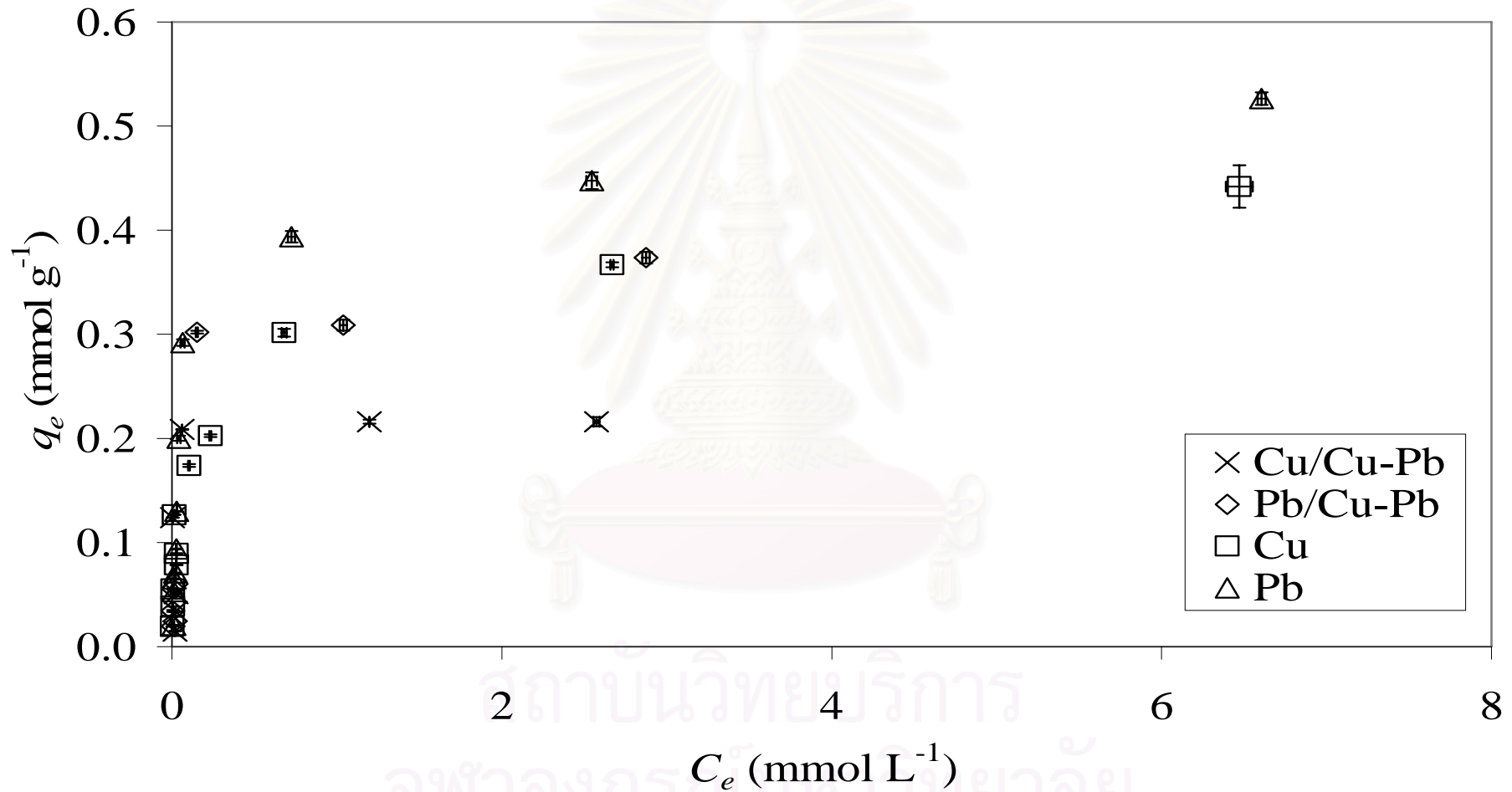Figure 4.8 Binary adsorption kinetics (shaking rate = 200 rpm, 25°C)

Figure 4.9 Single and binary adsorption isotherms of Cu(II) and Pb(II) (shaking rate = 200 rpm, 25°C)
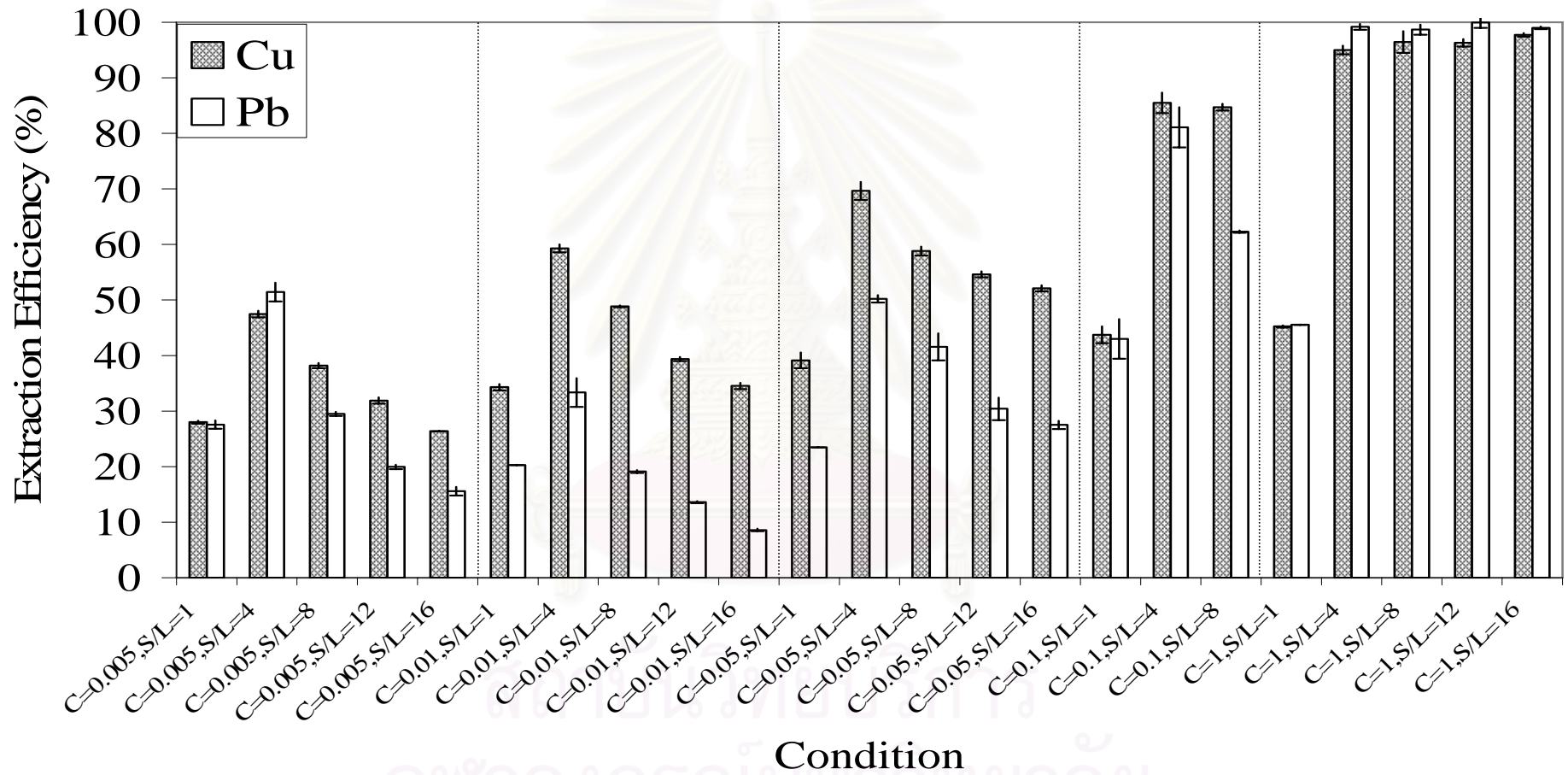
Figure 4.10 Desorption of Cu(II) and Pb(II) (shaking rate = 200 rpm, 25°C)
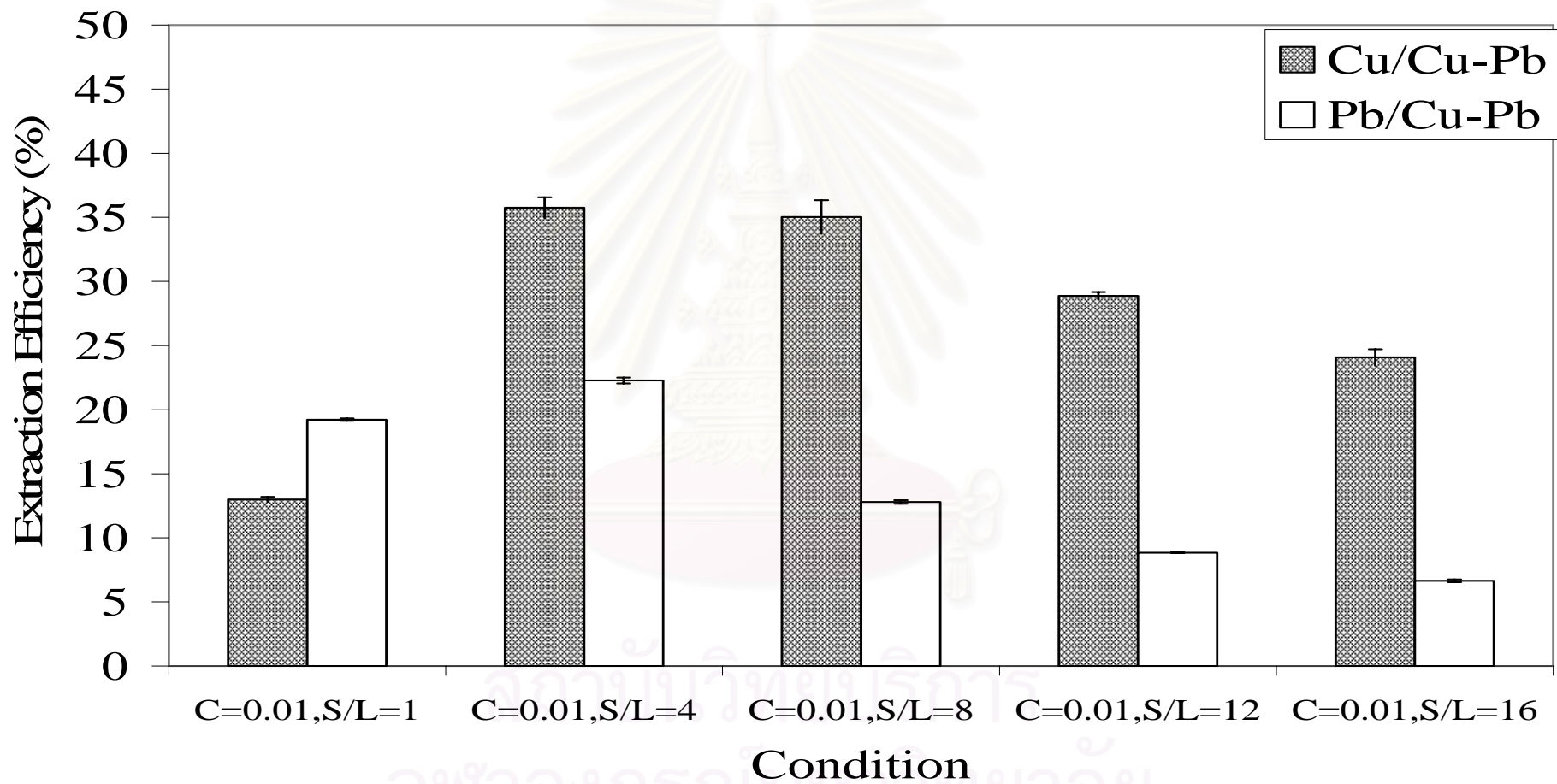
Figure 4.11 Binary desorption of Cu(II) and Pb(II) (shaking rate = 200 rpm, 25°C)
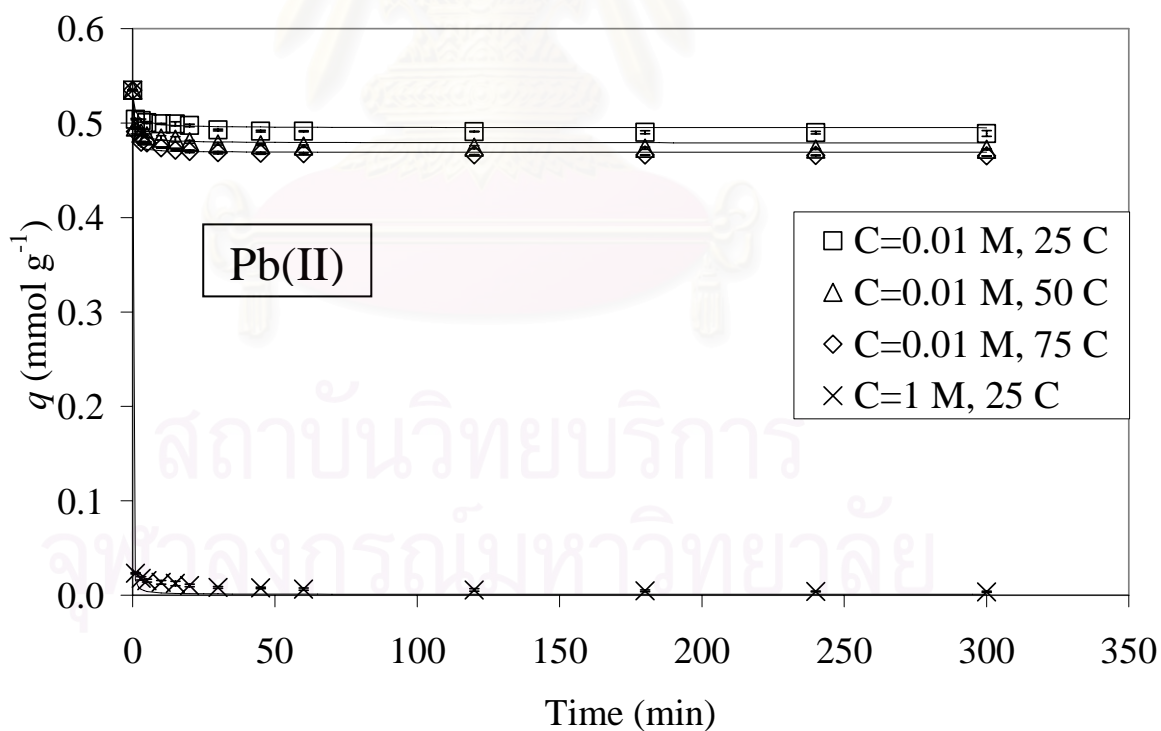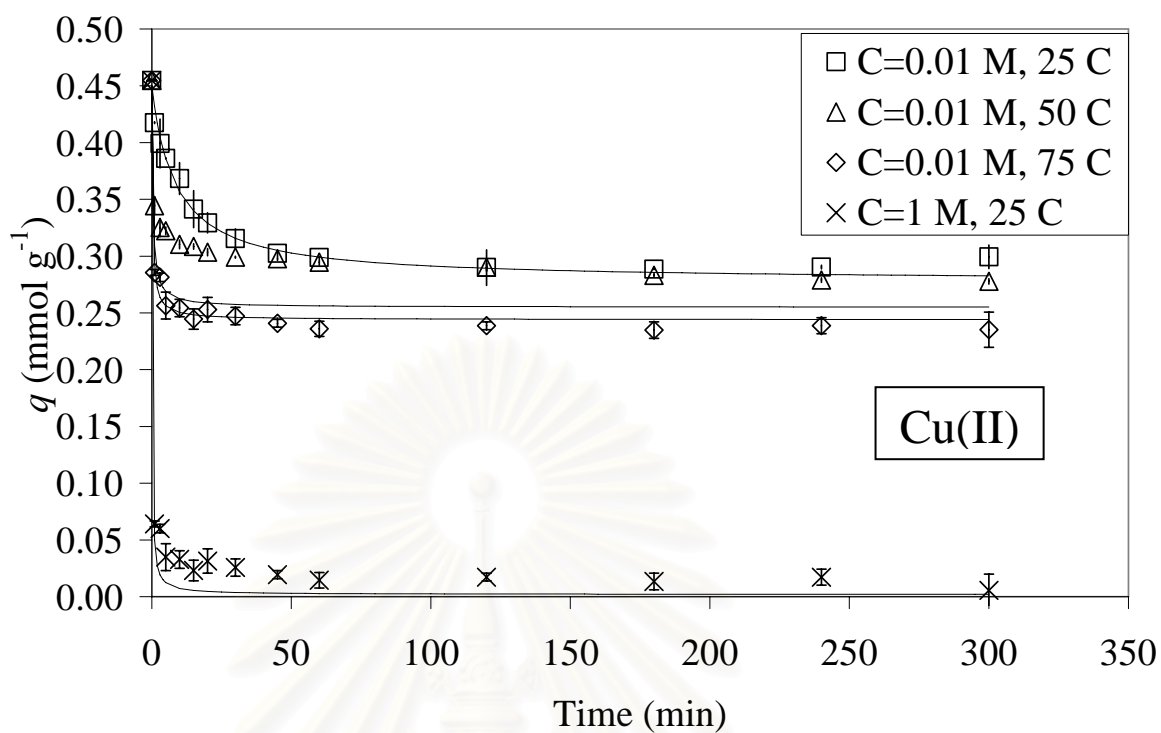
Figure 4.12 Desorption kinetics of single component systems

(shaking rate = 200 rpm, 25°C)
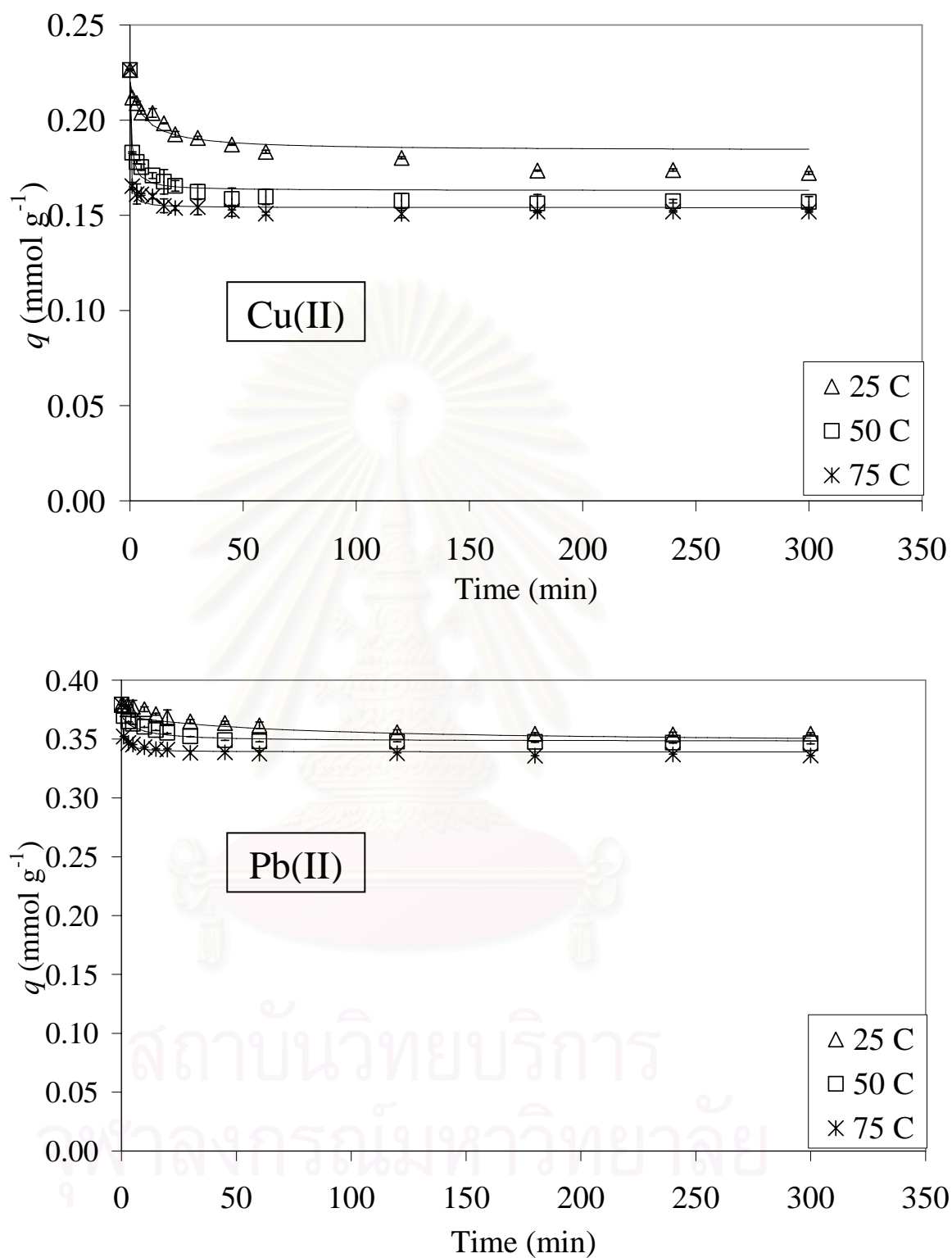
Figure 4.13 Desorption kinetics of binary component systems

(Citric acid concentration= 0.01 M, shaking rate = 200 rpm, 25°C)
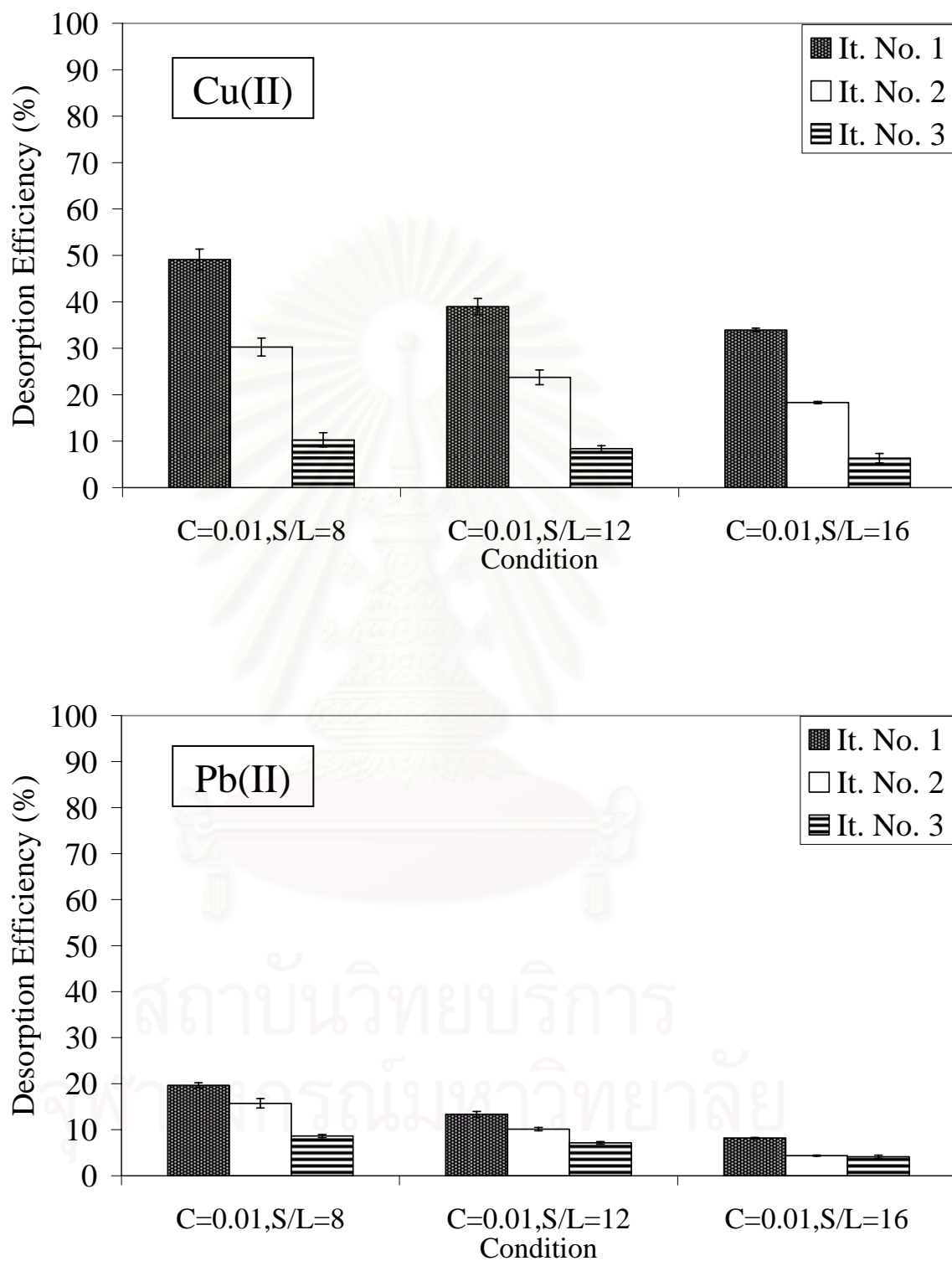
Figure 4.14 Iterative desorption for single component systems

(Citric acid concentration = 0.01 M, shaking rate = 200 rpm, 25°C)
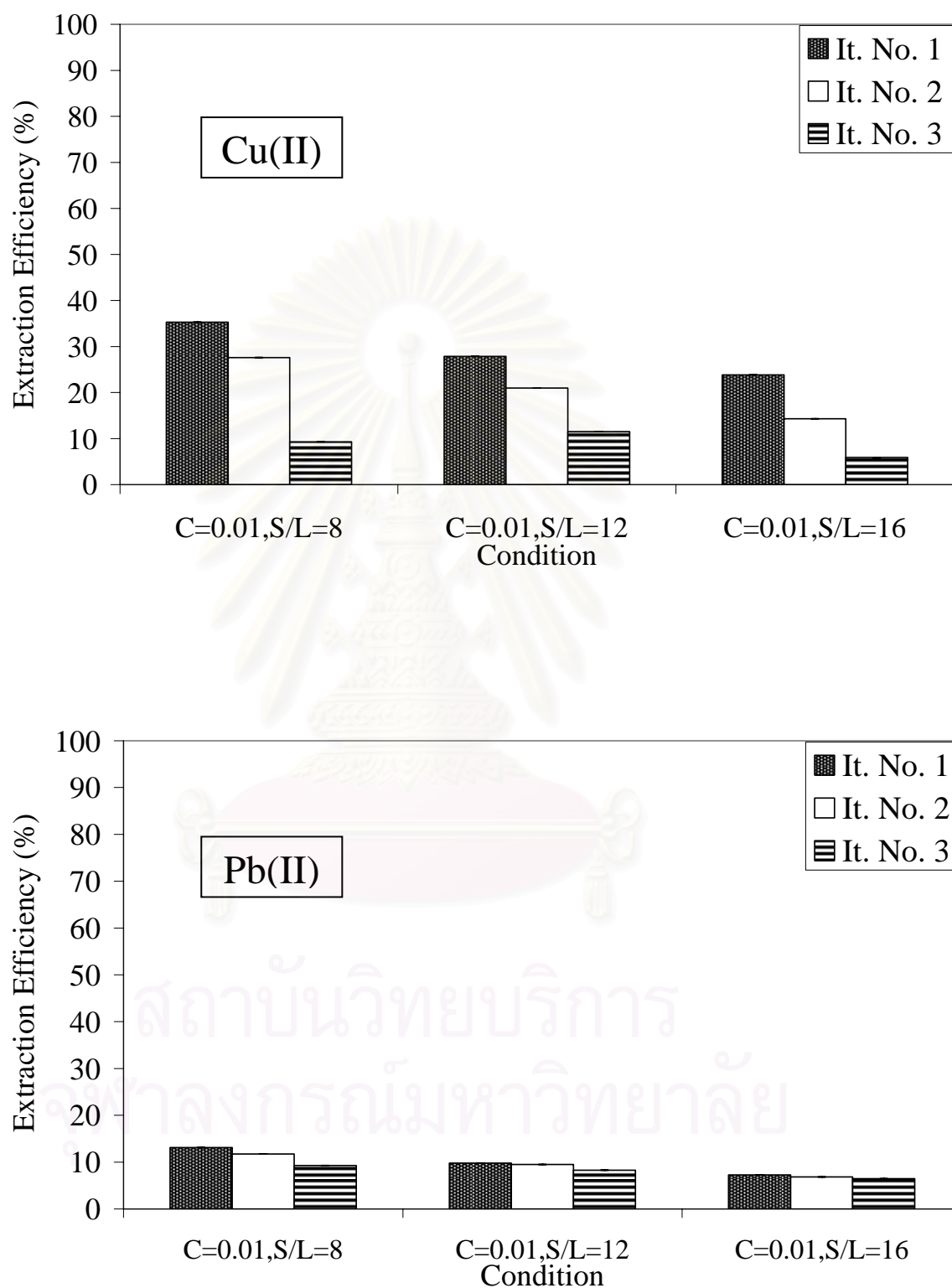
Figure 4.15 Iterative desorption for binary component systems

(Citric acid concentration = 0.01 M, shaking rate = 200 rpm, 25°C)

CHAPTER V

CONCLUSIONS AND RECOMMENDATIONS

5.1 Conclusions

The investigation in this work leads to the following conclusions:

1. Eucalyptus bark could provide effective activated carbon by phosphoric acid activation.

2. The adsorption for the heavy metal solutions occurred best at pH 5.

3. The pseudo second order was suited for prediction the kinetic parameter for adsorption and desorption of Cu(II) and Pb(II).

4. Adsorption isotherms of Cu(II) and Pb(II) fitted with Langmuir Isotherm.

5. The level of maximum adsorption capacity of this activated carbon was considered relatively high when compared with the reported values that were shown in Table 5.1.

6. Activated carbon from this work could adsorb more Pb(II) than Cu(II).

7. The desorption of Cu(II) with citric acid was more effective than that of Pb(II).

8. Increasing desorbing agent concentration and temperature increased desorption efficiency.

9. Optimal solid to liquid *(S/L) ratio* for the desorption of both metal ions was 4.

10. Desorbing agent concentration = 1 M and *S/L ratio* > 4 could recover 100% of the metal ions in single component system

11. Desorption of binary component system could separate metal ions only about 70% at desorbing agent concentration = 0.01 M and *S/L ratio* = 16.

12. Iterative desorption increased desorption efficiency but not desorption ratio.

5.2 Contributions

This research illustrates the feasibility in using eucalyptus bark to produce activated carbon for the recovery metal ions by adsorption and desorption. The adsorption capacities obtained from the activated carbon derived from this work compares well with those from literature. In fact, the activated carbon from eucalyptus bark seemed to have a reasonably high adsorption capacities towards the two metals investigated in this work. The results of this research will help facilitate the design of

the adsorption process for the removal of heavy metal ions from wastewater and recovery metal ions. However, the separation of the two heavy metals still cannot be achieved with high efficiency. Therefore the application regarding the recovery of each heavy metal from such wastewater still needs further experimental verifications.

5.3 Recommendations / Future works

Based on the results of this study, some recommendations for future studies can be proposed.

1. Powder activated carbon is difficult to handle in the actual treatment system, future works should study the production of granular activated carbon.
2. The pretreatment for development of effective of activated carbon might help enhance the separation efficiency of the two heavy metals.

Table 5.1 Comparison on the reported maximum adsorption capacities

Adsorbent	Adsorbents	Heavy metals	q_m (mmolg^{-1})
This work	Activated carbon	Cu(II)	0.450
TAN et al., 1985	Activated carbon	Pb(II)	0.289
Quek et al., 1998	Sago waste	Cu(II)	0.200
		Pb(II)	0.530
ARPA et al., 2000	smectile	Cu(II)	0.260
		Pb(II)	0.119
UZUN et al., 2000	commercial activated carbon	Pb(II)	0.230
Faur-Brasquet et al., 2002	AC pretreated with NaCl	Cu(II)	0.174
		Pb(II)	0.147
Chen et al., 2003	activated carbon pretreated with 1 M citric acid	Cu(II)	0.040
Feng et al., 2004	Rice husk ash	Cu(II)	0.230
		Pb(II)	0.064
Chen et al., 2004b	GAC	Cu(II)	0.110

Table 5.1 Comparison on the reported maximum adsorption capacities (cont.)

| Adsorbent	Adsorbent	Heavy metals	q_m (mmolg^{-1})
Machida et al., 2005	Activated carbon	Cu(II)	0.056
		Pb(II)	0.052
Pavasant et al., 2006	Dried *Caulerpa lentillifera*	Cu(II)	0.088
		Pb(II)	0.139

REFERENCES

Aksu, Z., and Dönmez, G. 2003. A comparative study on the biosorption characteristics of some yeast for Remazol Blue reactive dye. Chemosphere 50: 1075-1083.

ASTM. 2001. D 1762-84. Standard test method for chemical analysis of wood charcoal.

ASTM. 1999. D 4607-94. Standard test method for determination of iodine number of activated carbon.

ASTM. 1999. D 2866-94. Standard test method for total ash content of activated carbon.

Apiratikul, R. 2003. Biosorption of heavy metals mixture solution by green macroalga, *Caulerpa lentillifera*. Master's thesis. Program of Environmental Management, Graduate School, Chulalongkorn University.

Arriagada, R., Gercia, R., and Reyes, P. 1994. Steam and carbon dioxide activation of *Eucalyptus globulus* charcoal. J. Chem. Tech. Biotechnol. 60: 427-345.

Bartosch, C., Kiefer, R., and Höll, W.H. 2000. Separation of heavy metals by parametric pumping with variation of pH Part I: Application of cation exchangers in binary systems. Reactive & Functional Polymers 45: 197-210.

Castro, J.B., Bonelli, P.R., Cerrella, E.G., and Cukierman, A.L. 2000. Phosphoric acid activation of agricultural residues and bagasse from sugar cane: Influence of the experimental conditions on adsorption characteristics of activated carbons. Ind. Eng. Chem. Res. 39: 4166-4172.

Chen, J.P., and Wang, L. 2004a. Characterization of metal adsorption kinetic properties in batch and fixed-bed reactors. Chemosphere 54: 397-404.

Chen, J.P., and Wu, S. 2004b. Acid/base-treated activated carbons: characterization of functional groups and metal adsorptive properties. Langmuir 20: 2233-2242.

Chen, J.P., Wu, S., and Chong, K.H. 2003. Surface modification of a granular activated carbon by citric acid for enhancement of copper adsorption. Carbon 41: 1979-1986.

Doğan, M., Alkan M., Demirbas, Ö., Özdemir, Y., and Özmetin, C. 2006. Adsorption kinetics of maxilon blue GRL onto sepiolite from aqueous solutions. Chemical Engineering Journal 124: 89-101.

Eckenfelder, W.W. 2000. Industrial Water Pollution Control. Singapore: McGraw-Hill.

Faur-Brasquet, C., Reddad, Z., Kadirvelu, K., and Cloirec, P.L. 2002. Modeling the adsorption of metal ions (Cu2+, Ni2+,Pb2+) onto ACCs using surface complexation models. Applied surface science 196: 356-365.

Feng, Q., Lin, Q., Gong, F., Sugita, S., and Shoya, M. 2004. Adsorption of lead and mercury by rice husk ash. Journal of Colloid and Interface Science 278: 1-8

Girgis, B.S., Yunis, S.S., and Soliman, A.M. 2002. Characteristics of activated carbon from peanut hulls in relation to conditions of preparation. Mater. Lett. 57: 164–172.

Hammaini, A., González, F., Ballester, A., Blázquez, M.L., and Muňoz, J.A. Biosorption of heavy metals by activated sludge and their desorption characteristics. Journal of Environmental Management (In press).

Hasar, H. 2003. Adsorption of nickel(II) from aqueous solution onto activated carbon prepared from almond husk. Journal of Hazardous Materials B97: 49-57.

Ho, Y.S. and McKay, G. 1999. A kinetic study of dye sorption by biosorbent waste product pith. Resour Conser Recycl. 15(3-4): 171-193.

Isarasaenee, R. 1996. Production of activated carbon from used tires by superheated steam activation. Master's thesis. Program of Chemical Technology, Faculty of Science, Chulalongkorn University.

Jankowska, H., Swiatkowski, A., and Choma, J. 1991. Active Carbon. Warsaw: Ellis Horwood.

Japanese Standard Association. 1991. JIS K: 1470. Standard testing method of mythylene blue number of activated carbon.

Jeon, C., Yoo, Y.J., and Hoell W.H. 2005. Environmental effects and desorption characteristics on heavy metal removal using carboxylated alginic acid. Bioresource Technology 96: 15–19.

Jindaphunphairoth, V. 2000. Preparation of activated carbon from Eucalyptus camaldulensis Dehnh. by activation with carbon dioxide and superheated steam. Master's thesis. Program of Chemical Technology, Faculty of Science, Chulalongkorn University.

Kadirvalu, K., Kavipriya, M., Karthika, C., Vennilamani, N., and Pattabhi, S. 2004.

Mercury(II) adsorption by activated carbon made from sago waste. <u>Carbon</u> 42: 745-752.

Kaewsan, P. 2000. Single and Multi-Component Biosorption of Heavy Metal Ions by Biosorption by Marine Alga Durvillaea potatorum. PhD. Diss., Environmental Engineering, Griffith University, Queensland.

Kakitani, T., Hata, T., Kajimoto, T., and Imamura, Y. 2006. Designing a purification process for chromium-, copper- and arsenic-contaminated wood. <u>Waste Management</u> 26: 453-458

Kim, J.W., Sohn, M.H., Kim, D.S., Sohn, S.M., and Kwon, Y.S. 2001. Production of granular activated carbon from waste walnut shell and its adsorption characteristics for Cu^{2+} ion. <u>Journal of Hazardous Materials</u> 85: 301-315.

Kobya, M. 2004. Removal of Cr(VI) from aqueous solutions by adsorption onto hazelnut shell activated carbon: kinetic and equilibrium studies. <u>Bioresource Technology</u> 9: 317-321.

Kobya, M., Demirbas E., and Senturk, E., Ince, M. 2005. Adsorption of heavy metal ions from aqueous solutions by activated carbon prepared from apricot stone. <u>Bioresource Technology</u> 96: 1518-1521.

Krenkel, P.A. 1975. <u>Heavy Metals in the Aquatic Environment</u>. Pergamon Press Ltd, Oxford, England.

Krishnan, K.A., and Anirudhan, T.S. 2003. Removal of cadmium(II) from aqueous solutions by steam-activated sulphurised carbon prepared from sugar-cane bagasse pith: Kinetics and equilibrium studies. <u>Water SA</u> 29: 147-156.

Lagergren, S. 1898. Zur Theorie der sogenannten adsorption gelöster stoffe. Kungliga Svenska Vetenskapsakademiens. <u>Handlingar</u>, Band 24, No. 4.

Mohan, D., and Singh K.P. 2002. Single- and multi-component adsorption of cadmium and zinc using activated carbon derived from bagasse-agricultural waste. <u>Water research</u> 36: 2304-2318

Nadeem, M., Mahmood, A., Shahid, S.A., Shah, S.S., Khalid, A.M., and McKay, G. 2006. Sorption of Lead from Aqueous Solution by Chemically Modified Carbon Adsorbents. <u>Journal of Hazardous Materials</u> 138: 604-613.

Ninlanon, N. 1997. Production of activated carbon from mangrove wood using superheated steam and carbon dioxide. Master's thesis. Program of Chemical Technology, Faculty of Science, Chulalongkorn University

Palma, L.D., and Mecozzi, R., 2007. Heavy metals mobilization from harbour sediments using EDTA and citric acid as chelating agents. Journal of Hazardous Materials (In press).

Park, K.H., Mohapatra, D., and Reddy, B.R. 2006. A study on the acidified ferric chloride leaching of a complex (Cu–Ni–Co–Fe) matte. Separation and Purification Technology 51: 265-271.

Patnaik, P. 1999. A Comprehensive Guide to The Hazardous Properties of Chemical Substancees. New York: John Wiley & Son.

Patnukao, P., and Pavasant, P. 2006. Activated carbon from *Eucalyptus camaldulensis Dehn* bark using phosphoric acid activation. Bioresource Technology (In press).

Pavasant, P., Apiratikul, R., Sungkhum, V., Suthiparinyanont, P., Wattanachira, S., and Marhaba, T. 2003. Biosorption of Cu^{2+}, Cd^{2+}, Pb^{2+} and Zn^{2+} using dried marine green macroalga *Caulerpa lentillifera*. Bioresource Technology 97: 2321-2329.

Qin, F., Shan, and X., Wei, B., 2004. Effects of low-molecular-weight organic acids and residence time on desorption of Cu, Cd, and Pb from soils. Chemosphere 57: 253-263.

Quek, SY., Wase, DAJ., and Forster, CF. 1998. The use of sago waste for the sorption of lead and copper. Water SA 24: 251-256.

Suravattanasakul, T. 1998. Production of activated carbon from palm-oil shell by pyrolysis and steam activation in a fixed bed reactor. Master's thesis. Program of Polymer science, Faculty of Science, Chulalongkorn University.

Ücer, A., Uyanik, A., and Aygün, Ş.F. 2006. Adsorption of Cu(II), Cd(II), Zn(II), Mn(II) and Fe(III) ions by tannic acid immobilised activated carbon. Separation and Purification Technology 47: 113-118.

UZUN, İ., and GÜZEL, F. 2000. Adsorption of some heavy metal ions from aqueous solution by activated carbon and comparison of percent adsorption results of activated carbon with those of some other adsorbents. Turk J Chem 24: 291-297.

Volesky, B. 1990. Biosorption of heavy metals. (n.p.): CRC press.

Wu, H.L., Luo, Y.M., Christie, P., and Wong, M.H. 2003. Effects of EDTA and low molecular weight organic acids on soil solution properties of a heavy metal polluted soil. Chemosphere 50: 819–822.
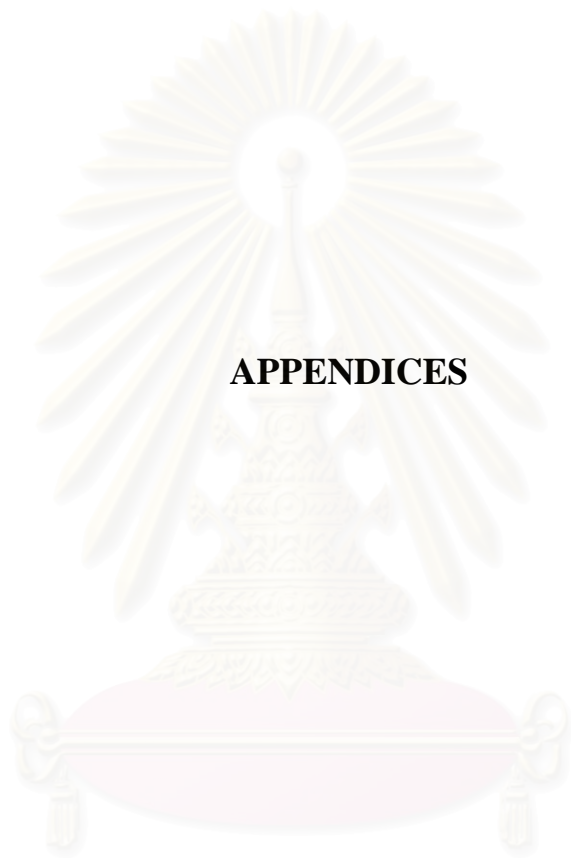
APPENDICES

APPENDIX A

Properties of heavy metals

Copper (Cu)

Atomic number	29
Atomic mass	63.546 g.mol^{-1}
Electronegativity according to Pauling	1.9
Density	8.09 g.cm^3 at 20°C
Melting point	1083°C
Boiling point	2595°C
Vanderwaals radius	0.128 nm
Ionic radius	0.096 nm (+1) ; 0.069 nm (+3)
Isotopes	6
Electronic shell	[Ar] 3d^{10} 4s^1
Energy of first ionisation	743.5 kJ.mol^{-1}
Energy of second ionisation	1946 kJ.mol^{-1}
Standard potential	+0.522 V (Cu$^+$ / Cu) ; +0.345 V (Cu^{2+} / Cu)
Discovered by	The ancients

Copper is a reddish metal with a face-centered cubic crystalline structure. It reflects red and orange light and absorbs other frequencies in the visible spectrum, due to its band structure, so it as a nice reddish color. It is malleable, ductile, and an extremely good conductor of both heat and electricity. It is softer than iron but harder than zinc and can be polished to a bright finish. It is found in group Ib of the periodic table, together with silver and gold. Copper has low chemical reactivity. In moist air it slowly forms a greenish surface film called patina; this coating protects the metal from further attack.

Applications

Most copper is used for electrical equipment (60%); construction, such as roofing and plumbing (20%); industrial machineri, such as heat exchangers (15%) and alloys

(5%). The main long established copper alloys are bronze, brass (a copper-zinc alloy), copper-tin-zinc, which was strong enough to make guns and cannons, and was known as gun metal, copper and nickel, known as cupronickel, which was the preferred metal for low-denomination coins. Copper is ideal for electrical wiring because it is easily worked, can be drawn into fine wire and has a high electrical conductivity.

Copper in the environment

Copper is a very common substance that occurs naturally in the environment and spreads through the environment through natural phenomena. Humans widely use copper. For instance it is applied in the industries and in agriculture. The production of copper has lifted over the last decades and due to this copper quantities in the environment have expanded.

The world's copper production is still rising. This basically means that more and more copper ends up in the environment. Rivers are depositing sludge on their banks that is contaminated with copper, due to the disposal of copper-containing wastewater. Copper enters the air, mainly through release during the combustion of fossil fuels. Copper in air will remain there for an eminent period of time, before it settles when it starts to rain. It will than end up mainly in soils. As a result soils may also contain large quantities of copper after copper from the air has settled.

Copper can be released into the environment by both natural sources and human activities. Examples of natural sources are wind-blown dust, decaying vegetation, forest fires and sea spray. A few examples of human activities that contribute to copper release have already been named. Other examples are mining, metal production, wood production and phosphate fertilizer production. Because copper is released both naturally and through human activity it is very widespread in the environment. Copper is often found near mines, industrial settings, landfills and waste disposals.

Most copper compounds will settle and be bound to either water sediment or soil particles. Soluble copper compounds form the largest threat to human health. Usually water-soluble copper compounds occur in the environment after release through application in agriculture.

World production of copper amounts to 12 million tonnes a year and exploitable reserves are aroun 300 million tonnes, which are expected to last for only another 25 years. About 2 million tonnes a year are reclaimed by recycling. Today

copper is mined as major deposists in Chile, Indonesia, USA, Australia and Canada, which together account for around 80% of the world's copper. The main ore is a yellow copper-iron sulfide called chalcopyrite ($CuFeS_2$).

Health effects of copper

Routes of exposition

Copper can be found in many kinds of food, in drinking water and in air. Because of that we absorb eminent quantities of copper each day by eating, drinking and breathing. The absorption of copper is necessary, because copper is a trace element that is essential for human health. Although humans can handle proportionally large concentrations of copper, too much copper can still cause eminent health problems.

Copper concentrations in air are usually quite low, so that exposure to copper through breathing is negligible. But people that live near smelters that process copper ore into metal do experience this kind of exposure.

People that live in houses that still have copper plumbing are exposed to higher levels of copper than most people, because copper is released into their drinking water through corrosion of pipes.

Occupational exposure to copper often occurs. In the work place environment copper contagion can lead to a flu-like condition known as metal fever. This condition will pass after two days and is caused by over sensitivity.

Effects

Long-term exposure to copper can cause irritation of the nose, mouth and eyes and it causes headaches, stomachaches, dizziness, vomiting and diarrhoea. Intentionally high uptakes of copper may cause liver and kidney damage and even death. Whether copper is carcinogenic has not been determined yet.

There are scientific articles that indicate a link between long-term exposure to high concentrations of copper and a decline in intelligence with young adolescents. Whether this should be of concern is a topic for further investigation.

Industrial exposure to copper fumes, dusts, or mists may result in metal fume fever with atrophic changes in nasal mucous membranes. Chronic copper poisoning results in Wilson's Disease, characterized by a hepatic cirrhosis, brain damage, demyelization, renal disease, and copper deposition in the cornea.

Environmental effects of copper

When copper ends up in soil it strongly attaches to organic matter and minerals. As a result it does not travel very far after release and it hardly ever enters groundwater. In surface water copper can travel great distances, either suspended on sludge particles or as free ions.

Copper does not break down in the environment and because of that it can accumulate in plants and animals when it is found in soils. On copper-rich soils only a limited number of plants has a chance of survival. That is why there is not much plant diversity near copper-disposing factories. Due to the effects upon plants copper is a serious threat to the productions of farmlands. Copper can seriously influence the proceedings of certain farmlands, depending upon the acidity of the soil and the presence of organic matter. Despite of this, copper-containing manures are still applied.

Copper can interrupt the activity in soils, as it negatively influences the activity of microrganisms and earthworms. The decomposition of organic matter may seriously slow down because of this.

When the soils of farmland are polluted with copper, animals will absorb concentrations that are damaging to their health. Mainly sheep suffer a great deal from copper poisoning, because the effects of copper are manifesting at fairly low concentrations.

Lead (Pb)

Atomic number	82
Atomic mass	207.2g.mol^{-1}
Electronegativity according to Pauling	1.8
Density	11.34 g.cm^3 at 20°C
Melting point	327°C
Boiling point	1755°C
Vanderwaals radius	0.154 nm
Ionic radius	0.132 nm (+2) ; 0.084 nm (+4)
Isotopes	13
Electronic shell	[Xe] 4f^{14}5d^{10} 6s^2 6p^2
Energy of first ionisation	715.4kJ.mol^{-1}
Energy of second ionisation	1450.0 kJ.mol^{-1}
Energy of third ionisation	3080.7 kJ.mol^{-1}
Energy of fourth ionisation	4082.3 kJ.mol^{-1}
Energy of fifth ionisation	6608 kJ.mol^{-1}
Discovered by	The ancients

Lead is a bluish-white lustrous metal. It is very soft, highly malleable, ductile, and a relatively poor conductor of electricity. It is very resistant to corrosion but tarnishes upon exposure to air. Lead isotopes are the end products of each of the three series of naturally occurring radioactive elements.

Applications

Lead pipes bearing the insignia of Roman emperors, used as drains from the baths, are still in service. Alloys include pewter and solder. Tetraethyl lead (PbEt$_4$) is still used in some grades of petrol (gasoline) but is being phased out on environmental grounds.

Lead is a major constituent of the lead-acid battery used extensively in car batteries. It is used as a coloring element in ceramic glazes, as projectiles, in some candles to threat the wick. It is the traditional base metal for organ pipes, and it is used as electrodes in the process of electrolysis. One if its major uses is in the glass of computer and television screens, where it shields the viewer from radiation. Other

uses are in sheeting, cables, solders, lead crystal glassware, ammunitions, bearings and as weight in sport equipment.

Lead in the environment

Native lead is rare in nature. Currently lead is usually found in ore with zinc, silver and copper and it is extracted together with these metals. The main lead mineral in Galena (PbS) and there are also deposits of cerrussite and anglesite which are mined. Galena is mined in Australia, which produces 19% of the world's new lead, followed by the USA, China, Peru' and Canada. Some is also mined in Mexico and West Germany. World production of new lead is 6 million tonnes a year, and workable reserves total are estimated 85 million tonnes, which is less than 15 year's supply.

Lead occurs naturally in the environment. However, most lead concentrations that are found in the environment are a result of human activities. Due to the application of lead in gasoline an unnatural lead-cycle has consisted. In car engines lead is burned, so that lead salts (chlorines, bromines, oxides) will originate.

These lead salts enter the environment through the exhausts of cars. The larger particles will drop to the ground immediately and pollute soils or surface waters, the smaller particles will travel long distances through air and remain in the atmosphere. Part of this lead will fall back on earth when it is raining. This lead-cycle caused by human production is much more extended than the natural lead-cycle. It has caused lead pollution to be a worldwide issue.

Health effects of lead

Lead is a soft metal that has known many applications over the years. It has been used widely since 5000 BC for application in metal products, cables and pipelines, but also in paints and pesticides. Lead is one out of four metals that have the most damaging effects on human health. It can enter the human body through uptake of food (65%), water (20%) and air (15%).

Foods such as fruit, vegetables, meats, grains, seafood, soft drinks and wine may contain significant amounts of lead. Cigarette smoke also contains small amounts of lead.

Lead can enter (drinking) water through corrosion of pipes. This is more likely to happen when the water is slightly acidic. That is why public water treatment systems

are now required to carry out pH-adjustments in water that will serve drinking purposes.

For as far as we know, lead fulfils no essential function in the human body, it can merely do harm after uptake from food, air or water.

Lead can cause several unwanted effects, such as:

- Disruption of the biosynthesis of haemoglobin and anaemia
- A rise in blood pressure
- Kidney damage
- Miscarriages and subtle abortions
- Disruption of nervous systems
- Brain damage
- Declined fertility of men through sperm damage
- Diminished learning abilities of children
- Behavioural disruptions of children, such as aggression, impulsive behavior and hyperactivity

Lead can enter a foetus through the placenta of the mother. Because of this it can cause serious damage to the nervous system and the brains of unborn children.

Environmental effects of lead

Not only leaded gasoline causes lead concentrations in the environment to rise. Other human activities, such as fuel combustion, industrial processes and solid waste combustion, also contribute.

Lead can end up in water and soils through corrosion of leaded pipelines in a water transporting system and through corrosion of leaded paints. It cannot be broken down; it can only converted to other forms.

Lead accumulates in the bodies of water organisms and soil organisms. These will experience health effects from lead poisoning. Health effects on shellfish can take place even when only very small concentrations of lead are present. Body functions of phytoplankton can be disturbed when lead interferes. Phytoplankton is an important source of oxygen production in seas and many larger sea-animals eat it. That is why we now begin to wonder whether lead pollution can influence global balances.

Soil functions are disturbed by lead intervention, especially near highways and farmlands, where extreme concentrations may be present. Soil organisms than suffer from lead poisoning, too.

Lead is a particularly dangerous chemical, as it can accumulate in individual organisms, but also in entire food chains. For more effects on freshwater ecosystem take a look at lead in freshwater

APPENDIX B

Paper Publications (Conference Articles)

Apipreeya Kongsuwan, Phussadee Patnukao, Prasert Pavasant. **Removal of Metal Ion from Synthetic Waste Water by Activated Carbon from Eucalyptus camaldulensis Dehn Bark.** 2006. JGSEE and Kyoto University 2nd Joint International Conference on: 21 - 23 Nov. 2006, Nai Lert Park Hotel, Bangkok.

92

The 2nd Joint International Conference on "Sustainable Energy and Environment (SEE 2006)"
21-23 November 2006, Bangkok, Thailand

E-041 (P)

Removal of Metal Ion from Synthetic Waste Water by Activated Carbon from *Eucalyptus camaldulensis Dehn* Bark

Apipreeya Kongsuwan[1] , Phussadee Patnukao[2] and Prasert Pavasant[1,*]

[1] Department of Chemical Engineering, Faculty of Engineering, Chulalongkorn University, Bangkok, 10330, Thailand
[2] National Research Center for Environmental and Hazardous Waste Management, Chulalongkorn University, Bangkok, 10330, Thailand

Abstract: *Eucalyptus bark could be effectively employed as a raw material for the production of activated carbon. The obtained activated carbon was utilized as adsorbent for treating synthetic wastewater containing Cu(II) and Pb(II). The optimum pH for the adsorption of Cu(II) and Pb(II) was 5. The adsorption reached equilibrium within 45 minutes for the whole range of initial heavy metal concentrations (0.1-10 mM). The results was found to match well with pseudo second-order kinetic model where equilibrium adsorption capacities and adsorption rate constant increased with initial heavy metal concentration. The adsorption isotherm followed Langmuir better than Freundlich isotherms. The maximum adsorption capacities of Cu(II) and Pb(II) adsorption were 4.5 and 5.4 mmol/g, respectively.*

Keywords: Removal, Adsorption, Activated Carbon, Heavy Metals, Isotherm

1. INTRODUCTION

With a rapid increase in global industrial activities, pollution derived from the uncontrolled escape of heavy metals such as copper nickel chromium and zinc has become serious. Heavy metals are detected in waste streams from mining operations, tanneries, electronics, electroplating and petrochemical industries in large quantities. These heavy metals have harmful effect on human physiology and other biological systems when they exceed the tolerance levels. The most widely used methods for removing heavy metals from wastewaters include ion exchange, chemical precipitation, reverse osmosis, evaporation, membrane filtration and adsorption [1]. Among various treatment technologies, activated carbon adsorption is commonly used because it was shown to be economically favorable (compared with ion exchange, liquid extraction or electrodialysis), technically easy (compared with precipitation or reverse osmosis) [2] and improved the efficiency of metallurgical removal particularly at low concentration range.

Recent work at the Department of Chemical Engineering, Faculty of Engineering, Chulalongkorn University, Thailand, has demonstrated a successful conversion of eucalyptus bark to activated carbon. This work therefore intended to employ this activated carbon product in the removal of heavy metal from the synthetic wastewater, and it was divided into two parts. The first part consisted of characterization of physicochemical properties of activated carbon used in this work. The second part was an experimental study of adsorption of metal ion by activated carbon. The results were evaluated with common kinetic models (First-order Lagergren, Pseudo second-order expression) to determine the reaction rate constants, and with common isotherm models (Langmuir and Freundlich isotherms) to examine for their adsorption capacities. The influence of pH was also investigated. In this work, a synthetic mixture solution of copper and lead was arbitrarily selected as a modeled adsorption system.

2. METHODOLOGY

2.1 Preparation of activated carbon

The raw material, eucalyptus bark, was prepared by impregnation into phosphoric acid (85% by weight) by using the weight ratio of raw material and phosphoric acid at 1:1. The mixture was carbonized in a muffle furnace at 500 °C for 1 h. The product was washed with hot distilled water until the pH of the leachate was 6 and dried in an oven at 105°C for 4 h. Finally, powder activated carbon was crushed and sieved in the size ranged between mesh number 325 (0.045 mm) and 100 (0.150 mm) and stored in a desiccator.

2.2 Activated carbon characteristics

- The surface morphology of activated carbon was visualized via scanning electron microscopy (SEM), the corresponding SEM micrographs were obtained using a scanning electron microscope (XL 30 ESEM FEG).
- Surface areas was calculated from adsorption isotherms using the method of Brunauer, Emmet and Teller (BET method). The BET surface area was determined by nitrogen adsorption (- 196°C) on surface area analyzer (Thermo Finnigan, Sorptomatic 1990).
- The ash content of the carbon was determined using a standard method according to ASTM D 2866-94 [3]. This method involved pre-drying the sample at 150°C, followed by burning in a muffle furnace at 650°C for 4 h in the presence of air. The ash content was calculated from the combustion residue. This test was repeated until constant ash content was obtained.
- Apparent (bulk) density of all samples was calculated as the ratio between weight and volume of packed dry material.
- The yield of activated carbon was defined as the ratio of the weight of the activated carbon product to that of the original eucalyptus bark, both weights were on a dry basis, i.e.

$$\%\text{Yield} = \frac{W_1}{W_0} \times 100 \tag{1}$$

where W_0 is the original mass of the precursor on a dry basis and W_1 is the mass of the carbon after activation, washing, and drying.

- The weight loss was calculated as the ratio of the weight of final activated carbons to that of initial raw materials according to the following equation:

Corresponding Author: prasert.p@chula.ac.th

93

The 2nd Joint International Conference on "Sustainable Energy and Environment (SEE 2006)"
E-041 (P)   *21-23 November 2006, Bangkok, Thailand*

$$\%\text{Weight loss} = \frac{(W_2 - W_0)}{(W_1 - W_0)} \times 100 \tag{2}$$

where W_0 is the weight of capsule with cover (g), W_1 the weight of capsule with cover plus original sample (g), and W_2 the weight of capsule with cover plus dried sample (g).

- The ultimate analysis of eucalyptus bark was performed in CHNS/O analyzer (Perkin Elmer PE2400 Series II), using gaseous products freed by pyrolysis in high-purity oxygen and chromatographic was detected with a thermal conductivity detector. The proximate analysis was developed following ASTM standards for chemical analysis of wood charcoal [4].
- The functional groups of activated carbon was analyzed by Fourier Transform Infared Spectrophotometer (FT-IR model 1760x).
- Iodine number was determined according to the ASTM standard method [5].
- Methylene blue number was determined according to Standard testing method of Methylene Blue Number of Activated Carbon (JIS K 1470-1991) [6].

2.3 Adsorption procedure

Stock solutions of Cu(II) and Pb(II) were prepared by dissolving reagent grade $Cu(NO_3)_2$ and $Pb(NO_3)_2$ in de-ionized water, respectively. pH was adjusted in the range from 1-6 by adding HNO_3 and NaOH aqueous solution to Cu(II) and Pb(II) solution. Adsorption was performed in batch experiments where 25 mL of heavy metal solutions was added to 0.1 g of activated carbon in conical flasks and mixed with rotary shaker at 200 rpm, 25 °C for 30 min. Solution and activated carbon were separated by filtering through a filter paper. The initial concentrations of Cu(II) and Pb(II) in the solution were varied from 0.1 to 10 mM. The concentration of heavy metals in the solutions was determined by an atomic absorption spectrometer.

2.4 Determination of the adsorption capacity

The sorption capacity was calculated from Equation (3),

$$q = \frac{V(C_i - C_e)}{1000W} \tag{3}$$

where q is adsorption capacity (mg/g), C_i the initial metal concentration (mg/L), C_e the concentration of metal at equilibrium (mg/L), W the adsorbent dosage (g) and V the solution volume (mL).

3. RESULTS AND DISCUSSION

3.1 Characterization of activated carbon

Table 1 summarizes the characteristics of the activated carbon obtained from the technique employed in this work. It is common to look first at the BET results as this is one of the most important properties of the activated carbon and Table 1 illustrates that activated carbon from this work had a relatively high specific surface areas (1239 m^2/g) when compared with those prepared from other agricultural by-products such as peanut hull (208 m^2/g), coir pith (595 m^2/g), eichhornia (266 m^2/g), cassava peel (200 m^2/g), coconut tree sawdust carbon (325 m^2/g) and sago waste (625 m^2/g) [7]. The difference could be due to the removal of considerable organic by-products and minerals presented in the activated carbon surface with the phosphoric acid during the activation process [8]. SEM micrographs indicated that the activated carbon product contained mainly microporous (more than 88.5%) and about 11.5% of mesopore. The morphology of the activated carbon surface is shown in Fig.1.

The functional groups on the surface of activated carbon were analyzed by Fourier Transform Infared Spectrophotometer demonstrate the existence of hydroxyl and amino groups which are mostly negatively charged.

Table 1 Characteristics of the activated carbon

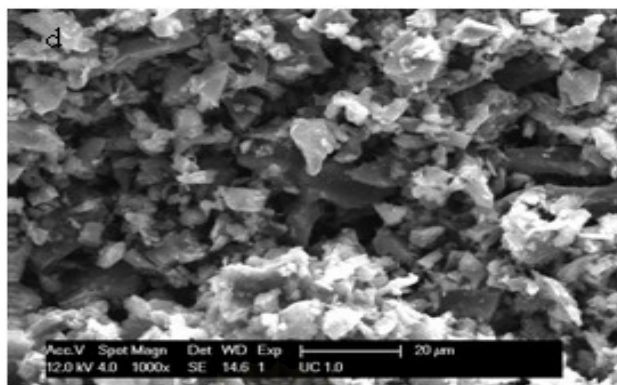| Parameter		Value
Yield	(%)	31.9
weight loss	(%)	54.6±0.5
Apparent (bulk) density	(g/cm³)	0.251
Moisture content	(%)	7
Ash content	(%)	4.88±0.09
C	(%)	62
H	(%)	4
Porous characteristics		
- BET specific surface area	(m²/g)	1239
- Micropore	(%)	88.5
- Mesopore	(%)	11.5
Iodine number	(mg/g)	918.6
Methylene blue	(mg/g)	427±2

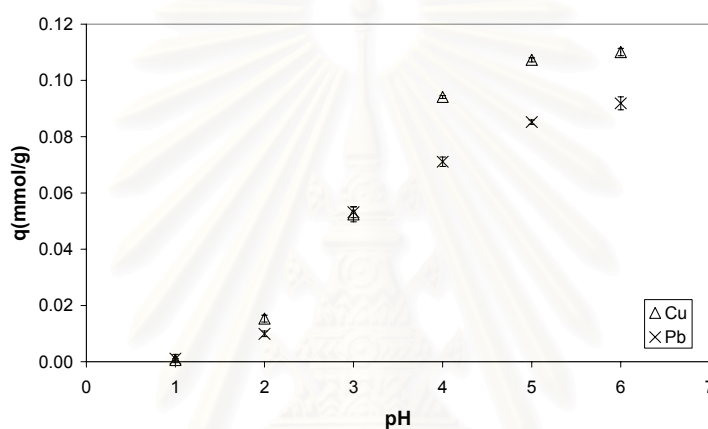**Fig. 1** SEM photograph of activated carbon

Fig. 2 Effect of pH on adsorption capacity

3.2 Adsorption studies
- Effect of pH for adsorption

The adsorption of metals was found to be strongly dependent on the pH of the solution. Fig.2 demonstrates that the optimum pH for the adsorption of Cu and Pb were about 5 which was rather acidic. At low pH (< 3), there was excessive protonation of the active sites at carbon surface and this often refuses the formation of links between metal ion and the active site. At moderate pH values (3-6), linked H^+ is released from the active sites and adsorbed amount of metal ions is generally found to increase. At higher pH values (>6), the precipitation is dominant or both ion exchange and aqueous metal hydroxide formation (not necessarily precipitation) may become significant mechanisms in the metal removal process. This condition is often not desirable as the metal precipitation could lead to a misunderstanding for the adsorption capacity. And in practice, metal precipitation is generally not a stabilized form of heavy metal as the precipitation can some time be very small in size, and upon the neutralization of the effluent from the wastewater treatment plant, the solubility of the metals increases resulting in a re-contamination of the waste outlet stream.

- Adsorption of metal ion

Adsorption kinetics

Batch experiments are carried out using Cu(II) and Pb(II) solutions at different initial concentrations (0.1-10mM). Figs.3 - 4 show the results on the adsorption kinetics of both metal ions. Kinetic curves were generally single, smooth and continuous, and the saturation could be expected to occur which indicated a monolayer adsorption of metal ion on the carbon surface. Cu(II) and Pb(II) adsorptions increased sharply during the initial stage and slowed down gradually when approaching equilibrium. These behaviors are quite common as they are attributed to saturation of the available adsorption sites [9].

As expected, the equilibrium adsorption capacity increased with increasing initial concentration. This equilibrium could be well described using the explanation regarding the dispersion force between metal ions and surface of activated carbon. As the positively charged ion approached the surface of the activate carbon, the surface of activated carbon was slightly induced to exhibit negatively charged property and the attraction between the two dipoles which was likely to lower the potential energy between them occurred and eventually brought about adsorption [10].
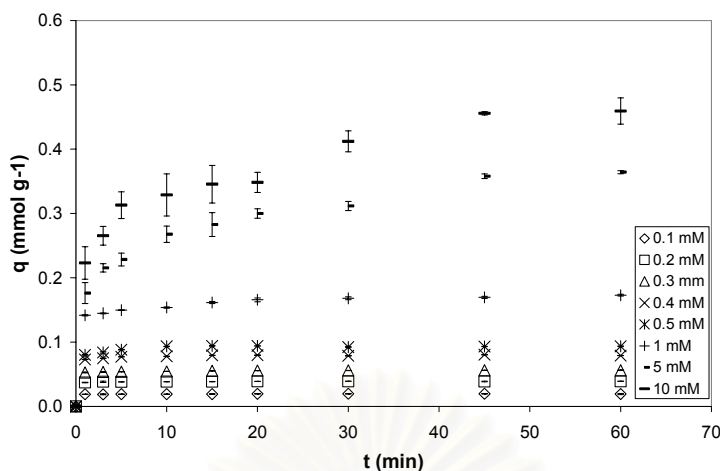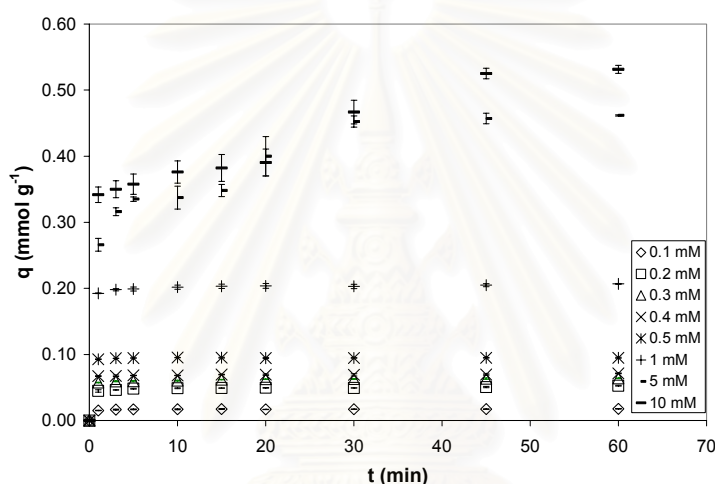
Fig. 3 Adsorption kinetics of Cu(II)

Fig. 4 Adsorption kinetics of Pb(II)

In order to describe the adsorption kinetics for Cu(II) and Pb(II) on activated carbon, the pseudo first-order [11] and the pseudo second order [12] were applied to the experimental data. Both equations are given by:

Pseudo first-order

$$\log(q_e - q) = \log q_e - \frac{k_1}{2.303}t \qquad (4)$$

Pseudo second-order

$$\frac{t}{q_e} = \frac{1}{k_2 q_e^2} + \frac{1}{q_e} \qquad (5)$$

where q_e and q are the amount of adsorbed adsorbate on the adsorbent at equilibrium and at time t, respectively (mmol g^{-1}); k_1 and k_2 are the adsorption rate constant for first-order and pseudo second-order, respectively.

The plots of these two kinetics models for Cu(II) and Pb(II) removal at different concentrations are presented in Figs.5 – 8. The relations were linear. The results demonstrated that Cu(II) adsorptions were appropriate to the first-order at high initial concentration and pseudo second-order for all initial concentration. In case of Pb(II) adsorptions, they were appropriate to both kinetics plots. Therefore the kinetic parameters such as rate constants and equilibrium adsorption capacities of adsorption for Cu(II) and Pb(II) were only described with pseudo second-order expression as they were suitable for both metals: they are summarized in Table 3. The results indicated that an increasing in the initial concentration of metal ion increased the equilibrium sorption capacity, q_e and adsorption rate constant, k_2.

Adsorption isotherm

Adsorption equilibrium is established when the concentration of metal ion in a bulk solution (C_e) is in dynamic with that of the interface (q_e). This level of equilibrium concentration depended significantly on the initial concentration of the metals and the results for this isotherm case is shown in Fig. 9. As a general observation, Pb(II) exhibited a higher maximum adsorption capacity than Cu(II).
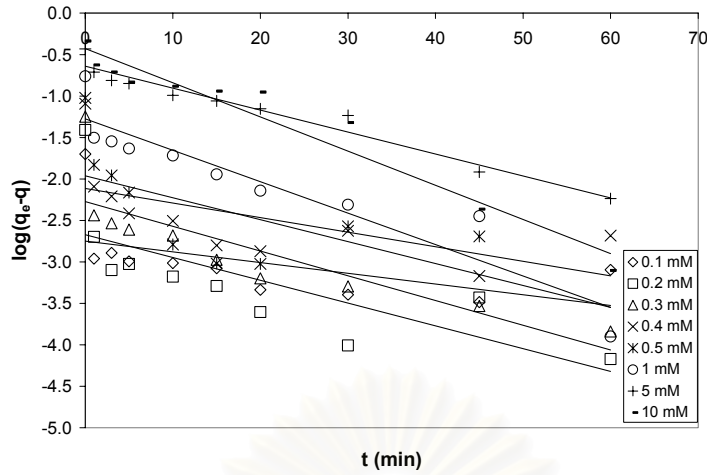
96

The 2nd Joint International Conference on "Sustainable Energy and Environment (SEE 2006)"
E-041 (P)   *21-23 November 2006, Bangkok, Thailand*

Fig. 5 First-order kinetics plots for the Cu(II) adsorption
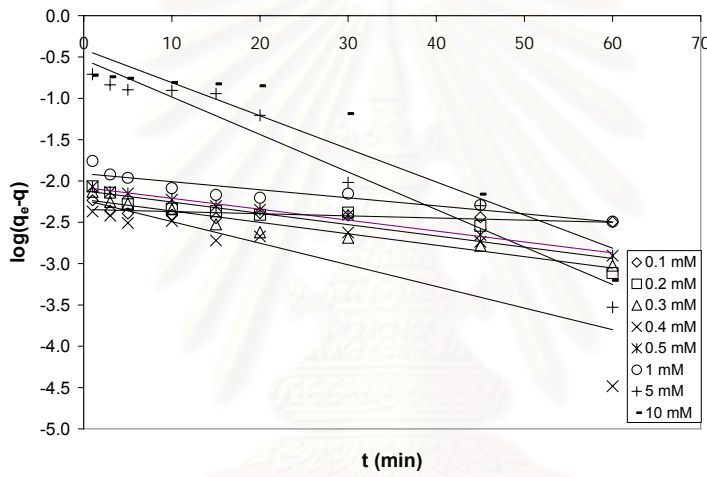

Fig. 6 First-order kinetics plots for the Pb(II) adsorption
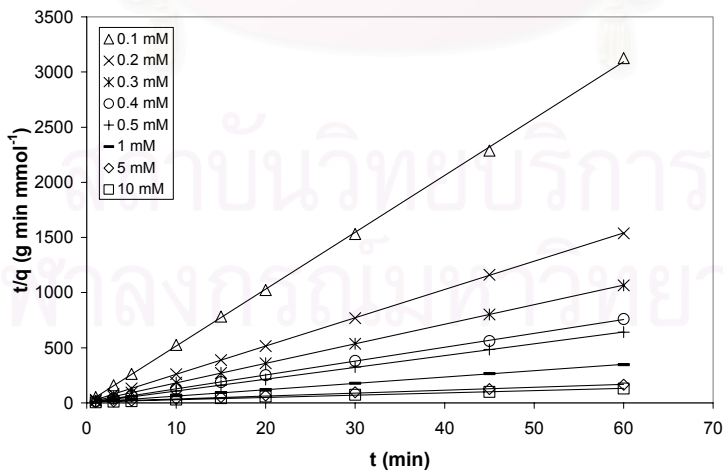

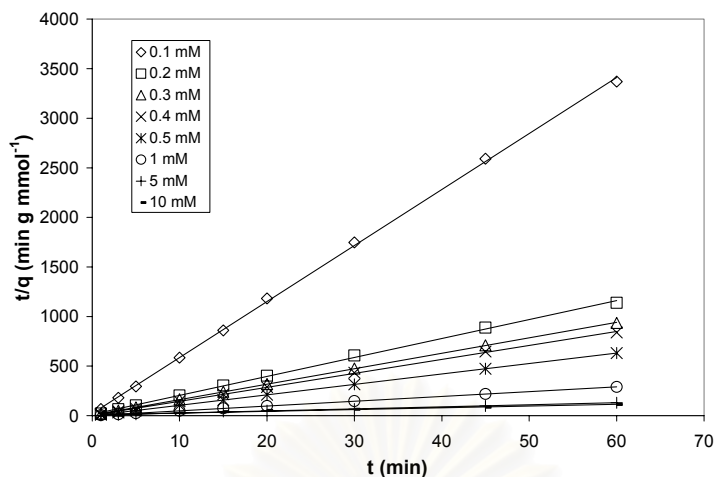**Fig. 7** Pseudo second-order kinetics plots for the Cu(II) adsorption

Fig. 8 Pseudo second-order kinetics plots for the Pb(II) adsorption

Table 2 R-square values of the first-order for the Cu(II) and Pb(II) adsorption

Initial concentration (mM)	Cu(II) R^2	Pb(II) R^2
0.1	0.3618	0.9995
0.2	0.7019	0.9988
0.3	0.9527	0.9211
0.4	0.4551	0.9999
0.5	0.2877	1.0000
1.0	0.8945	0.8388
5.0	0.9714	0.9476
10.0	0.9389	0.9847

Table 3 Kinetic parameters of the pseudo second-order for the Cu(II) and Pb(II) adsorption

Initial concentration (mM)	Cu(II)				Pb(II)			
	k (g mmol⁻¹ min⁻¹)	$q_{e,cal}$ (mmol g⁻¹)	$q_{e,exp}$ (mmol g⁻¹)	R^2	k (g mmol⁻¹ min⁻¹)	$q_{e,cal}$ (mmol g⁻¹)	$q_{e,exp}$ (mmol g⁻¹)	R^2
0.1	3.22×10^{-4}	1.94×10^{-2}	1.97×10^{-2}	0.9997	1.39×10^{-5}	1.77×10^{-2}	1.74×10^{-2}	0.9995
0.2	5.87×10^{-4}	3.90×10^{-2}	3.91×10^{-2}	1.0000	2.00×10^{-4}	5.23×10^{-2}	5.30×10^{-2}	0.9988
0.3	8.00×10^{-4}	5.64×10^{-2}	5.63×10^{-2}	1.0000	6.57×10^{-4}	6.42×10^{-2}	6.45×10^{-2}	0.9999
0.4	4.62×10^{-3}	7.95×10^{-2}	7.99×10^{-2}	0.9998	1.11×10^{-3}	7.10×10^{-2}	7.10×10^{-2}	0.9996
0.5	5.01×10^{-3}	9.36×10^{-2}	9.11×10^{-2}	0.9999	3.77×10^{-2}	9.50×10^{-2}	9.40×10^{-2}	1.0000
1.0	6.23×10^{-3}	1.74×10^{-1}	1.73×10^{-1}	0.9997	3.99×10^{-2}	2.07×10^{-1}	2.00×10^{-1}	0.9999
5.0	1.52×10^{-2}	3.77×10^{-1}	3.66×10^{-1}	0.9930	4.00×10^{-2}	4.80×10^{-1}	4.25×10^{-1}	0.9943
10.0	2.92×10^{-2}	4.79×10^{-1}	4.59×10^{-1}	0.9900	4.39×10^{-2}	5.51×10^{-1}	5.30×10^{-1}	0.9847

Generally there are two mathematical expressions used to describe the isotherm of the adsorption and they are Langmuir and Fruendlich equations. [13]. The Langmuir isotherm is given by:

$$q_e = \frac{bC_e q_m}{1+bC_e} \tag{6}$$

where q_m is the maximum adsorption capacity (mg/g), b a constant related to bonding energy of adsorption. The Langmuir parameters were obtain by fitting the experimental data to the linearized equation derived from Eq.(5):

$$\frac{C_e}{q_e} = \frac{C_e}{q_m} + \frac{1}{bq_m} \tag{7}$$

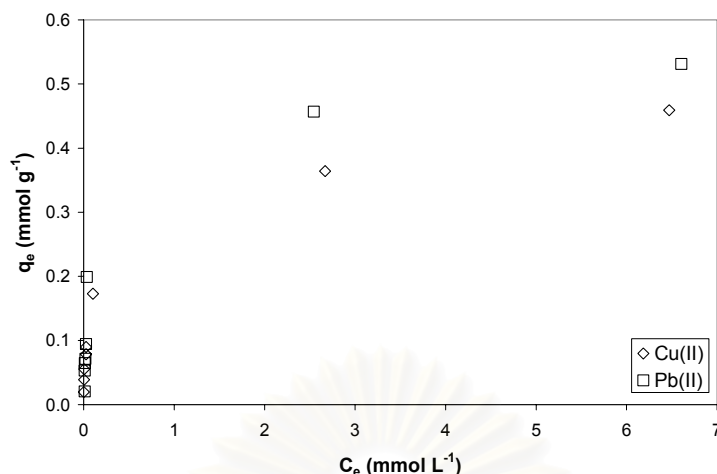The Langmuir plots for Cu(II) and Pb(II) adsorption are shown in Fig. 10.
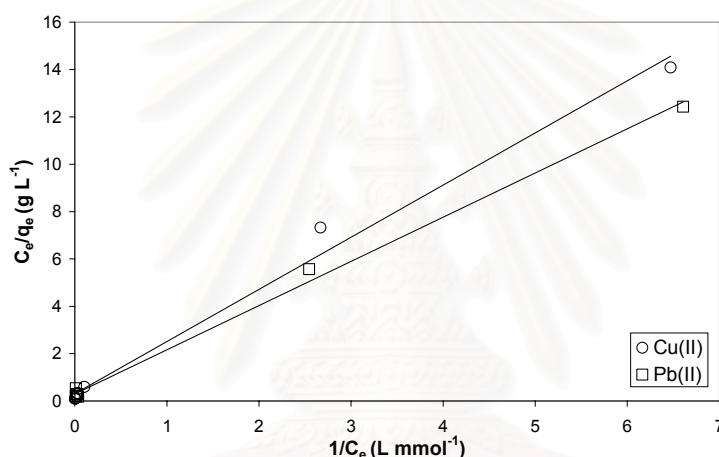
Fig. 9 Adsorption isotherm

Fig. 10 Langmuir isotherm plots for Cu(II) and Pb(II) adsorption

The Freundlich isotherm is given by:

$$q_e = K_F C_e^{1/n} \qquad (8)$$

where K_F and n are constants, and $n > 1$. The Freundlich isotherm is usually fitted to the logarithmic form:

$$\log q_e = \log K_F + (1/n)\log C_e \qquad (9)$$

The Freundlich isotherm plots for Cu(II) and Pb(II) isothermal adsorption are shown in Fig. 11. The parameters of Langmuir and Freundlich isotherm models for Cu(II) and Pb(II) are summarized in Table 3.

Table 4 demonstrates that the experimental data was fitted more favorably with Langmuir than Freundlich isotherms. This suggests that the adsorption of Cu(II) and Pb(II) could be monolayer-type [14]. A comparison between maximum adsorption capacities (q_m) between the two metals illustrated that Pb(II) had 120% sorption capacity of that of Cu(II) and the values of 1/n of less than 1 confirmed a favorable adsorption onto microporous adsorbent [2]. This level of sorption capacity was considered relatively high when compared with the reported values, e.g Sago waste (0.2 mmol Cu(II)/g, 0.23 mmol Pb(II)/g) [15], activated carbon (0.04 mmol Cu(II)/g /g) [16], activated carbon pretreated with 1 M citric acid (0.23 mmol Cu(II)/g /g) [17], Rice husk ash (0.064 mmol Pb(II)/g /g) [14].
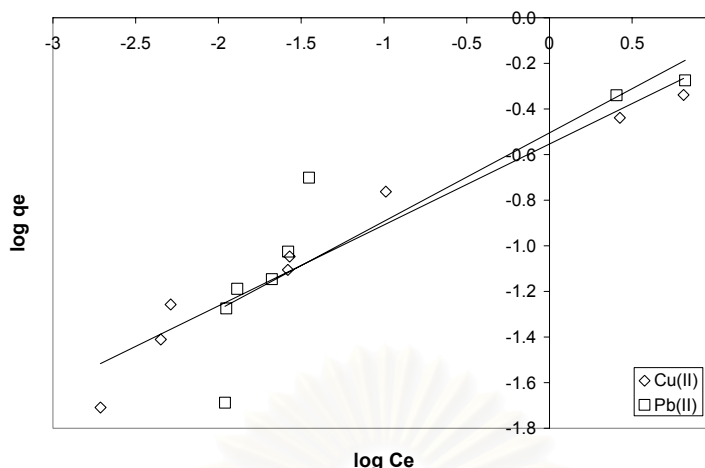
99

The 2nd Joint International Conference on "Sustainable Energy and Environment (SEE 2006)"
E-041 (P)
21-23 November 2006, Bangkok, Thailand

Fig. 11 Freundlich isotherm plots for Cu(II) and Pb(II) adsorption

Table 4 The parameters of Langmuir and Freundlich isotherm models

Heavy metal ion	Langmuir isotherm			Freundlich isotherm		
	q_m (mmol g^{-1})	B (L mmol^{-1})	R^2	K_F	1/n	R^2
Cu(II)	0.45	7.19	0.9911	0.54	0.49	0.9485
Pb(II)	0.55	6.23	0.9969	0.31	0.39	0.7976

4. CONCLUSION

The Cu(II) and Pb(II) adsorption by activated carbon from eucalyptus bark was evaluated here. The optimum pH for Cu(II) and Pb(II) adsorption on the activated carbon was pH 5. The adsorption reached equilibrium within 45 minutes for whole range of concentration (0.1-10 mM). The results on kinetics data was appropriately fitted with pseudo second-order kinetic model where adsorption rate constant and equilibrium adsorption capacities increased with initial heavy metal concentration. The adsorption isotherm followed Langmuir better than Freundlich isotherms. This work illustrates using of waste from industrial to recycle to be good adsorbent for removal metal ion from wastewater.

5. ACKNOWLEDGMENTS

6. REFERENCES

[1] Bartosch, C., Kiefer, R. and Höll, W.H. (2000) Separation of heavy metals by parametric pumping with variation of pH Part I: Application of cation exchangers in binary systems. Reactive & Functional Polymers, 45, pp. 197-210.
[2] Faur-Brasquet, C., Reddad, Z., Kadirvelu, K., and Cloirec, P.L. 2002. Modeling the adsorption of metal ions (Cu2+, Ni2+,Pb2+) onto ACCs using surface complexation models. Applied surface science, 196, pp. 356-365.
[3] American Standard of Testing Material. Standard test method for total ash content of activated carbon. Annual book of ASTM standards, D 2866-94, pp. 498-499.
[4] American Standard of Testing Material. Standard test method for chemical analysis of wood charcoal. Annual book of ASTM standards, D 1762-84.
[5] American Standard of Testing Material. Standard test method for determination of iodine number of activated carbon. Annual book of ASTM standards, D 4607-94, pp. 542-545.
[6] Japanese Standard Association. Standard testing method of mythylene blue number of activated carbon. Japanese industrial standard test method for activated carbon. JIS K 1470-1991.
[7] Kadirvalu, K., Kavipriya, M., Karthika, C., Vennilamani, N., Pattabhi, S. (2004). Mercury (II) adsorption by activated carbon made from sago waste. Carbon, 42, pp. 745-752.
[8] Chen, J.P., Wu, S., and Chong, K.H. (2003). Surface modification of a granular activated carbon by citric acid for enhancement of copper adsorption. Carbon, 41, pp. 1979-1986.
[9] Yardim, M.F., Budinova, T., Ekinci, E., Petrov, N., Razvigorova, M., Minkova, V. (2003). Removal of mercury (II) from aqueous solution by activated carbon obtain fromfurfural. Chemosphere, 53, pp. 835-841.
[10] Kim, D.S.(2003). Activated carbon from peach stones using phosphoric acid activation at medium temperatures.
[11] Lagergren, S., 1898. 'Zur Theorie der sogenannten adsorption gelöster stoffe'. Kungliga Svenska Vetenskapsakademiens. Handlingar, Band 24, No. 4.
[12] Ho, Y.S. and McKay, G., 1999. A kinetic study of dye sorption by biosorbent waste product pith. Resour Conser Recycl, 15(3-4), pp. 171-193.

100

The 2nd Joint International Conference on "Sustainable Energy and Environment (SEE 2006)"
21-23 November 2006, Bangkok, Thailand

E-041 (P)

[13] Eckenfelder, W.W. 2000. Industrial Water Pollution Control. McGraw-Hill Companies, Inc., Singapore, 417-450.

[14] Feng, Q., Lin, Q., Gong, F., Sugita, S., and Shoya, M., 2004. Adsorption of lead and mercury by rice husk ash. Journal of Colloid and Interface Science, 278, pp. 1-8

[15] Quek, S.Y., Wase, D.A.J.., and Forster, C.F. 1998. The use of sago waste for the sorption of lead and copper. Water SA, Vol. 24 No. 3.

[16] UZUN, İ., and GÜZEL, F. 2000. Adsorption of some heavy metal ions from aqueous solution by activated carbon and comparison of percent adsorption results of activated carbon with those of some other adsorbents. Turk J Chem, 24 , pp. 291-297.

[17] Chen, J.P., Wu, S., and Chong, K.H. 2003. Surface modification of a granular activated carbon by citric acid for enhancement of copper adsorption. Carbon, 41, pp. 1979-1986.

BIOGRAPHY

Miss Apipreeya Kongsuwan was born on 19th October, 1983 in Bangkok. She finished her secondary course from Samsenwittayalai School in March, 2001. After that, she studied in the major of Chemical Engineering in Faculty of Engineering at King Mongkut's University of Technology Thonburi. She continued her further study for Master's degree in Chemical Engineering at Chulalongkorn University. She participated in the Environmental Engineering Research Group and achieved her Master's degree in April, 2007.